Dissertation

submitted to the

Combined Faculties for the Natural Sciences and for Mathematics

of the Ruperto-Carola University of Heidelberg, Germany

for the degree of

Doctor of Natural Sciences

presented by

Diplom-Biochemikerin Petra Netter

born in: Bernburg (Saale)

Oral-examination: _____

Investigation of
Natural Killer cell detachment from tumor cells
-
Characterizing the termination of the
activating Natural Killer cell immunological synapse

Referees: PD Dr. Tobias Dick

Prof. Dr. Carsten Watzl

Im Gedenken an meine Mutter

There is one thing even more vital to science than intelligent methods;
and that is the sincere desire to find out the truth,
whatever it may be.

(Charles Pierce)

Table of contents

Acknowledgements

First of all, I would like to thank Prof. Dr. Carsten Watzl. Thank you for the excellent guidance and for always having the time for inspiring discussions. Your enthusiasm for science was a great motivation and guided me to become the scientist I am now.

Furthermore, I highly appreciate that PD Dr. Tobias Dick agreed to represent this scientific work to the Faculty of Natural Science of the University of Heidelberg.

I also thank all past and present members of the Watzl-lab:

Sabine Wingert	Doris Urlaub	Maren Claus
Christian Schütz	Moritz Amft	Martha-Lena Müller
Linda Drenkelforth	Melanie Ebel	Mina Sandusky
Birgitta Messmer	Sebastian Stark	Kevin Bode
Stephan Gütgemann	André Cohnen	Stephan Meinke
Frank Fasbender	Jürgen Damaschke	Doris Teutsch
Peter Bröde	Wolfgang Merkt	Peter Andorf
Stefanie Margraf	Simone Reipschläger	

Not to forget our visitors from all over the world:

Roberta Sommaggio	Mona Rady	Gregory Kemper

Thank you not only for the fruitful discussions and everything you taught me, but also for the huge amount of laughter and your friendship that made me enjoy my work even more. A special thanks goes to the ones of you who have been with me in a time of sorrow. You supported me with your understanding, help and warmth. I don't know if I could have kept going as I did if it weren't for you!

In addition, I thank all the members of the Institute for Immunology in Heidelberg who readily supported me when I asked for help or advice. And I also thank the people at the Leibniz Research Centre for Working Environment and Human Factors in Dortmund who welcomed us when we came here in 2012 and helped us to settle in.

Ein großes Dankeschön an meine Familie: meiner Mama, die mir gezeigt hat, niemals aufzugeben und für Träume zu kämpfen; meinem Papa für die Unterstützung bei allen meinen Entscheidungen und für die Kraft die er aufgebracht hat, als ich ihm nicht helfen konnte; meiner Schwester Heike und meinem Schwager André für ihre Unterstützung, selbst in den ungewöhnlichsten Situationen und dafür, dass sie immer für mich da sind.

Abschließend, möchte ich meinen Freunden danken, denn ohne sie wäre es einfach nicht das Gleiche:

Rowena, Agata, Anne, Stefanie, Caro, Jule, Selina, Saskia, Naima,

Robert, Dörte, Moritz, Gisela und Curdin.

Summary

The process of Natural Killer (NK) cell adhesion to target cells resulting in NK cell activation and cytotoxicity has been the subject of intense research. However, only very little is known about the detachment of NK cells from target cells after the lytic hit. Since NK cells are able to kill multiple targets in a serial manner, this detachment process could play a pivotal role for an effective cytotoxic NK cell response. We therefore established different assay systems, based on flow cytometry and microscopy, to study NK cell detachment in more detail. Using these assay systems we could demonstrate that recently detached NK cells showed signs of productive conjugates. We found evidence for degranulation and observed down-modulation of activating receptors. This was possibly caused by internalization after receptor engagement, a mechanism suggested to tune down the strength of the interaction between cells. In contrast, plasma membrane-bound metalloproteinases that mediate shedding of surface molecules and thereby also possibly decrease contact between effector and target cell, were not required.

In our flow cytometry-based system cultured human NK cells detached from K562 cells with a half-life of about 50 minutes. A similar trend was observed for the half-lives of NK:HeLa cell-contacts analyzed using life cell-microscopy. The maintenance of the NK:K562 conjugates required sustained early activating signaling, e.g. via Src- and Syk-family kinases, and was ATP-dependent. In contrast, MAP kinase and also PKCθ activity did not affect the formation nor the decay of conjugates. To investigate the involvement of inhibitory pathways in the detachment process we interfered with phosphatases and found that the serine-threonine phosphatase PP1 was important for the stability of conjugates. In addition to ongoing signaling, the flexibility of the actin cytoskeleton was indispensable to maintain NK:target cell contacts, whereas dynamics of microtubules had only limited impact.

Investigating the influence of target cell availability on the detachment revealed that contact to a new target accelerated the separation from a previous one. Therefore, the contact to a target may keep the NK cell in an activated status and thereby may support serial killing. To investigate the role of target cell viability on detachment we interfered with the target cell survival on various levels. Inhibition of myosin IIA, which is involved in exocytosis of lytic granules, led to reduced lysis and moderately decelerated detachment. Depletion of mature perforin by inhibition of the vacuolar H^+-ATPase led to a complete loss of NK cell cytotoxicity, while the formation of NK:target cell conjugates remained unaffected. Interestingly, this resulted in a drastic deceleration of NK cell detachment. If the loss of perforin was caused by monensin, a proton ionophor, lysis of target cells was abolished but the half-life of NK:target cell conjugates remained unaffected. Taken together these data indicate that not target cell survival as such, but some NK cell intrinsic mechanisms affect the detachment process.

In summary, we established assay systems that allow investigation of the detachment process from target cells and we found first evidences that maintenance of conjugates and the detachment are regulated processes. Thus, understanding the mechanisms leading to detachment may facilitate efforts to increase the efficiency of NK cell-mediated cytotoxicity.

Zusammenfassung

Adhäsion von NK-Zellen an Zielzellen führt zu deren Aktivierung und löst die von ihnen vermittelte Zytotoxizität aus. Dieser Prozess ist bereits intensiv erforscht. Über das Ablösen der NK- von Zielzellen nach dem Ausführen der Effektorfunktion ist im Gegensatz dazu bisher nur wenig bekannt. Da NK-Zellen in der Lage sind mehrere Zielzellen nacheinander zu zerstören, könnte das Ablösen eine entscheidende Rolle für eine effektive NK-Zell-vermittelte Immunantwort spielen. Daher haben wir verschiedene auf Durchflusszytometrie- und Mikroskopie-basierte Versuchssysteme etabliert, um das Freisetzen der Zielzelle von der NK-Zelle genauer zu untersuchen. Mit diesen Versuchssystemen konnten wir zeigen, dass kürzlich abgelöste NK-Zellen, Anzeichen produktiver Konjugate zeigten. Wir konnten Degranulation nachweisen und beobachteten die Herunterregulierung aktivierender Rezeptoren. Eine mögliche Ursache hierfür könnte Rezeptorinternalisierung sein, welche durch die Bindung des entsprechenden Liganden ausgelöst werden kann. Es wird angenommen, dass dieser Mechanismus die Stärke der Interaktion zwischen Zellen verringert. An die Plasmamembran gebundene Matrixmetalloproteinasen können Oberflächenmoleküle abschneiden und dadurch ebenfalls zum Verringern des Kontaktes zwischen Effektor- und Zielzelle beitragen. Jedoch zeigte deren Inhibierung keinen Einfluss auf die Beständigkeit von NK:Zielzell-Kontakten.

In unserem Durchflusszytometrie-basierten System bestimmten wir für Konjugate zwischen kultivierten humanen NK-Zellen und K652-Zellen eine Halbwertszeit von ungefähr 50 min. Die Untersuchung von NK:HeLa-Zellkontakten mittels Lebendzellmikroskopie zeigte eine vergleichbare Tendenz für die Halbwertszeit. Neben der Verfügbarkeit von ATP, benötigte die Aufrechterhaltung von NK:K562-Konjugaten anhaltende aktivierende Signale, beispielsweise über Src- und Syk-Kinasen. Dahingegen hatten MAP-Kinasen und PKCθ weder auf die Bildung noch auf den Zerfall der Konjugate einen Einfluss. Neben kontinuierlichen Signalen, ist die Flexibilität des Aktin-Zytoskeletts für die Aufrechterhaltung von NK:Zielzell-Kontakten unverzichtbar, wohingegen die Dynamik der Mikrotubulie nur von geringer Bedeutung war.

Weiterhin wurde untersucht, welchen Einfluss die Verfügbarkeit von weiteren Zielzellen auf das Ablösen hat. Das Ausbilden des Kontaktes zu einer neuen Zielzelle beschleunigte das Ablösen von der ursprünglichen Zielzelle. Das deutet darauf hin, dass der Kontakt zu einer Zielzelle möglicherweise den aktivierten Zustand der NK-Zelle aufrecht erhält und dadurch gegebenenfalls serielles Zerstören von Zielzellen unterstützt. Um die Rolle der Viabilität der Zielzellen für das Ablösen der NK-Zellen zu erforschen, haben wir versucht das Überleben der Zielzelle auf verschiedenen Ebenen zu beeinflussen. Inhibierung von Myosin IIA, das bei der Exozytose lytischer Granula benötigt wird, führte zu einer reduzierten Zielzelllyse und einem mäßig verlangsamten Zerfall der Konjugate. Durch Blockierung der vakuolären H^+-ATPase induzierten wir die Depletion von reifem Perforin. Das

verursachte einen kompletten Verlust der NK-Zell-Zytotoxizität wohingegen die Bildung von Konjugaten unbeeinflusst blieb. Interessanterweise führte dies zu einer drastischen Verlangsamung des Ablösens der NK- von den Zielzellen. Wurde der Verlust von Perforin durch das Protoneninonophor Monensin ausgelöst, wurde zwar die Zielzelllyse verhindert, aber die Halbwertszeit der NK:K562-Konjugate blieb unverändert. Diese Ergebnisse deuten darauf hin, dass nicht das Zielzellüberleben als solches, sondern NK-Zell-intrinsische Mechanismen das Freisetzen der Zielzelle beeinflussen.

In dieser Arbeit stellen wir Versuchssysteme vor, die eine Untersuchung des Ablösungsprozesses der NK-Zellen von Zielzellen ermöglichen. Weiterhin haben wir erste Hinweise darauf gefunden, dass sowohl die Aufrechterhaltung, als auch das Auflösen von Konjugaten regulierte Prozesse sind. Für Bestrebungen die Effizienz der NK-Zell-vermittelten Zytotoxizität zu erhöhen, ist das Verständnis der zugrunde liegenden Mechanismen von großer Bedeutung.

1. Introduction

1.1 General Natural Killer cell biology

Natural killer (NK) cells are essential innate effectors in early immune responses against viral infections and transformed cells. They constitute 5-15 % of the lymphocytes in the peripheral blood, but are also found in spleen, liver, lung, bone marrow and lymph nodes (Westermann&Pabst, 1992). There is a multiplicity of immunodeficiencies accompanied with total absence or impaired NK cell function (Orange, 2002). These are mostly caused by single gene mutations and in general associated with an increased susceptibility to herpes virus-infections. Additionally, low NK cell activity was shown to correlate with increased cancer risk (Imai et al., 2000). Human NK cells are typically described as $CD56^{+}$ $CD3^{-}$ $NKp46^{+}$ and divided in two distinct subpopulation based on the density of CD56 surface expression. $CD56^{bright}$ NK cells, mainly responding to soluble factors, show high cytokine and chemokine production. They express comparably low levels of CD16 and are a preceding developmental stage to $CD56^{dim}$ NK cells. The latter represent about 90 % of circulating NK cells with increased responsiveness to cell surface ligands and thus higher cytotoxic potential (Caligiuri, 2008; Long et al., 2013). As B and T cells, NK cells belong to the lymphocyte compartment (Blom&Spits, 2006), however due to the lack of somatical gene-rearrangement they do not carry clonotypic antigen-specific receptors (Long et al., 2013). Instead they express germ line-encoded receptors that bind to conserved molecular structures.

Induction of NK cell effector functions is tightly regulated by integration of activating and inhibitory signals (Long et al., 2013). During encounter of susceptible targets signaling cascades are induced that lead to activation and the formation of the activating NK cell immunological synapse (aNKIS), culminating in cytotoxic effector functions. Three main mechanisms for target cell elimination have been described: (i) Directed release of cytolytic effector proteins such as perforin and granzymes induces apoptosis of the target cell (Krzewski&Coligan, 2012). (ii) Opsonization of targets with immunoglobulins (Igs) induces antibody-mediated cellular cytotoxicity (ADCC) by binding of the Fc domain of the Ig to the activating receptor CD16 (FcγRIIIa) (Lanier et al., 1988). (iii) Binding and trimerization of the death receptors tumor necrosis factor-related apoptosis-inducing ligand (TRAIL)-R1-5 or Fas on the target cell by the respective ligands TRAIL and FasL on NK cells induces receptor-mediated apoptosis (Zamai et al., 1998; Chávez-Galán et al., 2009). Additionally, gene-transcription is initiated resulting in release of cytokines, e.g. interferon (IFN)-γ, tumor necrosis factor (TNF)-α and granulocyte-macrophage colony-stimulating factor (GM-CSF), which are important for recruitment and stimulation of other immune cell types (Campbell&Hasegawa, 2013). Besides this, regulatory NK cell functions were described. Via release of soluble factors or direct cell-

cell interaction they control other immune cell types, e.g. T cells and dendritic cells (DC) (Tian et al., 2012; Crome et al., 2013). Through to these activities NK cells have been postulated to play a crucial role in prevention of autoimmunity.

Two major mechanisms described for NK cell activation are "missing self" and "induced self" recognition. Kärre and colleagues proposed the "missing self" concept in 1990, stating that NK cells recognize and destroy malignant cells that lost self-MHC-I (Ljunggren&Karre, 1990; Karre, 2002). In healthy individuals NK cells bind MHC class I molecules expressed on autologous cells via inhibitory receptors e.g. Killer cell immunoglobulin-like receptors (KIRs). In contrast, during cellular stress expression of ligands for activating receptors is induced, triggering NK cell-mediated cytotoxicity. This "induced self" hypothesis was initially described for the activating receptor NKG2D (Diefenbach&Raulet, 2001) and later proposed to be also true for NKp30 (Kellner et al., 2012).
The strength of NK cell responsiveness is determined during their development. Interestingly, NK cells that lack inhibitory receptors for self-MHC I and thereby can not receive inhibitory signals become hyporesponsive, a mechanism required for self-tolerance (Raulet et al., 2001; Fernandez et al., 2005; Raulet, 2006). Recently, several models for this education process have been postulated. The "disarming model" suggests, that if NK cells constantly receive activating impulses with lacking inhibition they turn hyporesponsive. The "arming model" in contrast, proposes that NK cells become responsive through signals of at least one ITIM-bearing receptor that recognizes self-MHC-I (Raulet&Vance, 2006). This should prevent autoreactivity caused by lacking inhibition by self-MHC-I. This last model is also described with the word "licensing" (Kim et al., 2005). Recently, it was shown that licensing is reversible, depending on the MHC I-environment (Joncker et al., 2010). Another model, introduced by Brodin and colleagues in 2009 is the "rheostat model" stating that the more inhibitory signals could be received the higher is the responsiveness of the NK cell (Brodin et al., 2009; Joncker et al., 2009). The common feature of all these models is that NK cells express at least one functional inhibitory receptor specific for self-MHC-I to acquire functional competence.

Another emerging and surprising discovery in NK cell biology is the hypothesis of an NK cell memory, which initially was believed to be an exclusive feature of the adaptive immune system. Recent studies show that under certain circumstances NK cells mediate long-lived memory responses (Min-Oo et al., 2013). In mouse-systems three different origins of the memory-phenotype have been described: (i) mouse cytomegalovirus (MCMV)-induced memory, (ii) cytokine-induced memory and (iii) liver-restricted memory that is associated with recognition of haptens and thereby seem to be antigen-specific. Nevertheless, the relevance for the human system still has to be evaluated. But there are indications that certain virus infections, e.g. with cytomegalovirus (CMV), induce long-lived

specific NK cells (Min-Oo et al., 2013). The mechanisms and conditions of this feature are still not understood and subject of intense research. Deciphering this new concept would lead to another fundamental change in understanding the significance of NK cells for immunity.

1.2 The complexity of NK cell-mediated directed cellular cytotoxicity

The encounter of an NK cell with a susceptible target cell cumulating in directed cellular cytotoxicity is highly regulated and complex and requires the formation of the aNKIS. Initially, the immunological synapse (IS) was described for T cell interaction with antigen presenting cells (APCs) as "combination of a specialized junction, cell polarization, and positional stability" (Paul&Seder, 1994; Dustin et al., 1998). In 1999, Davis and colleagues showed that also NK cells formed synapses during inhibitory NK-target cell interactions (Davis et al., 1999). Two years later, activating Natural Killer cell synapses were described for the first time (Vyas et al., 2001). Until today immunological synapses as feature of cell-cell-interaction have also been found between other cell types of the immune system as well as between immune and non-immune cells (Orange, 2008). Understanding the IS as spatially and temporally structured rearrangement of various molecules, several functions for the IS in signaling, secretion and protein transfer have been postulated (Roda-Navarro&Reyburn, 2007; Krzewski&Strominger, 2008; Orange, 2008). The accumulation of adhesion molecules enables a firm attachment of the NK cell to the target cell, which supports ligation of a multitude of NK cell receptors. The formation of a thin cavity between NK and target cell, the so-called "synaptic cleft" facilitates directed release of lytic granules without harming bystander cells. Additionally, the small size of the cavity might ensure a high local concentration of the released effector molecules. This might also be important in terms of multiple killing events, since the reduced amount of cytolytic molecules required for one target saves energy. Recruitment of receptors and associating signaling molecules leads to local signal amplification. This accumulation might be one mechanism to facilitate overcoming of concentration-dependent activation thresholds. Furthermore, some studies describe the exchange of membrane fragments and embedded proteins between the two interacting cells (Onfelt et al., 2004; Roda-Navarro et al., 2004; Roda-Navarro&Reyburn, 2007). The purpose of this mechanism is still debated, but it might have a role in recycling mechanisms and regulation of NK cell activity. Moreover, it was also described to be involved in spreading of pathogens (Roda-Navarro&Reyburn, 2007; Krzewski&Strominger, 2008).

1.2.1 The Natural Killer cell immunological synapse

The process of synapse formation was reviewed in detail by J. S. Orange in 2008 and recently by Mace and colleagues (Orange, 2008; Mace et al., 2014). Although the steps occur in a certain sequence, a

linear descriptions of the events is difficult since most events occur simultaneously. Additionally, redundancy of signaling molecules and synergy of signaling pathways induced by coactivating receptors were described, indicating the complexity of this process. (Orange et al., 2003; Wulfing et al., 2003; Orange, 2008). The different stages of the aNKIS are pictured in figure 1.1 and can be roughly divided in (i) loose adhesion and ligation of integrins and receptors leading to initial signaling; (ii) actin cytoskeleton rearrangements and strengthening adhesion; (iii) recruitment and clustering of receptors promoting increased and sustained signaling; (iv) microtubule cytoskeleton reorganization; (v) granule convergence to the microtubule organizing center (MTOC) and polarization of MTOC/lytic granules to the IS; (vii) degranulation and recycling and (viii) disassembly of the IS.

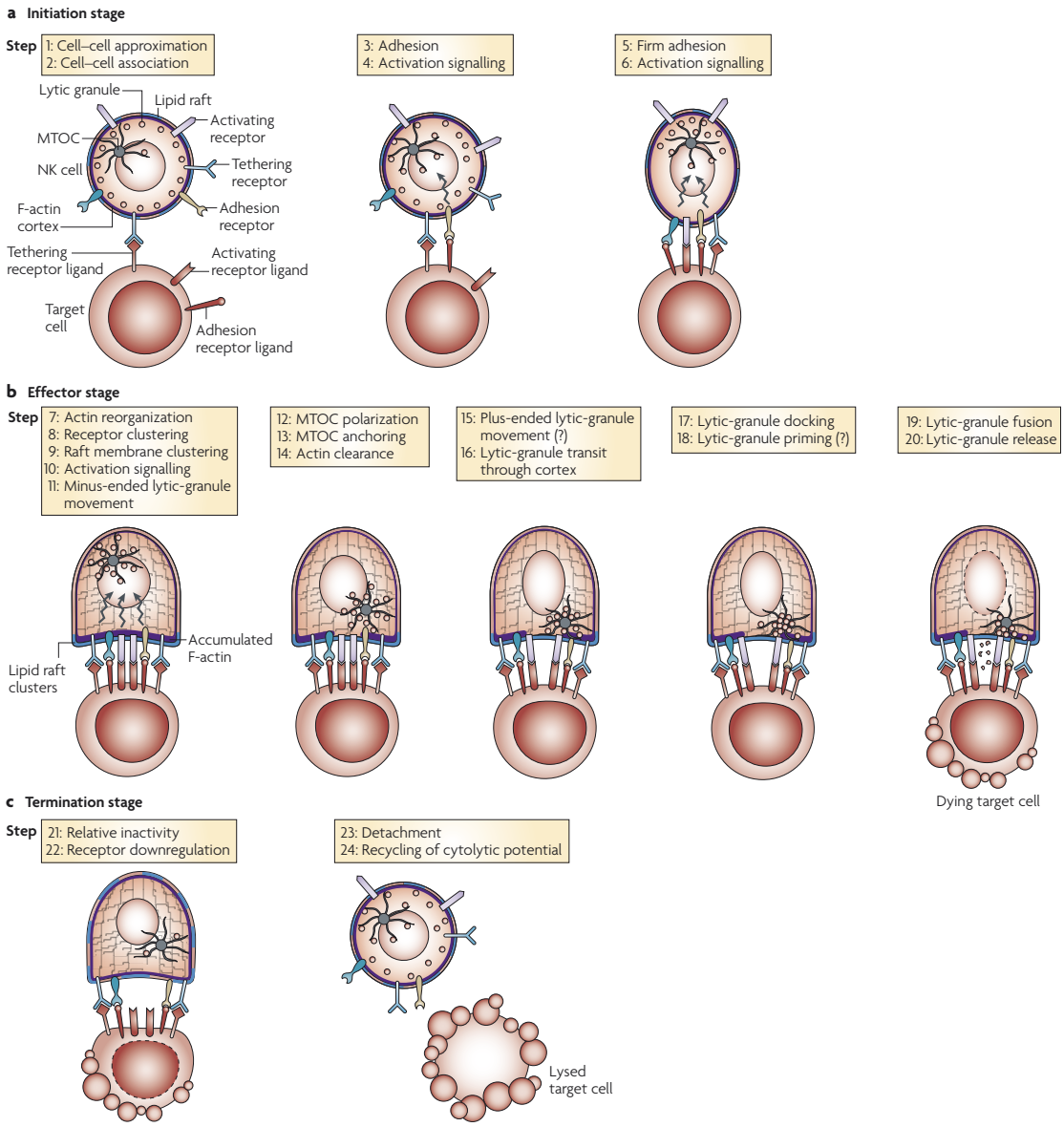

Fig. 1.1: Stages of the formation of the activating Natural Killer cell synapse. (Orange, 2008)

The initiation of the aNKIS formation

In the first tethering-like contact between NK and target cells adhesion molecules as integrins and selectins are bound initiating adhesion and signaling. Binding of the integrin lymphocyte function-associated antigen (LFA)-1 to intercellular adhesion molecules (ICAM)-1, -2 or -3 on the target cell is crucial for directed NK cell cytotoxicity (Bryceson et al., 2005). Subsequently, intracellular association of talin to LFA-1 is required for recruitment of vinculin, G-actin, and the actin polymerization machinery, including the actin nucleating protein complex Arp2/3 and Wiskott-Aldrich Syndrome-protein (WASp) (Mace et al., 2009; Mace et al., 2010; Ham et al., 2013).

Additionally, upon ICAM-1 binding, Src-mediated phosphorylation of Vav1 inducing the Vav1-Rac1 pathway is required to initiate actin cytoskeleton rearrangements (Riteau et al., 2003). Besides talin, availability of paxillin as well as activity of spleen tyrosine kinase (Syk), phospholipase C (PLC)-y and protein kinase C (PKC) were found to be essential for LFA-1-induced granule-polarization (March&Long, 2011). T cells require inside-out signals via activating receptors to induce conformational changes in LFA-1, that induce increased affinity and full function of the molecule. There are data suggesting that, although binding of activating receptors as 2B4 increases adhesion, LFA-1 can up-regulate its own adhesion by self-mediated inside-out signaling (Barber&Long, 2003; Hoffmann et al., 2011). However, co-stimulation of activating receptors is essential for the formation of a mature immunological synapse (Culley et al., 2009).

Subsequent to LFA-1 ligation, recruitment of activating receptors to the contact zone is induced enabling augmentation of activating interaction with the target cell. As shown in figure 1.2, NK cells express a vast variety of activating receptors which either signal on their own or associate with adaptor molecules as FcεR1γ-, TCRς-chains, DAP10 or DAP12 (Watzl&Long, 2010; Watzl&Urlaub, 2012; Koch et al., 2013; Long et al., 2013). The basis for activating signaling are either immunoreceptor tyrosine-based activation motifs (ITAMs) or other tyrosine-based activation motifs in the cytoplasmic tail of the receptor or the adaptor molecule. An overview of the induction of the main activating signaling pathways is shown in figure 1.3. In most cases triggering of a single receptor is not sufficient to induce activation. Instead co-stimulation of multiple receptors, occasionally in synergistic pairs, is required. The only known exception is Fc receptor FcγRIIIa (CD16), which can induce undirected degranulation after ligation in isolation (Bryceson et al., 2006).

The activating receptors NKp30, NKp44, NKp46 belong to the family of natural cytotoxicity receptors (NCRs). Although it is known that they play an important role in tumor surveillance, only a few ligands, mainly viral proteins, are discovered yet (Koch et al., 2013). NKp30 associates with CD3ς− and possibly FcεR1γ-chains and recognizes the tumor-associated antigens B7-H6 and BAT3 (Pende et al., 1999; Pogge von Strandmann et al., 2007; Brandt et al., 2009). In contrast to the

constitutively expressed NKp30 and NK46, NKp44 expression is induced during activation. It associates with DAP12 (Vitale et al., 1998). The proliferating cell nuclear antigen (PCNA) has been described as inhibitory cellular ligand for NKp44 (Rosental et al., 2011). In addition, NKp44L has recently been described as activating ligand that is expressed on a variety of tumor cell lines (Baychelier et al., 2013). NKp46 associates with the CD3ς- and FcεR1γ-chain (Vitale et al., 1998). No cellular ligand for NKp46 has been discovered yet. After ligation of the receptors the cytoplasmic ITAMs are phosphorylated by Src family kinases. This induces recruitment of spleen tyrosine kinase (Syk) and zeta chain-associated protein kinase (ZAP)-70 which in turn phosphorylate non-T cell activation linker (NTAL) and linker for the activation of T cells (LAT). Subsequently, these transmembrane adaptor molecules associate and activate signaling molecules as phosphatidylinositol 3-kinase (PI3K), phospholipase C (PLC) γ-1/-2 and members of the Vav family, which leads to induction Ca^{2+} flux, cytoskeleton rearrangements, cytotoxicity and cytokine release (Koch et al., 2013).

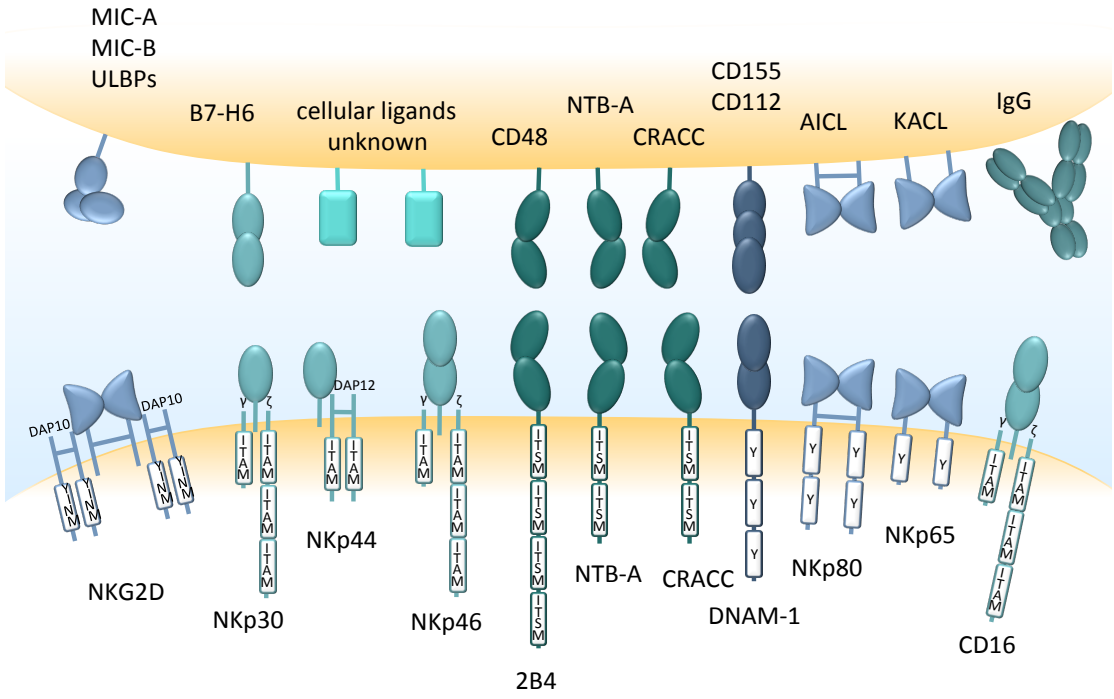

Fig. 1.2: Diversity of activating NK cell receptors. (Watzl&Urlaub, 2012)

On the contrary, NKG2D, NKp80 and SLAM family receptors signal via non-ITAM-based pathways (Watzl&Long, 2010; Long et al., 2013). C-type lectin like molecules, e.g. NKG2D and NKp80 are encoded in the Natural Killer gene complex (NKC) (Yokoyama&Plougastel, 2003). NKG2D binds to stress-induced ligands of MICA, MICB and ULBPs (López-Larrea et al., 2008). The receptor associates with DAP10, which contains a tyrosine-based signaling motif. Phosphorylated DAP10 binds PI3K or Grb2. Grb2 further interacts with Vav1. PI3K associated with DAP10 is

inducing signaling via other guanine nucleotide exchange factors (GEFs) and small GTPases, leading to adhesion, granule polarization and degranulation (Watzl&Long, 2010; Long et al., 2013). In contrast NKp80, which recognizes the activation-induced C-type lectin (AICL), signals independent of adaptor molecules since it contains an atypical hemi-ITAM in its cytoplasmic tail. However, the induced signaling pathway is not unraveled yet (Welte et al., 2006; Ruckrich&Steinle, 2013). A third group of well characterized activating receptors belong to the family of signaling lymphocytic activation molecule (SLAM) related receptors (SRR) (Veillette, 2006). NK cells express NTB-A, CRACC and 2B4 (Claus et al., 2008). All except for 2B4, which associates with CD48, display the characteristic homophilic binding. Their cytoplasmic part contains immunoreceptor tyrosine-based switch motifs (ITSMs). The ITSM in SLAM family receptors is associating with SLAM-associated protein (SAP) or Ewing's sarcoma-associated transcript (EAT)-2. SAP not only recruits Fyn, which phosphorylates Vav1 but also blocks binding of the inhibitory phosphatases SHIP-1, SHP-1 and SHP-2 (Watzl&Long, 2010). Signaling downstream of EAT-2 has not been resolved yet, although it is suggested to be activating. Another molecule of the SLAM receptor-family is CD2, which binds CD58 and in humans also weakly to CD48 (Selvaraj et al., 1987; Arulanandam et al., 1993). CD2 is recruited quickly the contact site after LFA-1 ligation (Orange et al., 2003) and was reported to be required for conjugate formation between NK92 and K562 cells (Zheng et al., 2009). Additionally, as also described for NKG2D, DNAM-1 and 2B4 it provides inside-out signals that increase LFA-1 affinity (Barber&Long, 2003; Bryceson et al., 2009). DNAM-1 does not belong to any of these families. It binds CD155 and nectin-2 and plays a role in LFA-1 mediated cellular adhesion (de Andrade et al., 2013). DNAM-1 does not associate with an ITAM-bearing adaptor molecule, but gets phosphorylated by PKC after receptor cross-linking. The phosphorylation is required for its association with LFA-1. Additionally, it was described that if CD2 is costimulated with 2B4 PLCγ-2 is activated (de Andrade et al., 2013).

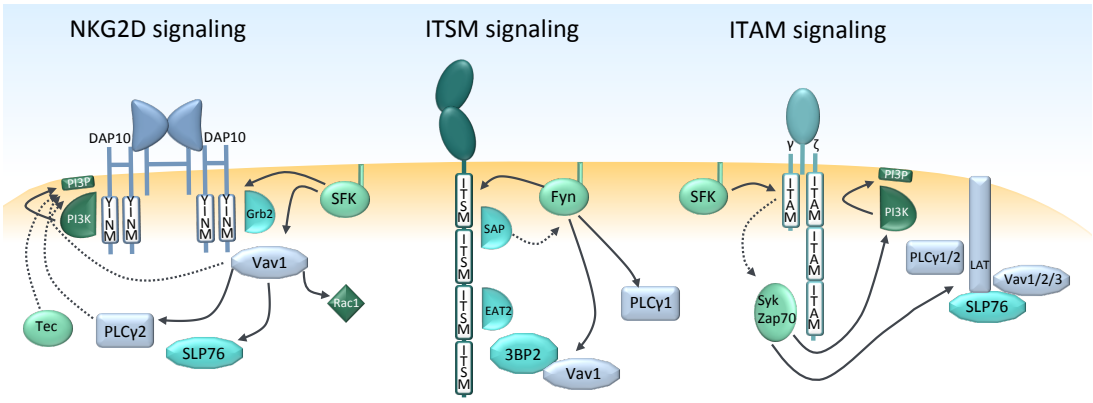

Fig. 1.3: Activating signaling pathways in human NK cells. (Watzl&Urlaub, 2012)

Signaling pathways induced by different activating receptors can be synergistic or redundant. But some molecules are indispensible for instance, Vav family members or PLCγ are required downstream of most activating receptors (Watzl&Long, 2010; Koch et al., 2013; Long et al., 2013).

As for T cells, organization of molecules at the NK cell synapse in supramolecular activation clusters (SMACs) was described (Orange, 2008; Dustin&Depoil, 2011). In T cells the clusters are further subdivided in the TCR-rich central (c) SMAC, the LFA-1-rich peripheral (p) SMAC and the distal (d) SMAC rich in F-actin (Dustin&Depoil, 2011). Granule secretion occurs through the pSMAC, to not disturb the activating receptor interactions in the cSMAC (Stinchcombe et al., 2001). In NK cells activating receptors, LFA-1 and F-actin accumulate in the pSMAC, whereas perforin was located in the cSMAC (Orange et al., 2003). However, the importance of the SMAC for cell function is still debated since it was found, that signaling events leading to activation also occur outside of the SMAC zones (Orange, 2008; Dustin, 2009).

The iNKIS – Prevention of cytotoxicity at early stages

Some data suggest that, in contrast to other lymphocytes, if the activating signaling in NK cells overcomes the inhibitory an "all-or-nothing response" is induced, that might not be tuned further (Lagrue et al., 2013). Therefore, inhibition of NK cells is an important mechanism to prevent false directed NK cell cytotoxicity. Protection of healthy cells is mediated via inhibition of NK cells by receptors of the Killer cell immunoglobulin-like receptor (KIR)-family, the immunoglobulin-like transcript (ILT) receptor family or the heterodimer NKG2A/CD94. All of these receptors contain immunoreceptor tyrosine-based inhibition motifs (ITMIs) in their cytoplasmic tail. Ligation by their cognate ligands induces phosphorylation of the ITIM leading to recruitment of the phosphatases SHP-1, -2 or SHIP-1 (Watzl&Long, 2010). SHP-1 inactivates Vav1 by dephosphorylation and thereby interrupts activating signaling at a very early and central point (Stebbins et al., 2003). In parallel to Vav1 inactivation, phosphorylation of Crk induces its dissociation from a signaling complex, which abrogates activating signaling (Peterson&Long, 2008). SHIP-1 reduces the phosphatidylinositol 3,4,5-trisphosphate (PIP3) level and thereby interferes with phosphatidyl-inositol-3-kinase (PI3K) induced signaling (Gumbleton&Kerr, 2013). There are evidences that inhibition can occur even earlier via restricting the increase of LFA-1 affinity or the recruitment of activating receptors to the contact site (Bryceson et al., 2006; Peterson&Long, 2008; Long et al., 2013). Additionally, clustering of inhibitory receptors at the contact zone was shown to prevent clustering of activating receptors and led to collapse of the actin cytoskeleton inducing retraction of the NK cell (Abeyweera et al., 2011).

Interestingly, the induced inhibition is locally restricted and does not induce general inhibition of the whole cell (Peterson&Long, 2008). Thereby non-susceptible bystander cells are protected if they are close enough to a susceptible target to allow simultaneous contact.

The effector stage of the aNKIS formation

If the activating signals are stronger than the inhibitory the formation of the aNKIS proceeds to the effector stage initiated by amplified activating signaling and induction of firm adhesion. The effector stage is characterized by actin reorganization, polarization of the degranulation machinery and release of cytotoxic granules towards the target cell.

Downstream of Vav1 activation, formation of F-actin is induced (Orange, 2008; Mace et al., 2009; Mace et al., 2010; Ham et al., 2013). A multiplicity of GEFs and GTPases, e.g. Cdc42, Rac1 and the recently discovered DOCK8 as well as a number of kinases, e.g. PIPKIγ and PKCθ are involved in this process (Krzewski et al., 2006; Sinai et al., 2010; Carlin et al., 2011; Mace et al., 2012; Ham et al., 2013). However, details of the signaling pathways are not completely resolved yet. The induced actin rearrangements facilitate receptor clustering, lipid-raft clustering and polarization of the whole cell and the lytic granules towards the target cell (Fassett et al., 2001; Orange, 2008; Lagrue et al., 2013). The accumulation of actin at the cell-cell-contact zone occurs within a few minutes and can persist for up to 30 min (Butler&Cooper, 2009).

In addition to actin rearrangements microtubule dynamics are vital for NK cell cytotoxicity since they facilitate lytic granule convergence to the microtubule-organizing center (MTOC) and the polarization to the contact zone (Katz et al., 1982; Lagrue et al., 2013). However, conjugation with the target cell was shown to occur independently of microtubules (Katz et al., 1982). The minus-end directed movement of the lytic granules to the MTOC does not require rearrangement of actin or microtubules, but is dependent on the motor-protein dynein and existing microtubules (Fig. 1.4 [1]) (Mentlik et al., 2010). It rapidly occurs after target cell contact, before the MTOC polarizes towards the IS and is a requirement for synapse maturation (Mentlik et al., 2010). Granule convergence induced by activating ligands or IL-2 requires Src kinases but no down-stream signaling (James et al., 2013) and is a prerequisite for polarization to the synapse (Katz et al., 1982; Stinchcombe et al., 2006; Banerjee et al., 2007; Mentlik et al., 2010). In contrast, in NK cells triggering of LFA-1 alone is sufficient to induce polarization of lytic granules (Barber et al., 2004; Bryceson et al., 2005; Hogg et al., 2011). Subsequent of granule convergence to the MTOC, both move towards the synapse. This process in contrast to granule convergence is depending on cytoskeletal rearrangements (Mace et al., 2014) and requires signaling events downstream of Src kinases (Bryceson et al., 2006). Activation of PI3K induces the MEK-ERK signaling pathway, but how ERK is involved in microtubule

reorganization is not clear (Jiang et al., 2000; Graham et al., 2006; Galandrini et al., 2013). Downstream of PI3K PLCγ hydrolyses phosphatidylinositol (4,5)-bisphosphate (PIP_2) to membrane bound diacylglycerol (DAG) and inositol 1,4,5-triphosphate (IP_3), which binds to receptors in the endoplasmatic reticulum (ER)-membrane inducing Ca^{2+} release, which is required for signaling and MTOC polarization (Bryceson et al., 2006; March&Long, 2011). Additionally, store-operated Ca^{2+} entry (SOCE) depending on ORAI1 and STIM1 is required for degranulation and cytotoxicity, but not for inside-out signals of LFA-1 or granule polarization (Maul-Pavicic et al., 2011). A variety of other molecules is involved in the movement of the MTOC/lytic granules to cell-cell contract site, e.g. Pyk2 (Gismondi et al., 1997; Sancho et al., 2000) or CIP4 (Banerjee et al., 2007). The transit of the lytic granules through the F-actin supposedly is mediated by the ATP-dependent motor protein myosin IIA (Andzelm et al., 2007; Sanborn et al., 2011). Recently it was shown, that lytic granules traverse through hypodense regions in the actin mesh at the synapse (Fig. 1.4 [2]) (Rak et al., 2011; Brown et al., 2011) and are highly motile at the IS (Mace et al., 2012).

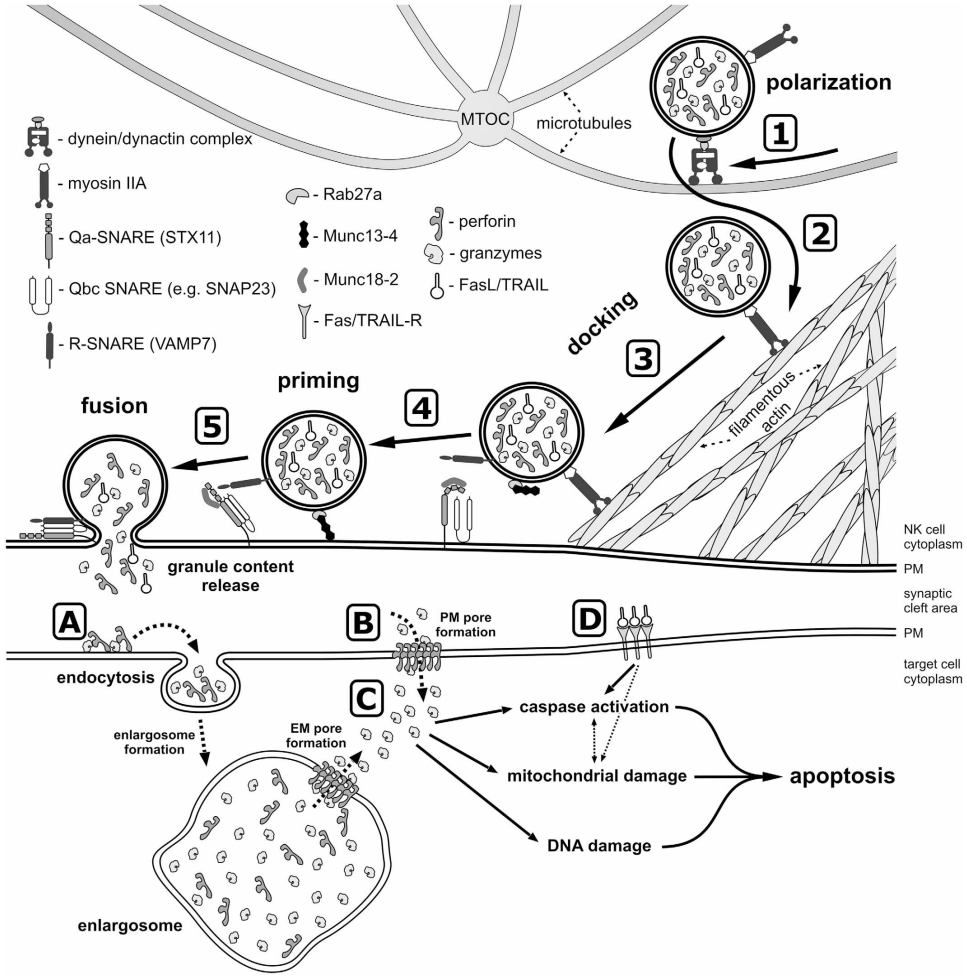

Fig. 1.4: Granule exocytosis in human NK cells and induction of apoptosis in the target cell. (Krzewski&Coligan, 2012)

Some activating receptors (e.g. NKp46 or CD2) need co-ligation of LFA-1 to induce this remodeling of cortical actin whereas others (e.g. CD16 or NKG2D) do not (Brown et al., 2012).

The docking of the granules at the plasma membrane involve SNARE proteins as Munc13-4, Syntaxin 11, Munc18-2 or VAMPs as well as the GTPase Rab27a (Fig. 1.4 [3&4]) (Casey et al., 2007; Cote et al., 2009; Wood et al., 2009; Liu et al., 2010; Elstak et al., 2011; Krzewski et al., 2011; Dabrazhynetskaya et al., 2012; Lopez et al., 2013). Additionally, Munc13-4 and Rab27a have been described to facilitate the final maturation of lytic granules before degranulation (Ménager et al., 2007). Two distinct modes of granule fusion with the plasma membrane have been described (Fig. 1.4 [5]). Complete fusion leads to release of the entire content whereas during incomplete fusion the content is only partly released (Liu et al., 2011). Following degranulation recycling of vesicles and cytotoxic molecules via endocytosis was described as energy saving mechanism in NK cell cytotoxicity (Liu et al., 2009; Li et al., 2011; Capuano et al., 2012). The endosomes were shown to polarize towards to MTOC (Stinchcombe et al., 2011). Additionally, re-internalization of Munc13-4 was observed and proposed to be required for serial killing (Capuano et al., 2012). Recently, two independent studies showed that an NK cell could deliver multiple lytic hits towards the same target cell (Lopez et al., 2013; Vanherberghen et al., 2013). This might be facilitated by lytic granules that arrive consecutively at the synapse (Vanherberghen et al., 2013).

The termination stage of the aNKIS formation

The termination stage of the aNKIS is characterized by the induction of apoptosis in the target cells and the detachment of the NK cell from the target cell.

Lytic granules are a complex structure containing a variety of molecules as enzymes and lytic proteins. Granzymes, perforin and granulysin are the most studied effector molecules. The granules show a particular way of packaging these molecules to minimize their activity (Metkar et al., 2002). The characteristic acidic intra-luminal pH of lytic granules is established by the membrane-bound vacuolar H^+-ATPase (Mellman et al., 1986). On one hand, the low pH enables activity of proteolytic enzymes required for perforin maturation (Voskoboinik et al., 2010). On the other hand, the low pH renders perforin unable to interact with calcium ions required for its activity (Voskoboinik et al., 2005). Additionally it was shown that under this condition perforin forms complexes with the proteoglycan serglycin, which allows packaging that renders the molecules inactive. However, the requirement of serglycin for self-protection is debated (Voskoboinik et al., 2010). Perforin is generated as a 70 kDa immature precursor in the ER. Maturation by the cleavage of a C-terminal signaling sequence by cathepsin L occurs in the lytic granules (Uellner et al., 1997; Konjar et al., 2010). Granzyme A and B are the most abundant members of the granzyme family found in human NK cells (Lieberman, 2003).

They are transported to the lytic granules as pro-enzymes and are processed by cathepsin C and H to the active form, which also form a complex with serglycin for tight packaging (Krzewski&Coligan, 2012). During degranulation the cytotoxic molecules are released into the synaptic cleft. The neutral pH leads to release of perforin from serglycin and its activation. Subsequently, perforin binds to the target cell membrane in a Ca^{2+}-dependent manner and forms pores by oligomerization (Fig. 1.3 [B]) (Baran et al., 2009). Interestingly, the NK cell is not affected by the released perforin (Lopez et al., 2013). Cleavage of perforin by surface cathepsin B or coverage of the NK cell membrane by CD107a after degranulation are discussed as possible mechanisms that protect the NK cells (Balaji et al., 2002; Cohnen et al., 2013). The perforin pore-formation is a prerequisite for granzyme entry into the target cell (Keefe et al., 2005; Thiery et al., 2011). There are different mechanisms debated for granzyme uptake. Originally it was postulated that the perforin-pores allow diffusion of granzyme from the synaptic cleft into the target cell cytoplasm. More recently, data suggest that granzyme is released into the target cell cytoplasm from endosomes in a perforin-dependent way. Endocytosis was described to be initiated either as membrane repair response or by binding of the perforin-serglycin-granzyme macromolecular complex to Mannose 6-phosphate receptors or to be clathrin-mediated (Fig. 1.4 [A]) (Krzewski&Coligan, 2012). Once in the cytoplasm, the highly specific serine proteases induce caspase-dependent and –independent apoptosis (Fig. 1.4 [C]). Granzyme B cleaves caspase 3 and other caspases leading to induction of the caspase cascade. By cleavage of BH3-interactin domain death agonist (BID), granzyme B induces damage of the mitochondrial outer membrane, leading to release of pro-apoptotic molecules into the cytoplasm (Wowk&Trapani, 2004). Additionally, it also targets the mitochondrial membrane directly without the necessity of cytosolic mediators (Lieberman, 2003).

There are studies describing the formation of nanotubes between the target and the detaching NK cell (Onfelt et al., 2004; Roda-Navarro et al., 2004; Chauveau et al., 2010; Comerci et al., 2012). Several functional properties have been proposed for these long thin “closed-ended connections” between NK and target cells (Davis, 2009). Chauveau and colleagues found a correlation between nanotube formation and target cell lysis (Chauveau et al., 2010). Additionally, accumulation of receptors and signaling molecules in nanotubes and the transmission of intercellular calcium fluxes were described (Davis, 2009). Furthermore, a recent study found that certain receptor-ligand pairs could promote nanotube formation (Comerci et al., 2012). Recent advances in microscopy leading to increased resolution might facilitate new insights in the importance of nanotubes for NK cell function.

1.3 NK cells are serial killers

A strategy of NK cells and also cytotoxic T lymphocytes (CTLs) to augment their cytotoxic potential is the ability to lyse multiple targets, a mechanism named "serial killing". It was described first for T cells in 1975 by Zagury and colleagues (Zagury et al., 1975) and later in 1981 for NK cells as well (Ullberg&Jondal, 1981). Originally the potential to lyse multiple targets was observed in cytotoxicity assays, where only the amount of specific lysis compared to the E:T ratio allowed conclusions about the average number of targets that could be killed by one effector (Zagury et al., 1975; Ullberg&Jondal, 1981). In later studies, time-lapse microscopy allowed live cell imaging and thereby the pursuit of individual cells over an extended period of time (Sanderson, 1976; Rothstein et al., 1978; Bhat&Watzl, 2007; Choi&Mitchison, 2013; Vanherberghen et al., 2013). Recent data suggests, that individual NK cells can kill up to 14 targets consecutively (Bhat&Watzl, 2007; Choi&Mitchison, 2013; Vanherberghen et al., 2013). But this differs strongly between individual cells, since most NK cells kill less or not at all (Choi&Mitchison, 2013; Vanherberghen et al., 2013). Supporting these observations, Tomescu and colleagues showed that a recently degranulated NK cell is as effective in killing as one that did not degranulate before (Tomescu et al., 2009). Recycling mechanisms described above for lytic proteins, membrane parts and molecules involved in degranulation, as well as studies that indicate rapid *de novo* formation of lytic granules after target cell recognition would support this finding (Liu et al., 2005; Liu et al., 2009; Li et al., 2011; Liu et al., 2011; Capuano et al., 2012). However, earlier studies describe exhaustion and induction of apoptosis induced by target cells (Bajpai&Brahmi, 1994; Yamauchi et al., 1996; Taga et al., 1999; Poggi et al., 2005; Warren, 2011).
Choi and Mitchison recently discovered that in sequential killing events, the first kill was slower than the following ones. This would suggest that in addition to an increased number of killed targets the speed of action is augmented by serial killing. They hypothesized that this is due to integration of the signals from the previous and the current target. Therefore, maintaining the contact with the previous target until the encounter of a new target keeps the NK cell in an activated status, a mechanism they termed "kinetic priming". This could be facilitated by simultaneous contact with multiple targets, which was described (Bhat&Watzl, 2007; Choi&Mitchison, 2013; Lopez et al., 2013). Although quick consecutive killing events were observed, so far no evidence indicates, that NK cells could kill multiple targets simultaneously, which was described for T cells (Wiedemann et al., 2006; Lopez et al., 2013). Understanding and inducing the ability for serial killing could expand the perspective of NK and T cell in therapeutic applications, e.g. in cancer treatment. First evidences indicate that bispecific antibodies can reinforce serial killing (Hoffmann et al., 2005; Bhat&Watzl, 2007).

To facilitate serial killing as such, the NK cell needs to disengage from the previous target to functionally interact with a new one. The synapse breakage and detachment of the NK from the target

cell has not yet been studied in detail. Recently, there were a few indications as to when the detachment occurs in relation to the target cell death. Vanherberghen and colleagues (2013) analyzed NK cell target cell interaction at the single cell level. They observed that fast target cell death induced by a strong cytotoxic response led to shorter contacts compared to conjugates with slow target cell death. Therefore, they propose that the duration of the contact depends on viability and membrane integrity of the target cell. Additionally, they observed that the NK cells remained attached after breakage of the synapse and hypothesize that these two mechanisms are independently regulated.

2. Aim of the thesis

For efficient augmentation of NK cell-mediated cytotoxicity by serial killing, the detachment process plays a pivotal role. However, only little is known about what exactly induces detachment of NK cells from target cells or which events are involved. Since research on events following the lytic hit was just emerging, no verified assay systems were available. Therefore, the first objective of the study was to establish assay systems that allow investigation of the decay of NK:target cell-conjugates. With these tools, we aimed to better characterize the phenotype of detached NK cells and to illuminate events that are possibly involved in the detachment process. For that purpose we used inhibitors targeting various steps that are known to be indispensible for NK cell cytotoxicity.

By investigating these diverse aspects possibly involved in detachment, the aim of this study was to gain a better understanding of this last step in cytolytic NK:target cell interactions.

3. Materials and Methods

3.1 Materials

3.1.1 Antibodies

Goat monoclonal antibodies

Name (clone)	Conjugate	Source, Reference
anti-PKCθ (C19)	--	Santa Cruz Biotechnology, Heidelberg, Deutschland

Mouse monoclonal antibodies

Name (clone)	Conjugate	Source, Reference
IgG control (MOPC-21)	PE, FITC	Biolegend, San Diego, CA, US
IgG control (MOPC-21)	--	Sigma-Aldrich, St. Louis, MO, US
IgG control (MOPC-31C)	Pe/Cy5	BD Biosciences, San Jose, CA, US
anti-2B4 (C1.7)	--	(Valiante&Trinchieri, 1993)
anti-2B4 (C1.7)	FITC, PE	Biolegend, San Diego, CA, US
anti-CD3 (HIT3a)	PE	Biolegend, San Diego, CA, US
anti-CD11a (HI111)	PE/Cy5	Biolegend, San Diego, CA, US
anti-CD16 (3G8)	PE	Biolegend, San Diego, CA, US
anti-CD56 (MEM-188)	FITC, PE	Biolegend, San Diego, CA, US
anti-CD69 (FN50)	PE	Biolegend, San Diego, CA, US
anti-CD158a (EB6)	PE	Beckman Coulter, Krefeld, Germany
anti-CD158b1/b2 (GL183)	PE	Beckman Coulter, Krefeld, Germany
anti-DNAM1 (DX11)	PE	BD Biosciences, San Jose, CA, US
anti-LAMP1 (H4A3)	FITC, APC	Biolegend, San Diego, CA, US
anti-LAMP1 (H4A3)	PE/Cy5	BD Biosciences, San Jose, CA, US
anti-NKG2A (Z199)	PE	Beckman Coulter, Krefeld, Germany
anti-NKG2C (134591)	PE	R&D, Minneapolis, MN, USA
anti-NKG2D (149810)	--	R&D Systems, Minneapolis, MN USA
anti-NKG2D (1D11)	PE	Biolegend, San Diego, CA, US
anti-NKp30 (p30-15)	PE	Biolegend, San Diego, CA, US
anti-NKp44 (P44-8)	PE	Biolegend, San Diego, CA, US
anti-NKp46 (9E2)	PE	Biolegend, San Diego, CA, US
anti-human perforin (dG9)	FITC	Biolegend, San Diego, CA, US
anti-human perforin (Pf-344)	--	Mabtech, Hamburg, Germany
anti-phospho-tyrosine (4G10)	biotin	Millipore, Temecula, CA, US

Rabbit polyclonal antibodies

Name	Conjugate	Source, Reference
anti-actin	--	Sigma-Aldrich, St. Louis, MO, US
anti-PKCα	--	Cell Signaling Technology, Danvers, MA, US

Secondary antibodies

Name	Conjugate	Source, Reference
donkey-anti-goat IgG (H+L)	HRPO	Jackson ImmunoResearch Laboratories/ Dianova, Hamburg, Germany
goat-anti-mouse IgG (H+L)	HRPO	Jackson ImmunoResearch Laboratories/ Dianova, Hamburg, Germany
goat-anti-rabbit IgG (H+L)	HRPO	Jackson ImmunoResearch Laboratories/ Dianova, Hamburg, Germany

3.1.2 Buffers

2.5 x NRSB (non-reducing sample buffer):	5 % (w/v)	SDS
	25 % (v/v)	Glycerol
	0.05 % (w/v)	Bromphenol Blue
	0.156 mM	Tris-HCl, pH = 6.8
5 x RSB (reducing sample buffer):	10 % (w/v)	SDS
	50 % (v/v)	Glycerol
	25 % (v/v)	2-Mercaptoethanol
	0.1 % (w/v)	Bromphenol Blue
	0.3125 mM	Tris-HCl, pH = 6.8
4 % paraformaldehyde	32 g	Paraformaldehyde, powder
	80 mL	10 x PBS
	ad 800 mL	ddH_2O
	Water was heated to 60 °C using a hot plate with stirring. After adding PFA powder, the solution was covered and maintained at 60 °C. NaOH was added and the stirring continued until the solution became clear. 10 x PBS was added and the pH adjusted to 7.2 using HCl. After filtration the PFA was kept on ice to cool down, aliquoted and stored at -20 °C	
Annexin V-binding buffer (10 x)	0.1 M	Hepes
	25 mM	$CaCl_2$
	1.4 M	NaCl
FACS-buffer	1 x	DPBS (Life Technologies)
	2 % (v/v)	fetal calf serum
PBS (10x)	1.37 M	NaCl
	27 mM	KCl
	100 mM	$NaH_2PO_4 \times 2H_2O$
	18 mM	KH_2PO_4

PBST/NaCl:	1 x 0.05 % (v/v) 0.5 M	PBS Tween 20 NaCl
MOPS buffer 20x (Invitrogen)		
Triton X-100 lysis buffer:	150 mM 20 mM 10 % (v/v) 0.5 % (v/v) 2 mM 10 mM 1 mM 1 mM	NaCl Tris-HCl, pH 7.4 Glycerol Triton X-100 EDTA NaF PMSF Na-orthovanadate
Western blot transfer buffer:	24 mM 129 mM 20 % (v/v)	Tris Glycin MeOH

3.1.3 Eukaryotic cells

Culture media, fetal calf serum (FCS), non-essential amino acids and sodium pyruvate were purchased from Gibco (Invitrogen/LifeTechnologies, Darmstadt, Germany); human serum from PromoCell (Heidelberg, Germany) and purified human interleukin (IL)-2 from the NIH Cytokine Repository (Bethesda, MD, US). If not indicated otherwise, all media were supplemented with 10 % (v/v) FCS and 1 % (v/v) penicillin/streptomycin (Gibco/Invitrogen/LifeTechnologies, Darmstadt, Germany). Vericyte medium was obtained from Medicyte (Heidelberg, Germany).

Name	Cell type	Culture medium
721.221	Human EBV-transfected B cell line	IMDM
HeLa	Human cervical cancer cell line	DMEM
HeLa-CD48	Human cervical cancer cell line, stably transfected with human CD48	DMEM + 1 µg/mL puromycin
JY	Human EBV-transfected B cell line	RPMI 1640, 10 % FCS, 1 % P/S, 0,1 % 2-mercaptoethanol
K562	Human erythroleukemic cell line	IMDM
Primary human NK cells	Isolated from peripheral blood mononuclear cells (PBMCs) by negative selection	IMDM, 10 % (v/v) human serum, 1 % (v/v) non-essential amino acids, 1 % (v/v) sodium pyruvate, 100 IU/ml IL-2 Vericyte medium

3.1.4 Inhibitors

Name	Target	Source
PD98059	MAPK pathway	Cayman Chemical, Ann Arbor, MI, US
PP1	Src-family tyrosine kinases	Biomol, Hamburg, Germany
Syk Inhibitor IV	SYK	Calbiochem/Merck Millipore, Billerica, MA, US
U73122	PLC	Biomol, Hamburg, Germany
U73343	Inactive analog of U73122	Biomol, Hamburg, Germany
Wortmannin	PI3K	Biomol, Hamburg, Germany
Concanamycin A	V-H^+-ATPase	Sigma-Aldrich, St. Louis, MO, US
Bafilomycin A1	V-H^+-ATPase	BioViotica, Göttingen, Germany
(+)-/(-)-Blebbistatin	Myosin IIA	Cayman Chemical, Ann Arbor, MI, US
GM6001 (Ilomastat)	Collagenase (MMP)	US Biological, Swampscott, MA, US
Batimastat	MMPs	Calbiochem/Merck Millipore, Billerica, MA, US
Piceatannol	Syk family kinases	Cayman Chemical, Ann Arbor, MI, US
Cytochalasin D	Disruption of F-actin filaments	US Biological, Swampscott, MA, US
Jasplakinolide	Induces actin polymerization	Enzo Life Sciences, Lörrach, Germany
Nocodazole	Promotes tubulin depolymerization	Calbiochem/Merck Millipore, Billerica, MA, US
Paclitaxel	Promotes assembly of microtubules, prevents microtubule depolymerization	Cell Signaling Technology, Danvers, MA, US
Calyculin A	PP2A, PP1	Calbiochem/Merck Millipore, Billerica, MA, US
Okadaic Acid	PP1, PP2A, PP3	Cayman Chemical, Ann Arbor, MI, US
AEB071 (Sotrastaurin)	Protein kinase C (PKC)	Axon Medchem, Groningen, Netherlands
PKCθ pseudosubstrate inhibitor, myristoylated	PKCθ	Calbiochem/Merck Millipore, Billerica, MA, US
U0126	MEK1/2	Cayman Chemical, Ann Arbor, MI, US
SB202190	p38 MAP kinase	Biomol, Hamburg, Germany
Sodium azide	Mitochondrial oxidative phosphorylation	Carl Roth, Karlsruhe, Germany
Cycloheximide	Inhibits protein synthesis in eukaryotes (translocation step)	Sigma-Aldrich, St. Louis, MO, US
(S)-MG132	Proteasome, inhibits NFκB activation	Cayman Chemical, Ann Arbor, MI, US

3.1.5 Kits

Name	Source
ATPlite – Luminescence ATP Detection Assay System	PerkinElmer, Rodgau, Germany
Dynabeads Untouched human NK cell Kit	Invitrogen/LifeTechnologies, Darmstadt, Germany
P3 primary cell 4D Nucleofector X Kit L	Lonza, Cologne, Germany
PKH26 Red Fluorescent Cell Linker Kit for General Cell Membrane Labeling	Sigma-Aldrich, St. Louis, MO, US
PKH67 Green Fluorescent Cell Linker Kit for General Cell Membrane Labeling	Sigma-Aldrich, St. Louis, MO, US

3.1.6 Plasmids

Name	Source
pBABEplus-CD48	Hoffmann et al., 2011

3.1.7 Reagents

Most reagents were purchased from Carl Roth (Karlsruhe, Germany), Sigma-Aldrich (Seelze, Germany), Merck/ Millipore (Darmstadt, Germany) and AppliChem (Darmstadt, Germany).

Name	Source
Albumin Fraction V	Carl Roth, Karlsruhe, Germany
Annexin V-PE/Annexin V-FITC	BD Biosciences, San Jose, CA, US
BD FACS Permeabilizing Solution 2	BD Biosciences, San Jose, CA, US
CellTracker Violet BMQC	Molecular Probes/LifeTechnologies, Darmstadt, Germany
Clear blue X ray films, CL-Xposure	Pierce/Thermo Fisher Scientific, Rockford, IL, US
Chromium-51	Hartmann Analytic, Braunschweig, Germany
Immobilon-P-PVDF membrane	EMD Millipore Corporation, Billerica, MA, US
Ionomycin	Calbiochem/Merck Millipore, Billerica, MA, US
Lymphocyte Separation Medium (LSM) 1077	PAA Laboratories, Cölbe, Germany
Monensin	Sigma-Aldrich, St. Louis, MO, US
Non-fat dry milk powder	Saliter, Obergünzburg, Germany
NuPAGE Gels	Invitrogen/LifeTechnologies, Darmstadt, Germany
Paraformaldehyde	Sigma-Aldrich, St. Louis, MO, US
Precision Plus Protein™ All Blue Standards	Bio-Rad Laboratories, Munich, Germany
Phorbol 12-myristate 13-acetate (PMA)	Sigma-Aldrich, St. Louis, MO, US
Puromycin	Calbiochem/Merck Millipore, Billerica, MA, US
Recombinant human interleukin (IL)-15	PAN Biotech, Aidenbach, Germany
SuperSignal West Pico and Dura Substrate	Pierce/Thermo Fisher Scientific, Rockford, IL, US

Name	Source
Tecin (recombinant human interleukin (IL)-2)	NIH Cytokine Repository
WesternBright Sirius HRPO substrate	Advansta, Menlo Park, CA, US

3.1.8 siRNAs

All siRNAs were purchased from Dharmacon/Thermo Fisher Scientific (Rockford, IL, US). They were resuspended to 20 µM in ddH_2O according to the manufacturers protocol. After determination of the concentration using a NanoDrop 2000 spectrometer (Thermo Fisher Scientific, Rockford, IL US), the RNA was aliquoted and stored at -20 °C.

Name	Target	Sequence
Control siRNA (non-targeting siRNA #1)		not available
siRNA PKRCQ (ON-TARGET plus, #09)	human PKCθ	GCUCGCUGCUUAAGAGAUA
siRNA PKRCQ (ON-TARGET plus, #10)	human PKCθ	CCACACAGAUUUAAAGUCU
siRNA PKRCQ (ON-TARGET plus, #11)	human PKCθ	GCAAUUCACAAGAAGUGUA
siRNA PKRCQ (ON-TARGET plus, #12)	human PKCθ	CCACAAGGAGAGAUUCAAA
siRNA PRF1 (ON-TARGET plus, #06)	human perforin 1	UGGAAGGGCUCACGGACAA
siRNA PRF1 (ON-TARGET plus, #07)	human perforin 1	GGUCAGUGCGGCUGGAUUU
siRNA PRF1 (ON-TARGET plus, #08)	human perforin 1	CUACAGUUUCCAUGUGGUA
siRNA PRF1 (ON-TARGET plus, #09)	human perforin 1	GGCCAUCACACCUCCAUUA

3.1.9 Flow chamber system

Name	Source
Cover glasses	Paul Marienfeld GmbH & Co. KG, Lauda-Königshofen, Germany
Microscope slides	Paul Marienfeld GmbH & Co. KG, Lauda-Königshofen, Germany
Discofix® 3-way Stopcock	B. Braun Melsungen AG, Melsungen, Germany
Female/male connectors	Ibidi GmbH, Martinsried, Germany
µ-Slide VI 0.4	Ibidi GmbH, Martinsried, Germany
Silicone Tubing 1.6 mm ID	Ibidi GmbH, Martinsried, Germany
Y Tube Fitting 1.6 mm	Ibidi GmbH, Martinsried, Germany
Syringe (luer; 50 mL and 2 mL)	B. Braun Melsungen AG, Melsungen, Germany
Perfusor secura FT	B. Braun Melsungen AG, Melsungen, Germany

3.2 Methods

3.2.1 Cellular biology

Cell culture

All cells were grown at 37 °C and 5 % CO_2 in a humidified incubator under sterile conditions. Cell lines were split on a regular basis every two to three days. Cell culture flasks were exchanged every two weeks. Cells were frozen in FCS containing 10 % DMSO at -75 °C and stored in liquid nitrogen. Cell lines were thawed on a regular basis. FCS, donor horse serum and human serum were heat inactivated by incubation at 56 °C for 30 min prior to use.

NK cell isolation

Peripheral blood mononuclear cells (PBMC) were isolated from whole blood via density centrifugation over LSM solution. NK cells were purified from PBMC using a NK cell negative selection kit (Invitrogen) according to the manufacturers protocol. The purity was controlled using flow cytometry. 90 to 99 % of the cells were $CD3^-$ $CD56^+$ $NKp46^+$.

NK cell culture with feeder cells

Isolated NK cells were resuspended in culture medium supplemented with 5 ng/mL recombinant human IL-15 and 200 IU/mL recombinant human IL-2, mixed with irradiated (30 Grey) JY feeder cells ($5x10^5$ cells/mL) and plated in 96-U-well plates at densities ranging from $1x10^6$ to $2x10^6$ cells/mL. This step was repeated after seven days of culture. Growing cultures were expanded 1:1 in culture medium. Cells were used for experiments two to five weeks after isolation.

NK cell culture in Vericyte medium

Purified NK cells were cultured in Vericyte medium (Medicyte) according to the manufacturers protocol. Briefly, they were seeded at $1x10^6$ cells/mL in 96-U-well plates. Medium was exchanged three days after purification and subsequently split to $1x10^6$ cells/mL if the density exceeded $2x10^6$ cells/mL. Otherwise the medium was exchanged latest after seven days. For experiments cells were used between two and five weeks after purification.

Inhibitor pre-treatment

Where indicated, NK cells or target cells where pre-treated with inhibitors at $5x10^5$ to $1x10^6$ cells/mL in culture medium at 37 °C/5 % CO_2 for 30 to 60 min. The inhibitors were present in the assay in the indicated concentrations. For experiments with concanamycin A and bafilomycin A1 NK cells were

pre-treated for 3 h at 37 °C/5 % CO_2. The cells were washed in medium before application in the experiments. These inhibitors were not present during the assays.

Cell lysis

Pelleted cells were resuspended in ice-cold 0.5 % triton X-100 lysis buffer at a density of $2x10^7$ cells/mL and incubated on ice for 20 min. The lysates were clarified by centrifugation at 20,000 x g/4 °C for at least 15 min, transferred to fresh tubes and stored at -20 °C.

Chromium-release assay

To determine the cytotoxic capacity of NK cells, ^{51}Cr-release assays were performed in 96-U-well plates. In assays with titrations of inhibitors (log2), human primary IL-2 activated NK cells were used at an E:T 5:1 or 4:1. In assays where inhibitor concentrations were kept constant the E:T was titrated (log2) starting at 20:1, 10:1 or 5:1. Target cells grown to mid-log phase were labeled at $5x10^5$ in 100 µL medium with 100 µCi ^{51}Cr (3.7 MBq) for 1 h at 37 °C. Subsequently, cells were washed twice and resuspended to $5x10^4$/mL in medium. 5,000 cells/well were used in all assays. Spontaneous release was measured using target cells incubated in medium alone. The maximum release was determined by incubating the target cells in 1 % triton X-100 during the time of the assay. In assays with inhibitor present, background toxicity by the treatment was controlled by incubating target cells in the highest concentration of the inhibitor, as well as the respective solvent control without NK cells. All samples were done in triplicates. Plates were incubated for 4 h at 37 °C, 5 % CO_2. Supernatant was harvested and ^{51}Cr release was measured in a WIZARD^2 Automatic Gamma Counter (PerkinElmer, Rodgau, Germany). Percent specific lysis was calculated as $\left[\frac{(\text{experimental release} - \text{spontaneous release})}{(\text{maximum release} - \text{spontaneous release})}\right]$ x 100.

Flow cytometry

Cell staining for flow cytometry

Cell staining was performed in 96-V-well plates. $1x10^5$ to $2x10^5$ cells were resuspended in 50 µL cold fluorescence-activated cell sorting (FACS)-buffer. The respective amount of fluorophore-conjugated antibody was added and the samples were incubated for 20 min on ice. After washing, the cells were resuspended in FACS-buffer and analyzed on a BD FACSCalibur. Results were evaluated using the FlowJo software from Tree Star Inc.

Cell viability assay

Cell viability assays were performed in 96-V-well plates. 50,000 cells were resuspended in 25 µL 1 x annexin-V binding buffer. 1.25 µL/sample annexin-V were added and the cells incubated for 15 min in the dark at room temperature. As positive control 0.2 µL 2 % triton X-100 was added to the

reaction. The staining reaction was stopped by addition of 200 µL cold 1 x annexin-V binding buffer per sample and placement on ice. The amount of annexin V^+ cells was determined immediately using the FACSCalibur. The increase in Annexin V^+ staining compared to untreated cells was evaluated using the FlowJo software from Tree Star Inc. According to background fluorescence of various inhibitors, either FITC- or PE-conjugated annexin V was used.

Degranulation assay (Alter et al., 2004)

Degranulation assays were performed in 96-V-well plates. Target cells were grown to mid-log-phase. $5x10^4$ human primary IL-2-activated NK cells were mixed with $1x10^5$ target cells at a final volume of 100 µL Medium? PBS?. Where mentioned, inhibitors or respective solvent controls were added to the reaction. 1.25 µL anti-LAMP1 or IgG control were added to the samples. Depending on the auto-fluorescence of the applied inhibitors, FITC- or PE/Cy5-conjugates antibodies were used. As positive control for degranulation NK cells were treated with 1 µg/mL ionomycin and 10 nM PMA. Samples were centrifuged at 20 x g/room temperature for 2 min and incubated for 2 h to 4 h at 37 °C/5 % CO_2. The cells were centrifuged at 400 x g/4 °C for 5 min, resuspended in 50 µL FACS-buffer per reaction and stained for 20 min on ice with either CD56-PE or IgG-PE. After washing, the samples were resuspended in cold FACS-buffer, kept on ice and analyzed immediately using a FACSCalibur. The amount of $CD107a^+$ cells of the $CD56^+$ NK cell population was evaluated using the FlowJo software from Tree Star Inc. NK cells incubated without targets cells were used to determine spontaneous and inhibitor-induced degranulation.

Cell labeling for flow cytometry-based conjugation and detachment assays

For all conjugation and detachment assays, cells were labeled with PKH Fluorescent Cell Linker Kits for General Cell Membrane Labeling (Sigma-Aldrich) according to the manufacturers protocol with minor changes. Cells were washed twice in PBS and resuspended to $1x10^7$ cells/mL in diluent C. An equal volume of $2x10^{-6}$ to $4x10^{-6}$ M dye working solution in diluent C was added and the samples incubated for 5 min at room temperature. The reaction was stopped by addition of an equal amount of fetal calf serum and incubation for 1 min. The samples were washed three times in culture medium and incubated at $6x10^5$ to $8x10^5$ cells/mL at 37 °C/5 % CO_2. Prior to use cells were counted, washed and resuspended to the required density.

For some assays target cells were labeled with CellTracker Violet BMCQ (Molecular Probes) according to the manufacturers protocol with a final dye concentration of 5 µM. Briefly, cells were resuspended at $1x10^6$ to $1x10^5$ cells/mL in pre-warmed staining solution (CellTracker Violet diluted in IMDM without any supplements) and incubated at 37 °C for 30 min. Subsequently, cells were

washed and incubated for another 30 min in pre-warmed IMDM without supplements, washed once and applied in assays.

Flow cytometry-based conjugation assay (based on (Burshtyn, 2010))

Conjugation assays were performed in 1.5 mL tubes. To distinguish the cell populations, effector cells were usually labeled with PKH26 Fluorescent Cell Linker and target cells with PKH67 Fluorescent Cell Linker. $5x10^4$ human primary IL-2-activated NK cells were mixed with $1x10^5$ target cells at a final volume of 100 µL medium, centrifuged at 20 x g/room temperature for 1 min and incubated at 37 °C. The reaction was stopped at various time points between 0 to 60 min by vortexing and addition of 100 µL 4 % paraformaldehyde. The samples were kept on ice and analyzed immediately using the BD FACSCalibur. The amount of NK cells engaged in conjugates compared to the total amount of NK cells was evaluated using the FlowJo software from Tree Star Inc.

Conjugate decay assay with non-adherent target cells (based on (Culley et al., 2009))

To distinguish the cell populations, effector cells were usually labeled with PKH26 Fluorescent Cell Linker and target cells with PKH67 Fluorescent Cell Linker. $5x10^5$/mL NK and $1x10^6$/mL target cells in assay medium (IMDM, 10 % FCS, 1 % penicillin/streptomycin) were mixed, centrifuged at 20 x g/room temperature for 3 min and transferred to 37 °C for 30 min (pre-coincubation period). Pre-coincubated mixed cells were diluted 1:25 in assay medium and aliquoted. The samples were incubated rotating at 37 °C. The reactions were stopped after 0, 10, 20, 40, 60 and 90 min by vortexing and addition of an equal amount 4 % paraformaldehyde. After incubation at room temperature for 10 min, samples were centrifuged at 400 x g/4 °C for 5 min, resuspended in FACS-buffer and analyzed on a BD FACSCalibur. As controls $4x10^4$/mL single NK and $8x10^4$/mL target cells were pre-incubated separately and combined at the point of dilution, aliquoted and treated as the pre-mixed samples. Control reactions were stopped 0, 40 and 90 min after dilution. The amount of NK cells engaged in conjugates compared to the total amount of NK cells was evaluated using the FlowJo Software from Tree Star Inc. The half-life of the conjugates was determined using the formula for a one-phase exponential decay:

$$\tau = \frac{\ln\left(\frac{Y_{50} - Plateau}{Span}\right)}{-K}$$

τ	–	Half-life [min]
ln	–	Natural logarithm
Y	–	Amount of remaining conjugates [%]
Span	–	Span between the exponentially determined maximum and minimal amount of remaining conjugates
Plateau	–	Exponentially determined minimal amount of remaining conjugates [%]
K	–	Rate constant [min^{-1}]

Conjugate decay assay with adherent target cells

The conjugate decay assay with adherent target cells was performed in 6-well plates. As targets HeLa-CD48 cells were used. Target cells were seeded at $0.75x10^5$ cells/well 1 d prior use, to obtain a confluent layer. Before the assay, medium was removed, cells were washed once in complete culture medium and $3x10^6$ to $5x10^6$ NK cells in 1 mL were added to each well. The plate was centrifuged for 3 min at 20 x g/room temperature and incubated for 30 min at 37 °C/5 % CO_2. To remove all unbound NK cells, medium was harvested, wells washed twice with complete culture medium and the plate centrifuged upside down covered with a second 6-well plate at 400 x g/5 min/room temperature. Harvested and washing media were combined and kept on ice. Fresh medium was added and the samples incubated with agitation at 37 °C/5 % CO_2 on a "Sunflower" 3D Mini–Shaker (BioSan, Riga, Latvia). This harvesting and washing-step was repeated after 30, 60 and 90 min. For each time point the harvested supernatants and washing media were combined and kept on ice. After the last harvesting step the number of the cells in the combined media was determined, the samples centrifuged at 400 x g/4 °C for 5 min and resuspended to $2x10^6$ cells/mL. Cells were stained for flow cytometry in a 96 well V-bottom-plate. For each staining reaction 50 µL NK cell suspension were used. Cells were analyzed for expression of various surface receptors using PE-conjugated antibodies: 2B4, CD69, CD158e, DNAM1, EB6, GL183, NKG2D, NKG2A, NKG2C, NKp30, NKp44 or NKp46. To each staining reaction anti-CD56-FITC (NK cell specific marker) and anti-LAMP1-PE/Cy5 (detection of NK cell degranulation) were added. IgG-isotype controls for all fluorophores were applied in a separate staining. The samples were stained for 20 min on ice in the dark, washed once, resuspended in FACS-buffer and analyzed on a FACSCalibur. The surface expression of the receptors was evaluated using the FlowJo Software from Tree Star Inc. and compared with the expression before contact to the target cells.

Determination of intracellular ATP level (ATPlite-kit)

Cellular ATP levels were determined using the ATPlite-kit from PerkinElmer (Rodgau, Germany) according to the manufacturers protocol. A black 96-flat clear bottom well plate was used. For each treatment a background control, containing medium with inhibitor alone, was added. The luminescence was detected using an Infinite M200 Pro (Tecan Group Ltd., Männedorf, Germany).

siRNA transfection

NK cells were transfected with 40 pmol of the respective siRNA using the Amaxa P3 primary cell 4D Nucleofector X Kit, program DK-100 according to the manufacturers protocol. $3x10^6$ NK cells per reaction were pelleted at 90 x g for 10 min, gently resuspended in P3 primary cell solution containing siRNA, transferred to a cuvette and transfected. The samples were immediately transferred to

37 °C/5 % CO_2 and incubated for 3 min. 250 µL pre-warmed RPMI without any supplements were added and the samples incubated for another 10 min at 37 °C/5 % CO_2. Cells were transferred to 1.15 mL pre-warmed IMDM per sample (supplemented with 10 % (v/v) human serum, 1 % (v/v) non-essential amino acids, 1 % (v/v) sodium pyruvate) in a 24-well plate. After 20 h medium was exchanged and recombinant human IL-2 added to a final concentration of 100 IU/mL. Cells were used for experiments 48 h post transfection. To determine the efficiency of the transfection at least $3.5x10^4$ cells were lysed and analyzed using western blot.

3.2.2 Microscopy

Time lapse microscopy

Time lapse experiments were done in µ-slide^{VI} luer (Ibidi). HeLa-cells were seeded at $6x10^5$/mL one day prior use and incubated at 37 °C/5 % CO_2. NK cells were labeled with PKH26 Fluorescent Cell Linker and resuspended at $2x10^6$ cells/mL in degased pre-warmed phenolred-free assay medium. All parts of the flow chamber system (except for the pump) were equilibrated to 37 °C 24 h before use. As medium for the assay phenol red-free IMDM supplemented with 10 % (v/v) FCS and 1 % (v/v) penicillin/streptomycin (Gibco/Invitrogen/LifeTechnologies, Darmstadt, Germany) was used, which was degased for at least 30 min and warmed to 37 °C directly before use. The medium in the reservoirs of the flow chamber was gently aspirated and the medium in the chamber exchanged for the degased assay medium. The syringes (B. Braun Melsungen AG, Melsungen, Germany) were connected via 1.6 mm ID silicon tubing (Ibidi GmbH, Martinsried, Germany) and 3-way Stopcocks (B. Braun Melsungen AG, Melsungen, Germany) to the flow chamber. During set up all remaining air bubbles were removed before the system was attached to the flow chamber. The flow chamber was placed in a climate chamber providing 37 °C/5 % CO_2. The first images were acquired before addition of the NK cells, then NK cells were added and allowed to attach for 30 min. After this, a flow with 32.5 mL/h was applied using a Perfusor secura FT pump (B. Braun Melsungen AG, Melsungen, Germany). The resulting shear stress was 0,96 dyn/cm^2. Images were acquired about every 75 sec with an IX 81 motorized inverted microscope (Olympus, Hamburg, Germany) and analyzed using the ImageJ software from the National Institute of Health (Bethesda, MD, US).

3.2.3 Protein biochemistry

SDS-Polyacrylamide gel electrophoresis (SDS-PAGE)

Cell lysates were mixed with 5x reducing sample buffer, and boiled for 5 min at 95 °C. The samples were cooled on ice and were shortly centrifuged. A maximum of 20 µL lysate and 5 µL precision blue

standard (BioRad) were loaded onto a 10 % or 4–12 % BisTris-NuPAGE gels (LifeTechnologies) and separated for 1 h 15 min at 150 V in 1 x MOPS buffer.
For analysis of perforin expression with the anti-human perforin antibody Pf344 (MabTech), samples were analyzed under non-reducing, denaturating conditions.

Western blot

Following SDS-PAGE proteins were transferred to a polyvinylidene difluoride (PVDF) membrane (Millipore), (activated with methanol,) for 1.5 h at 200 mA in Western blot transfer buffer. After transfer, membranes were incubated in blocking buffer for at least 1 h at room temperature, washed three times in PBST and incubated with primary antibody over night at 4 C. Subsequently, the membrane was washed three times in PBST/NaCl and incubated with the appropriate horseradish-peroxidase (HRPO)-conjugated secondary antibody (1:5,000-1:20,000 in blocking buffer) for at least 1 h at room temperature. After another 3 times of washing in PBST, the membrane was developed using SuperSignal West Pico/Dura or WesternBright Sirius HRPO substrate and X-ray films. X-ray films were scanned with a Perfection V700 Photo (Epson, Munich, Germany) using the Universal Silver Fast Launcher (LaserSoft Imaging AG, Kiel, Germany) and analyzed using ImageJ software from the National Institute of Health (Bethesda, MD, US).

3.2.4 Statistical analyses

Statistical analysis was performed using Prism 4.0 (GraphPad Software Inc., San Diego, CA, US). Values < 0.05 were esteemed significant and marked by a single asterisk. ** denotes values < 0.01; *** < 0.001, ns marks not significant values. If not otherwise indicated a paired one-tailed student's t-test was applied.

4. Results

4.1 Establishment of a flow cytometry-based assay system to determine the NK-tumor cell conjugate half-life

In NK cell research a strong focus lies on processes leading to activation and the thereby initiated effector functions. The steps between target cell encounter and the lytic hit are fairly well understood (Orange, 2008; Mace et al., 2014). In contrast, the subsequent process of the detachment of the NK from the target cell has not been evaluated specifically so far. This is one of the reasons why approaches to study this event are limited. Some groups used microscopy to visualize the whole event of NK-target cell interaction but did not analyze the detachment as such (Mace et al., 2012; Choi&Mitchison, 2013; Vanherberghen et al., 2013).

Therefore, we established an assay system based on an approach described by Culley and colleagues (2009) to characterize this process by using flow cytometry (Culley et al., 2009). Primary human IL-2-activated NK cells and K562 as susceptible target cell line were membrane labeled with PKH dyes. This labeling allows analysis of living cells without disturbing their function. The labeled cells were mixed and coincubated for 30 min in a small volume to allow conjugate formation (Fig. 4.1 A). This period will subsequently be referred to as "pre-coincubation". After this time the conjugate formation was still in a log-phase, with more conjugates forming than decomposing, but with a considerable amount of conjugates already generated. In general about 25 to 40 % if NK cells were engaged in conjugates at this time point. (data not shown). To stop the formation of new conjugates the samples were diluted 1:25, aliquoted and rotated for up to 90 min (Fig. 4.1 C). This treatment successfully prevented the formation of new conjugates. Separately incubated effector and target cells, that were mixed at the point of dilution showed a background of only 1 to 2 % NK cells in conjugates (data not shown).

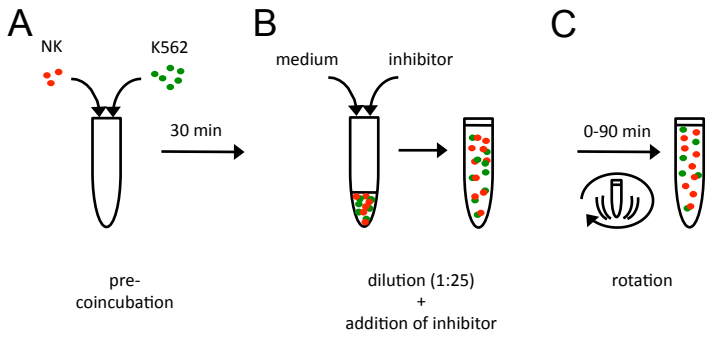

Fig. 4.1: Scheme for the detachment assay. (A) PKH26-labeled human IL-2-activated NK cells were mixed 1:2 with PKH67-labeled K562 cells and pre-coincubated for 30 min. (B) Samples were diluted 1:25 and aliquoted. If indicated inhibitors were added at this point. (C) Diluted samples were rotated for up to 90 min, before the reaction was stopped by vortexing and fixation with PFA.

Before fixation with PFA the samples were briefly vortexed to separate loose NK:K562 contacts that were not considered as functional conjugates. The membrane label in different colors allowed distinguishing NK (FL-2$^+$) from target cell (FL-1$^+$) populations in a scatter plot analysis. NK:K562-conjugates appear as double positive events. The amount of NK cells that are engaged in conjugates was determined as percentage of all NK cells in the assay (Fig. 4.2 A). To compare the data the value was normalized to the amount of NK cells in conjugates at the time point of dilution after 30 min pre-coincubation and plotted against the time. The values on the x-axis represent the time elapsed after dilution. To evaluate the data and determine the half-life of the conjugates the data were analyzed with a non-linear regression using the model of a one phase exponential decay (Fig. 4.2 B). With a coefficient of determination (R^2) of usually >0.98, this model reflects the primary data best. The half-life describes the time after which half of the originally formed conjugates did separate (indicated in figure 4.2 B by the dotted line). The pre-coincubation period is not included in this time since the actual age of the conjugates at the point of dilution could be between 0 to 30 min. In our system the observed half-life was 47.0 ± 11.8 min, with donor dependent differences since the experiments were done with primary human NK (Fig. 4.2 C).

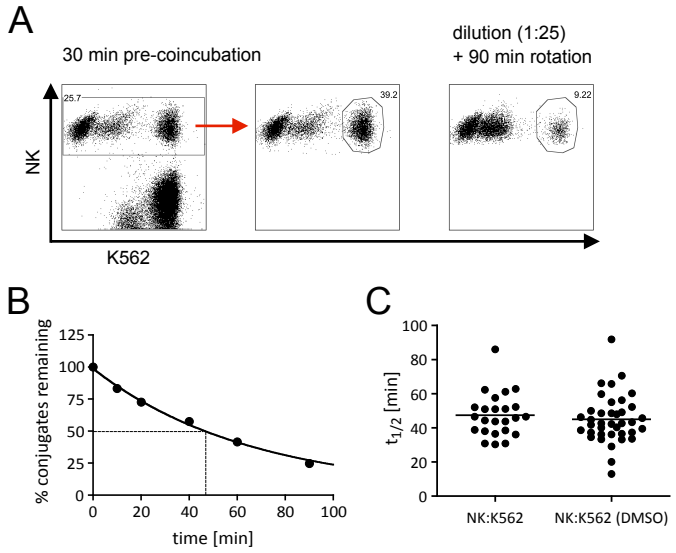

Fig. 4.2: Gating strategy and determination of the conjugate half-life. (A) In a scatter plot PKH26-labeled NK cells were discriminated from PKH67-labeled K562. The double positive population represents NK:K562-conjugates. The gate was set on all events positive for PKH26 and the number of NK cells engaged in conjugates determined as percent of all NK cells in the assay. This was done for samples after 30 min pre-coincubation (0 min), and at 10, 20, 40, 60 and 90 min after dilution. (B) The percentage of NK cells in conjugates for the various time points was normalized to the value after 30 min pre-coincubation, plotted as percentage of conjugates remaining against the time and fitted as a one phase exponential decay (representative example). (C) The half-life of conjugates formed by untreated (n=24) and DMSO-treated NK cells (n=38).

To determine factors influencing the detachment various inhibitors against different targets were applied in the assay. To not interfere with the formation of the conjugates the inhibitors were added at the point of dilution (Fig. 4.1 B). DMSO was used as solvent for most of the inhibitors used. Thus, we checked if it is affecting the detachment. Treatment with DMSO did not alter the half-life as shown in figure 4.2 C (45.1 ± 14.1 min).

To further inquire the influence of the set up, the assay was performed with varying E:T ratios and pre-coincubation times. The half-life changed only slightly if the E:T ratios were 1:1, 1:2 or 1:3 (34.6 ± 6.5 min, 38.4 ± 10.9 min or 37.3 ± 10.4 min, resp.). For an E:T of 1:5 the half-life of 48.1 ± 9.6 min was in general increased to a certain extent compared to the lower ratios (Fig. 4.3 A). Changing the pre-coincubation time to 20 min instead of 30 min did also not alter the half-life (53.8 ± 33.8 min vs. 50.7 ± 37.7 min) (Fig. 4.3 B).

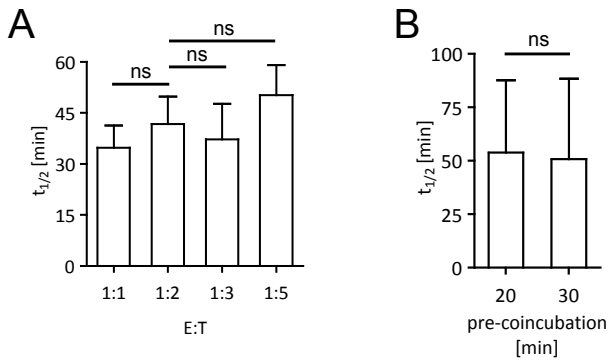

Fig. 4.3: Minor changes in the E:T ratio and the duration of the pre-coincubation time do not alter the half-life. (A) Half-life of NK:K562-conjugates determined in detachment assays with (A) different E:T ratios (1:1, 1:3: n=3; 1:2, 1:5: n=5) or (B) varying pre-coincubation times (E:T=1:2; n=4). (A, B) Graphs show mean ± SD. Paired two-tailed students t- test; ns=not significant.

4.2 Availability of new targets in close proximity accelerates the decay of existing conjugates

Recently, Choi and Mitchison (2013) proposed a model of "kinetic priming", suggesting that the NK cell remains attached to a previous target until a new one induces the detachment (Choi&Mitchison, 2013). A mechanism that would allow sustained signaling in the NK cell resulting in an accelerated cytolytic function. To test this in our assay system, an exceeding amount of new targets was added at the point of dilution (initial K562:fresh K562 = 1:200). To distinguish the subsequently added targets from the initial ones, they were labeled in a third color (CellTracker violet). Since agitation prevented the formation of new conjugates, the samples were incubated motionless after dilution. In figure 4.4 a representative example is shown. Without addition of fresh target cells and without rotation the decay was strongly decelerated ($t_{1/2}$ = 102.7 min) compared to the control with rotation ($t_{1/2}$ = 36.5 min). If fresh targets were added at the point of dilution and the samples were not rotated, the detachment was almost as fast as in the condition without fresh targets with rotation ($t_{1/2}$ = 40.4 min) and the control with addition of fresh targets with rotation ($t_{1/2}$ = 39.6 min). Simultaneously, the amount of NK cells in conjugates with new target cells increased over time, if the samples were kept motionless, indicating that the addition of fresh susceptible targets increases the decay of the "old" conjugates in favor of the formation of "new" conjugates with the freshly added NK cells. In the control condition with rotation the formation of conjugates occurred only at late time points and to a minimal extent. In an additional control the freshly added target cells were fixed with PFA before application in the assay. This

treatment successfully prevents formation of conjugates (data not shown). In the condition with addition of fresh fixed target cells, the decay was comparable to the condition with no addition of fresh target cells and without rotation. Considering the dilution of initially added susceptible targets in the freshly added unsusceptible targets, the probability that a NK cells encounters another one of these while engaged in a conjugate is comparably small. This indicates that the decelerated decay during motionless incubation without addition of fresh targets is not due to an equilibrium of decay and formation of new conjugates with the initial targets, but rather to sustained attachment. Similar results were obtained for two more donors (data not shown).

Thus, in agreement with the hypothesis of Choi and Mitchison, availability of a new target in close proximity induced detachment form the previous conjugate, possibly by reorientation of the cell polarity.

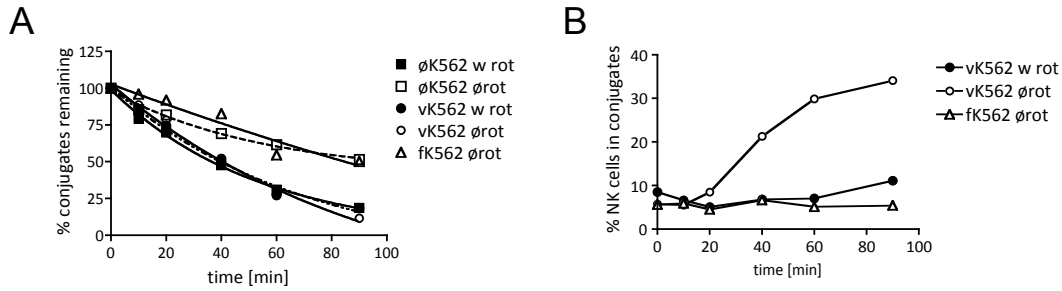

Fig. 4.4: Availability of fresh target cells accelerates the decay of pre-formed NK:K562-conjugates. In the decay assay conditions with addition of fresh viable (v) or fixed (f) K562 cells at the point of dilution were compared to the standard condition without addition of fresh target cells (øK562) The samples were either incubated motionless (ørot) or rotating (w rot). (A) Decay curves for the five compared conditions. (B) Formation of conjugates with freshly added targets. Time point 0 resembles the point of dilution.

4.3 Establishment of a microscopy–based flow chamber system to visualize NK cell detachment from target cells

In addition to analyzing the detachment in a flow-cytometry-based approach, we aimed to visualize the process using live-cell imaging. This allowed investigation of the detachment on the single-cell level. We established a flow-chamber system with HeLa cells as susceptible targets. Therefore, HeLa cells were grown in the flow chamber at a low density and NK cells were added in an exceeding amount to enable the formation of a high number of conjugates. After 30 min pre-coincubation time, the flow of medium with 35 mL/h was started. The induced shear stress was about 1 dyn/cm^2, commonly used for flow chamber assays (Gonzales&Wick, 1996; André et al., 2000; Tager et al., 2003). It is slightly lower than the level of shear stress in small blood vessels (Balagopalan et al., 2011). For comparison the shear stress found in arteries is about 100 dyn/cm^2 and in veins 5 dyn/cm^2 (Pries et al., 1995). The flow was applied to prevent the formation of new conjugates by detaching NK cells

and to break loose cell-cell contacts that might not be mature synapses. The cells were observed for about 60 min after initiation of the flow with images taken every 74 sec. NK cells that were not washed away directly after starting the flow were followed until they detached from the target cell or until the end of the observation time. If multiple NK cells encountered a target and if these could not be distinguished, they were excluded from the analysis. Similarly, NK cells that were attached to a target and washed away still connected to the target were also excluded.

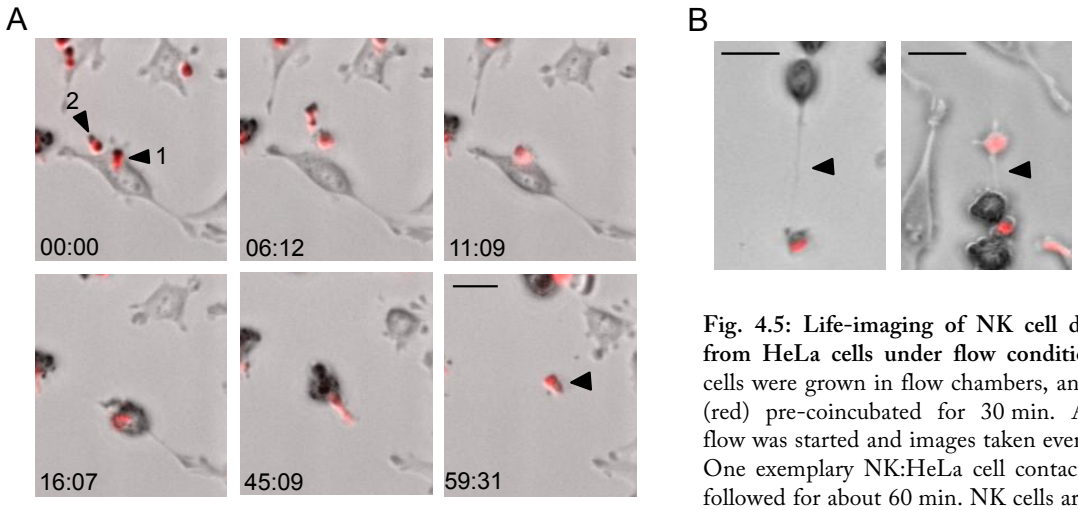

Fig. 4.5: Life-imaging of NK cell detachment from HeLa cells under flow conditions. HeLa cells were grown in flow chambers, and NK cells (red) pre-coincubated for 30 min. A medium flow was started and images taken every 74 s. (A) One exemplary NK:HeLa cell contact, that was followed for about 60 min. NK cells are indicated by black arrows. (B) Examples for nanotube-like structures formed between NK and HeLa cells. (A, B) Scale bar = 40 pixel.

Figure 4.5 A shows an example of a NK:HeLa cell contact. Two NK cells were attached to the target at the beginning of the observation. One (#2) was washed away already after about 6 min, whereas the other NK cell (#1) remained attached. The target rounded after about 16 min and was washed away after 59 min, breaking the contact to the NK cell. For two different donors the decrease of the amount of NK cells attached to HeLa cells is displayed over time in figure 4.6 (left graphs). Additionally, the half-life of the cell-cell interactions was determined using the fit for a one-phase-exponential-decay (right graphs). 67 NK:HeLa cell contacts observed for donor 1 had a half- life of 28.1 min. 66 NK cells of donor 2 were in contact with HeLa cells, and the determined half-life was 49.5 min. As seen in the flow cytometry-based decay assay, there are donor-dependent differences for the half-life. However, the overall time frame for the detachment seemed to match with the flow cytometry-based assay. Interestingly, as described in the literature (Onfelt et al., 2004; Roda-Navarro et al., 2004; Chauveau et al., 2010; Comerci et al., 2012), we also observed formation of nanotube-like structures between NK and HeLa cells (Fig. 4.5 B).

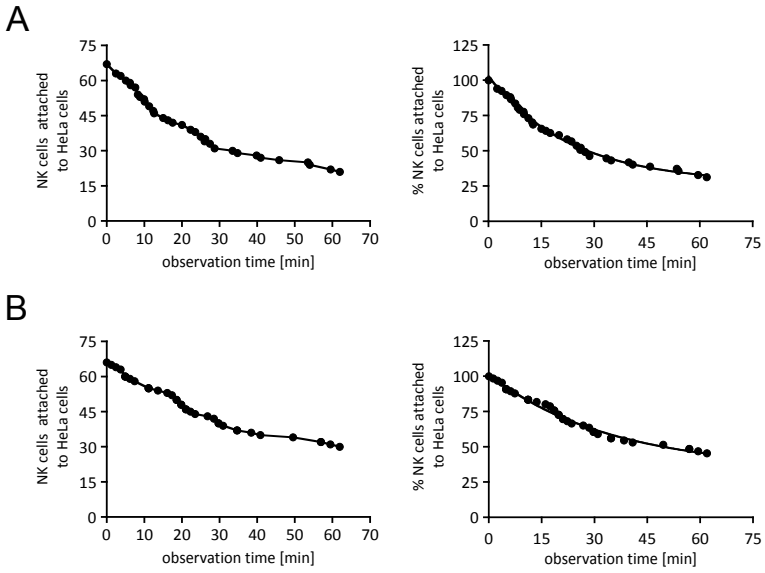

Fig. 4.6: Analysis of NK cell detachment from HeLa-target cells observed via life cell-imaging. For two different donors (A, B) the amount of NK cells connected to HeLa cells was determined and plotted against the observation time (left curves). The data were fitted with a one-phase exponential decay (right curves) and the half-life determined.

4.4 Surface receptor expression patterns of detached NK cells

Various NK cell receptors, e.g. 2B4 or NKG2D, were shown to be down-modulated after antibody-mediated cross-linking or ligand binding (Sandusky et al., 2006; Roda-Navarro&Reyburn, 2009). Diminishing interaction with the target cell is discussed to be one mechanism leading to detachment.

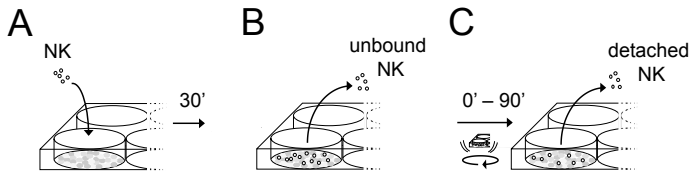

Fig 4.7: Scheme of the detachment assay with adherent target cells. NK cells were added to a confluent layer of HeLa-CD48 cells and pre-co-incubated for 30 min. After removal of unbound NK cells the conjugates were 3D-rotated for up to 90 min at 37 °C. Detached NK cells were harvested after 30 min, between 30 to 60 min and between 60 to 90 min after removal of the unbound NK cells and analyzed for surface expression of various receptors using flow cytometry.

To gain access to recently detached NK cells that certainly had target cell contact, a detachment assay with adherent target cells was established. NK cells were added to a confluent layer of HeLa cells transfected with CD48, the ligand for 2B4 (HeLa-CD48). The cells were incubated for 30 min to allow conjugate formation (Fig. 4.7 A). After this pre-coincubation all unbound NK cells were removed and the formed conjugates further incubated under three-dimensional rotation (Fig. 4.7 B) to prevent formation of new conjugates by detached NK cells. Subsequently, NK cells that detached in the following 30 min, between 30 and 60 min and between 60 and 90 min were harvested (Fig. 4.7 C) and analyzed for their surface expression pattern compared to NK cells before target cell contact. To compare different donors the relative fluorescence intensity (RFI) was determined for each time point

and receptor. Figure 4.8 shows the summary of the obtained data for various receptors. CD56 as NK cell marker was used to exclude HeLa cells from the analysis. CD11a as part of the lymphocyte-function associated antigen (LFA)-1 was analyzed to inquire possible changes in the integrin surface level. CD69 as early activation marker provides information about the activation status of the NK cells. CD107a serves as a marker for degranulation indicating induced effector functions by target cell contact. In addition to the natural cytotoxicity receptors NKp30, NKp44 and NKp46 the activating receptors 2B4, DNAM-1, and NKG2D were analyzed. As inhibitory receptor, NKG2A that forms a heterodimer with CD94 was included in the survey. Additionally, the expression of CD158 a, b1/b2 and e was determined. Since these were expressed very weakly or not at all they were excluded from the analysis.

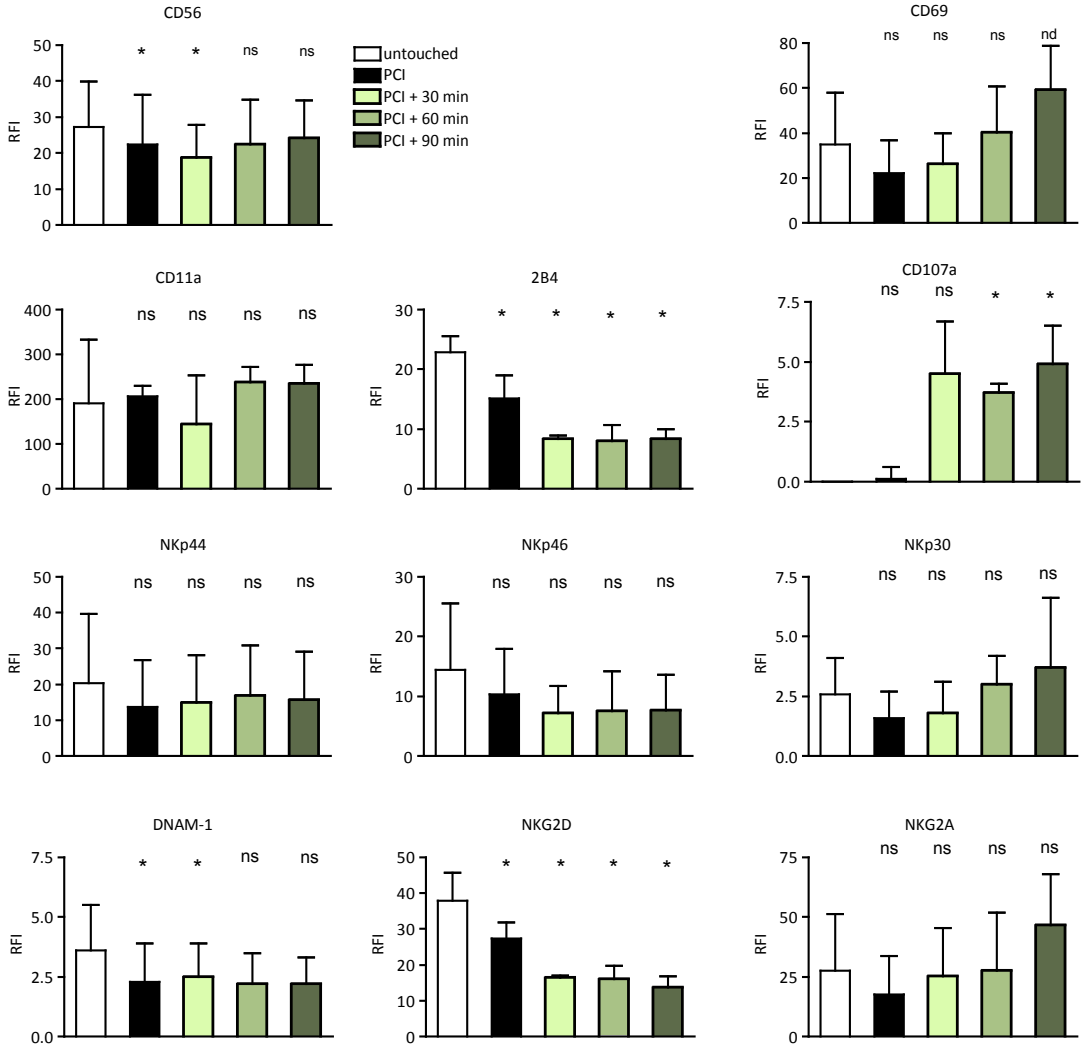

Fig. 4.8: The surface expression pattern of various receptors is altered after detachment. Relative fluorescence intensity (RFI) of various NK cell receptors before addition to HeLa-CD48 target cells, on NK cells removed after 30 min pre-coincubation, additional 30 min, 30 to 60 min and 60 to 90 min. (n=3). PCI = pre-coincubation. paired two-tailed students t-test (*< 0.05)

Interestingly, all molecules except for CD11a and CD107a showed a lower RFI after 30 min pre-coincubation compared to the corresponding untouched NK cells. This is possibly due to the handling of the cells during the assay. When analyzing NK cells after detaching from the target cells we found that amount of CD56 and CD11a increased back to the levels of untouched cells, whereas the expression of NKp44 and DNAM-1 did not change after the initial decrease. As described in literature, expression of 2B4 and NKG2D was significantly reduced by target cell contact. NKp46, although not significantly, did show a similar trend, indicating that the same mechanism might also be true for this receptor. The third group of receptors CD69, NK30 and NKG2A were higher expressed on late detaching NK cells. Again this was rather a trend then a significant change. The altered surface expression pattern of these receptors could be a sign of down-modulation of the receptors after activation. Alternatively, since the experiments were conducted with bulk NK cells, the differences could be due to diverse features of distinct subpopulations.

The increase in CD107a surface expression that was already detectable 30 min after pre-coincubation indicates that the NK cells were in functional contacts with the target cells, which induced degranulation most probably leading to lysis.

4.5 The Role of PKCθ on the stability of the NK cell aIS

Studies on the immunological synapse between $CD4^+$ T cells and antigen presenting cells (APCs) revealed an importance of PKCθ for the breakage of the synapse (Sims et al., 2007). In YTS cells PKCθ was found to phosphorylate WASp-interacting protein (WIP) after target cell contact and thereby enable the recruitment of myosin II A and actin to the WIP-WASp-multi protein complex (Krzewski et al., 2006). In mouse NK cells, Tassi and colleagues (2008) found a necessity of PKCθ for ITAM-mediated IFNγ-secretion (Tassi et al., 2008). To assess if PKCθ is also important for destabilizing the aNKIS we interfered with this signaling molecule using specific inhibitors and RNAi technology. First, AEB071 (also called sotrastaurin), a PKC specific inhibitor with increased selectivity for PKCθ (Ki = 0.22 nM) was applied (Evenou et al., 2009). In a ^{51}chromium release assay the effects of the inhibitor on the cytotoxic potential of NK cells was evaluated. Inhibition of PKCs led to a dose-dependent reduction of the lysis of K562 target cells (Fig 4.9 A). At an E:T ratio of 5:1 the treatment with 250 nM AEB071 reduced the lysis by 15.1 ± 7.5 % compared to the solvent control DMSO. Increasing the concentration to 500 nM led to a stronger reduction of 48.7 ± 6.0 % (Fig. 4.9 A). Although the cytotoxicity was impaired, the higher concentration of the inhibitor did not affect the formation of conjugates (Fig. 4.9 B). In contrast to the data for $CD4^+$ T cells, inhibition of PKCθ did not changed the detachment of NK cells. No significant difference between the half-life of

conjugates of AEB071-treated NK cells compared to the solvent-treated NK cells was observed (Fig 4.9 C).

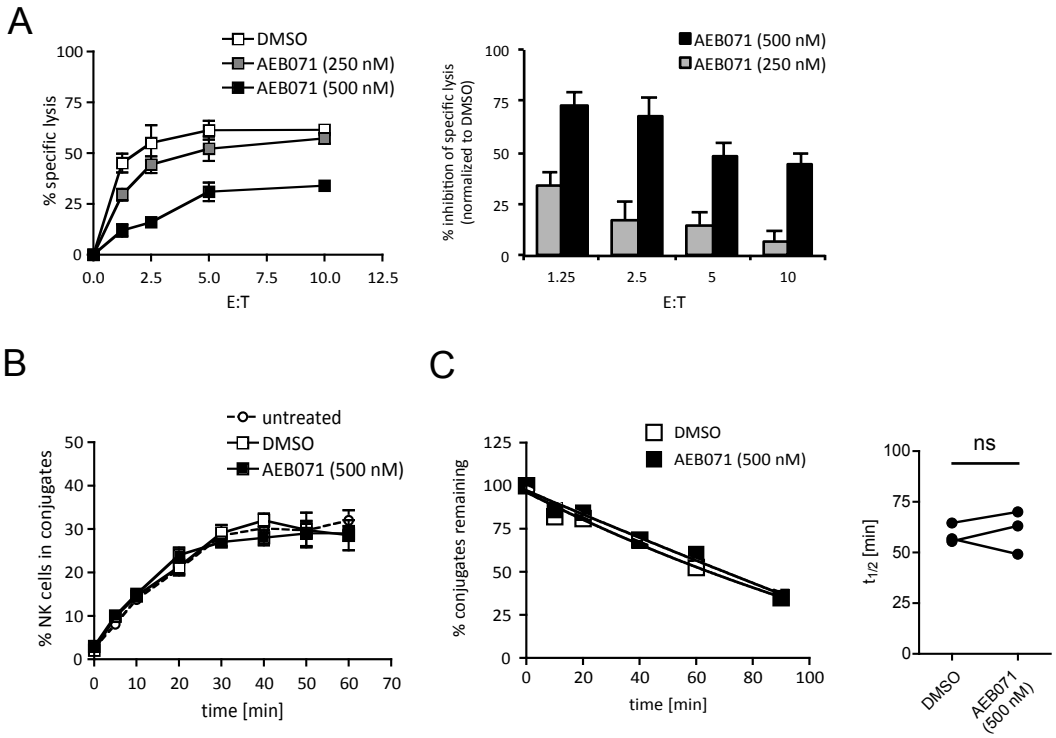

Fig 4.9: Inhibition of PKCs by AEB071 (sotrastaurin) reduces the cytotoxicity but does not affect formation or stability of conjugates. NK cells were pre-treated for 1 h with 250 nM (▣) or 500 nM AEB071 (■) or DMSO (□) as solvent control. The inhibitor concentration present during the pre-incubation was kept constant during the assays with K562 cells as target cells. (A) Standard ^{51}chromium release assay. The curve of one representative example (left) and the quantification of the experiments with three different donors (right) are shown as mean ± SD. (B) Conjugate formation assay. The curves represent the mean values ± SD of 3 different donors. (C) Conjugate decay assay. Decay curves of one representative example and quantification of 3 different donors are shown as mean ± SD. (p=0.3699)

Since AEB071 might also inhibit other PKC isoforms as PKCα (Ki = 0.95 nM) or PKCβI (Ki = 0.64 nM) the more selective myristoylated pseudosubstrate inhibitor was tested to verify the obtained data. For 3 of 4 donors the lysis of K562 cells was reduced by about 27 % after treatment of the NK cells. One donor did not respond to the treatment, indicating donor-dependent differences in the responsiveness to the treatment (Fig. 4.10 A). Compared to the inhibition induced by the two different AEB071 concentrations the effect of the pseudosubstrate inhibitor is intermediate, suggesting that higher concentrations of AEB071 might already inhibit other isoforms than PKCθ alone. In a third approach, PKCθ was knocked down by specific siRNAs targeting the *PKRCQ* mRNA. Four oligonucleotides were tested either alone or in different combinations. The most effective combinations were #9/#10 or a mix of all four, leading to a reduction of PKCθ protein by 80 % (Fig. 4.10 B). To test the influence of the siRNAs on other isoforms, exemplarily the expression of

PKCα was determined. It was not altered by the transfection (Fig. 4.10 B). Surprisingly, the reduction of PKCθ expression did not affect the cytotoxicity towards K562 target cells (Fig. 4.10 C).

In summary, these data indicate that PKCθ itself has limited if any influence on target cell lysis, whereas other isoforms might be required for full efficiency of NK cell effector functions. However, for the formation and maintenance of NK-target cell conjugates PKCθ and most probably other isoforms as PKCα or PKCβ did not seem to be essential.

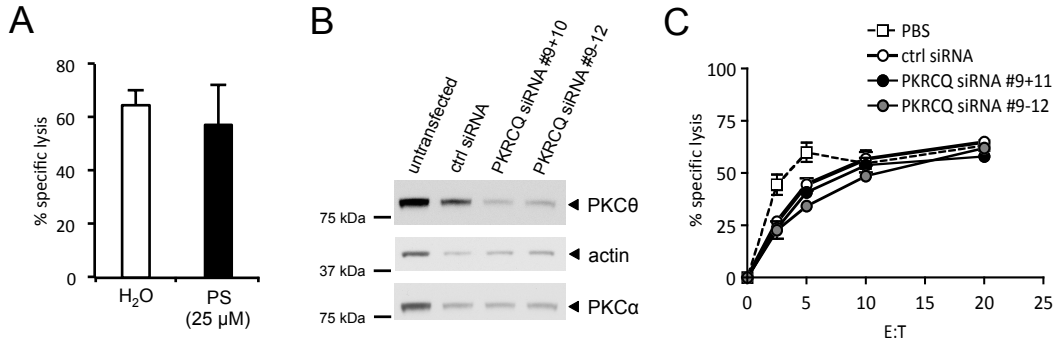

Fig. 4.10: Specific inhibition of PKCθ by its pseudosubstrate or knock-down of the kinase by RNAi does not alter the cytotoxicity towards K562 target cells. (A) NK cells were pre-treated for 30 min with 25 µM myristoylated PKCθ pseudosubstrate (PS) before addition of K562 target cells. The inhibitor concentration was kept constant during the assay. (E:T=5:1; n=4, mean ± SD). (B and C) NK cells were transfected with either control siRNA (20 pmol) or a mix from PKCRQ siRNAs #9 and #10 (10 pmol each) or a mix from PKCRQ siRNAs #9, #10, #11 and #12 (5 pmol each). 48 h post transfection one part of the cells was lysed for western blot analysis (B). Standard ^{51}chromium release assay. One representative experiment is shown as mean ± SEM (n=2).

4.6 Signaling pathways

4.6.1 Early but not late sustained activating signaling is required for conjugate stability

The formation of an aNKIS is strongly depending on signaling pathways induced by the interaction of activating NK cells receptors with their respective ligands. The formation of a functional NK cell synapse is considered to occur in distinct and tightly regulated steps (Orange et al., 2003; Orange, 2008). The pathways induced by triggering activating receptors are complex and partly redundant (Watzl&Long, 2010). Additionally, signaling via the integrin LFA-1 contributes to the activation (Long et al., 2013). Principle players in the signaling cascades are for instance protein tyrosine kinases (PTKs), e.g. Src- and Syk-family kinases that activate various molecules as SLP76, Vav1, PLCγ or WASp, inducing gene transcription and cytoskeletal remodeling. Additionally, triggering PI3K leads to activation of MAP kinase pathways cumulating in granule polarization and exocytosis (Vyas et al., 2002). The question arose, if these signaling molecules involved in the formation also are required for the maintenance of NK-target cell conjugates. Hence, we applied various specific inhibitors in the decay assay. Adding the reagents at the point of dilution guarantees an undisturbed formation of conjugates. The course of the decay would give information about the role of the signaling molecules for the stability of the conjugates.

Initially, early signaling events as Src- and Syk-family kinases, as well as PLCγ and PI3K were targeted. The effect of the inhibitors on the effector function of the NK cells was tested in a cytotoxicity assay. All inhibitors, except for wortmannin (PI3K), led to a significant reduction of the cytotoxicity (Fig. 4.11 A), emphasizing the importance of these signaling events for NK cell function. When these inhibitors were applied in the detachment assay, all of them, including wortmannin, significantly reduced the half-life of the conjugates.

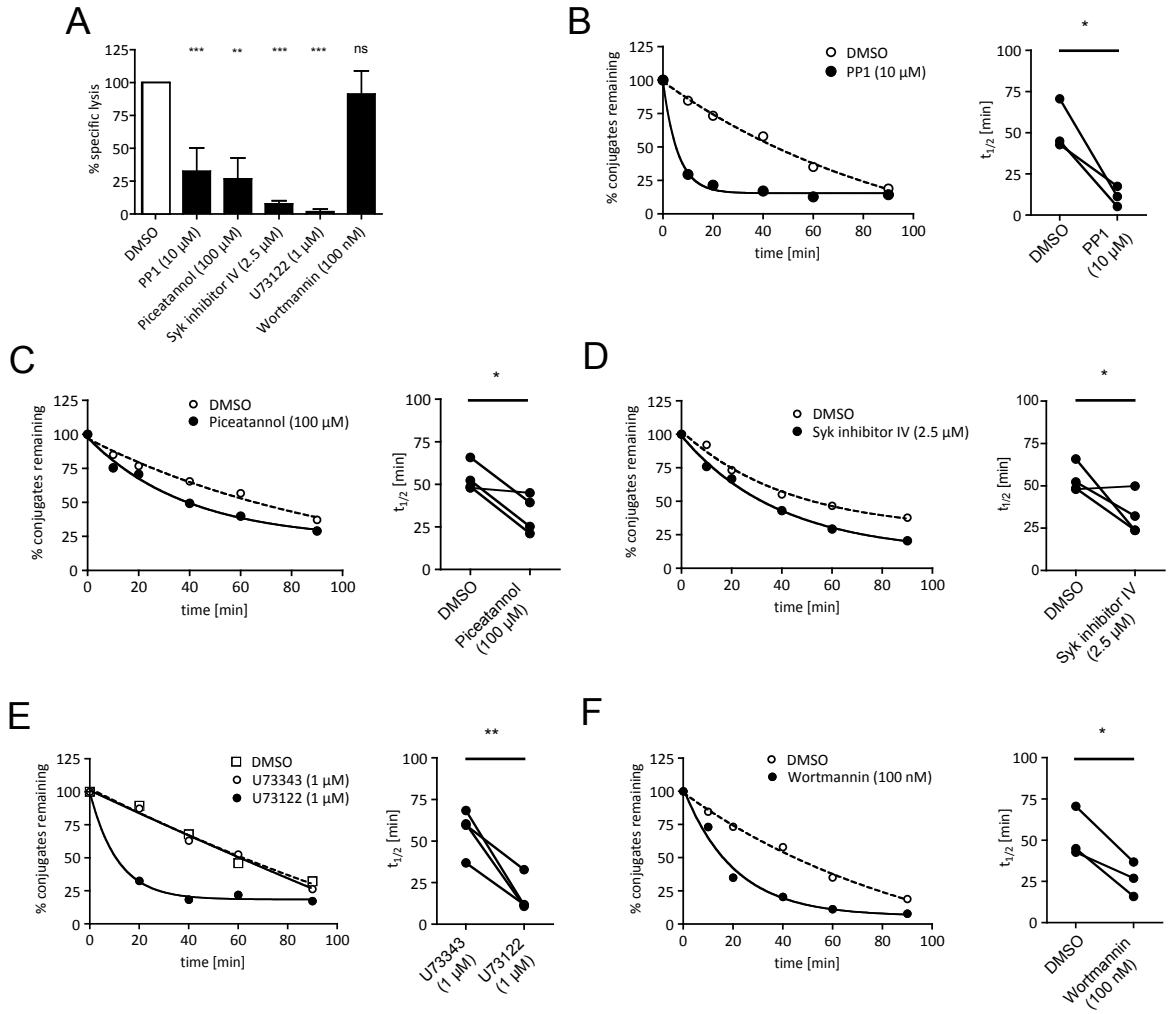

Fig. 4.11: Disruption of early signaling events impairs the cytolytic potential of NK cells and accelerates the decay of NK:K562-conjugates. Specific inhibitors targeting various signaling events were employed in standard 4 h ^{51}chromium release (A) and conjugate decay assays (B-F). (A) NK cells were pre-treated for 30 min with the respective inhibitor before addition of K562 target cells at an E:T ratio of 5:1. Values are shown as mean ± SD. (n=4, for PP1 and wortmannin n=5). (B-F) Inhibitors were added at the point of dilution after 30 min pre-coincubation. For each treatment a representative conjugate decay curve and the quantification for 3 to 4 different donors is shown. (*< 0.05; ** < 0.01).

In Fig. 4.11 B-F exemplary decay curves are shown. Inhibition of Src family kinases, as Lck, Fyn, Src or Hck, by PP1 led to an average reduction of the half-life by 77 % from 52.7 ± 15.5 min to 11.3 ± 6.2 min compared to the solvent control (Fig. 4.11 B). Likewise, interfering with Syk-family

kinases by piceatannol or Syk inhibitor IV also decreased the conjugate stability. Piceatannol, which has a slightly broader spectrum of targets at a concentration of 100 µM (Syk and Lyn) reduced the half-life by about 40 % from 53.7 ± 8.3 min to 32.7 ± 11.3 min. Syk inhibitor IV shows a higher selectivity for Syk without affecting other Syk- or also Src-family kinases. The reduction of the half-life by 40 % was comparable to the effect caused by piceatannol treatment (53.7 ± 8.3 min to 32.4 ± 13.3 min compared to DMSO; Fig. 4.11 C and D). These data indicate that Src- and Syk-kinases are indispensable for conjugate stability. Furthermore, targeting PLCγ, which induces Ca^{2+} flux and PKC activation, by the inhibitor U73122 decreased conjugate stability even stronger than inhibition of Src- and Syk-kinases. The half-life was reduced by 70 % from 59.5 ± 12.2 min to 16.2 ± 11.1 min compared to the inactive analog U73343 (Fig. 4.11 D). Inhibition of PI3K by wortmannin, although it did not show any effect on the cytotoxicity (Fig. 4.11 A), reduced the conjugate half-life by 50 % from 52.7 ± 15.5 min to 26.6 ± 10.4 min (Fig. 4.11 E).

Taken together these data indicate a pivotal role of ongoing early signaling in the NK cell not only for cytotoxicity but also for the maintenance of conjugates.

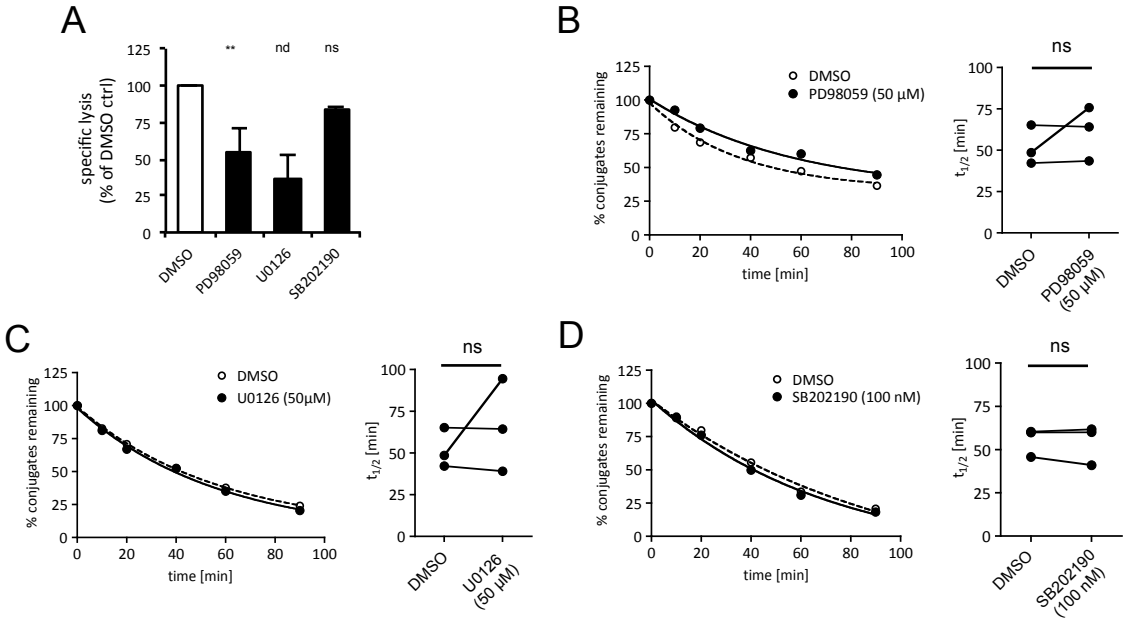

Fig. 4.12: Late activating signaling events are required for full cytolytic capacity of NK cells, but not for the maintenance of NK:K562-conjugates. (A) NK cells were pre-treated for 30 min with the MAPK inhibitors PD98059, U0126 or SB202190 before addition of K562 target cells at an E:T of 5:1. The inhibitor was present during the 4 h standard ^{51}chromium release assay. The values are shown as mean ± SD. (PD98059: n=3, U0126: n=2; SB: n=4). (B-D) The inhibitors were added to a standard conjugate decay assay at the point of dilution in the indicated concentration. For each treatment a representative decay curve and the quantification of experiments with three different donors are shown. (*< 0.05; ** < 0.01).

Signaling molecules that act further downstream of PI3K such as mitogen-activated protein kinase (MAPK) cascades are crucial for polarization and degranulation of the NK cells (Vyas et al., 2002).

Inhibition of MEK1/2 by PD98059 or U0126 reduced the cytotoxicity by 46 % to 67 %, respectively. But if the inhibitors were applied in the decay assay no effect on the half-life was observed (DMSO: 52.4 ± 12.4 min, PD98059: 61.1 ± 16.3 min, U0126: 66.0 ± 27.7 min; Fig. 4.12 B, C). The serine-threonine kinase p38 has been reported to play a role for cytokine production under certain conditions (Mainiero et al., 2000) and to have a regulatory function in target cell lysis (Chini et al., 2000). Inhibition of p38 by SB202190 did not influence the lysis of target cells or the stability of conjugates. The half-life (60.1 ± 0.3 min) was unchanged compared to the solvent control DMSO (61.0± 1.2 min; Fig. 4.12 D).

In summary, the data suggest that signaling events further downstream of PI3K are required for full effector functions of NK cells but not for their potential to remain in conjugates.

4.6.2 Inhibitory signaling

Triggering of inhibitory NK cell receptors that contain a cytoplasmic immunoreceptor tyrosine-based inhibition motif (ITIM) leads to recruitment of the tyrosine phosphatases SHP-1 and SHP-2. SHP-1 in turn dephosphorylates Vav1 and thereby interrupts initial steps of NK cell activation (Watzl&Long, 2010). Since sustained early activating signaling is required for conjugate stability, the question arose if phosphatases might induce detachment by ceasing activation steps. NSC87877 and 119901 were described as inhibitors of the phosphatases SHP-1 and SHP-2 (Chen et al., 2006; Wahle et al., 2007). But when tested, we did not observe any changes in NK cell cytotoxicity (data not shown).

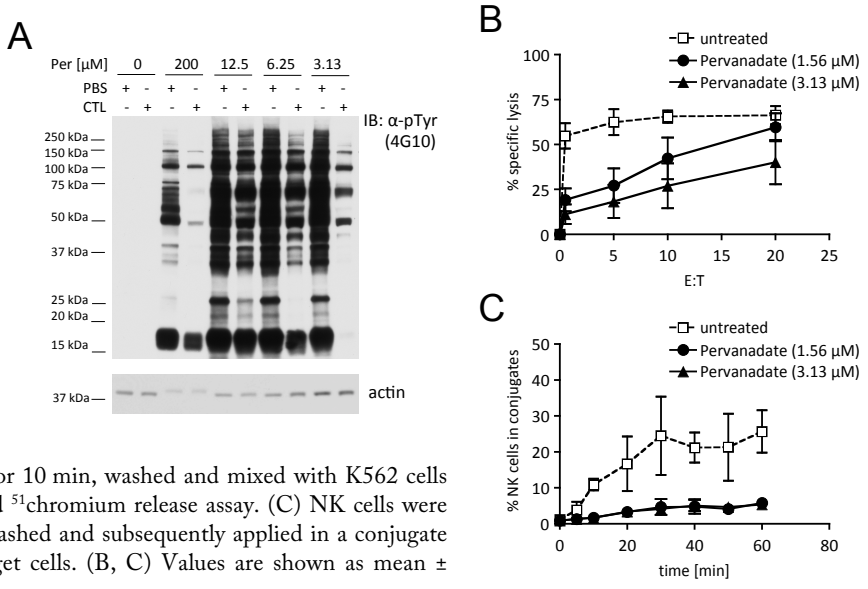

Fig. 4.13: Inhibition of tyrosine phosphatases by pervanadate affects cytotoxicity of NK cells and their ability to form conjugates with target cells. (A) NK cells resuspended in PBS or assay medium (CTL) were treated for 10 min with various pervanadate concentrations, washed, lysed and probed for tyrosine phosphorylation (4G10) and actin as a loading control. (B) NK cells were pre-treated for 10 min, washed and mixed with K562 cells at various E:T in a 4 h standard ^{51}chromium release assay. (C) NK cells were pre-treated with pervanadate, washed and subsequently applied in a conjugate formation assay with K562 target cells. (B, C) Values are shown as mean ± SD. (n=3).

Therefore, the general tyrosine phosphatase inhibitor pervanadate was used (Huyer et al., 1997). By irreversibly oxidizing the catalytic cysteine residue of protein tyrosine-phosphatases it induces an

increase of overall tyrosine phosphorylation. Pervanadate was titrated to determine the lowest concentration that still induces increased tyrosine phosphorylation in assay medium without affecting the NK cell viability. The NK cells were treated for 10 min and analyzed for tyrosine phosphorylation. Untreated IL-2-activated NK cells do not show detectable background phosphorylation. The highest concentration of 200 µM pervanadate led to an increased phosphorylation in both PBS and assay medium. But this amount might be toxic and affect the viability of the cells indicated by the weaker actin signal. Lower concentrations starting from 12.5 µM down to 3.13 µM also increased tyrosine phosphorylation without affecting the actin level, indicating that these concentrations are still effective without being toxic (Fig. 4.13 A). Since the lowest concentration of 3.13 µM still increases the level of tyrosine phosphorylation, it was used for the following experiments. Additionally, the concentration was further reduced to 1.56 µM. In a cytotoxicity assay against K562 cells these concentrations reduce the lysis in a dose-dependent manner (Fig. 4.13 B). Because long-term treatment of the NK cells with pervanadate induces apoptosis (data not shown), the NK cells were pre-treated, washed and applied in a conjugate formation assay without addition of pervanadate. Inhibiting tyrosine phosphatases strongly reduced the ability of the NK cells to form conjugates compared to untreated cells (Fig. 4.13 C). Thus, since tyrosine phosphatases in general are required for normal activation and function of NK cells their role in detachment could not be determined in the assay system used here.

Besides phosphorylation of tyrosine residues, a number of signaling molecules, e.g. Akt or Erk, are regulated via serine- or threonine phosphorylation. Treatment of NK cells with the S/T phosphatase inhibitor calyculin A was shown to reduce NK cell-mediated cytotoxicity (Bajpai and Brahmi, 1994). The S/T phosphatase PP2A was found to negatively regulate IL-2 signaling in NK cells (Ross et al., 2010). Other than that, not many details about S/T phosphatases in NK cells are known. We targeted S/T phosphatases with two inhibitors. Okadaic acid has a broader spectrum interfering with PP1 (IC_{50} = 10-50 nM), both isoforms of PP2A (IC_{50} = 0.5 nM) and PP3 (IC_{50} = 4 nM). Calyculin A is targeting only PP1 (IC_{50} = 2 nM) and PP2A (IC_{50} = 0.5-1 nM). Titration of okadaic acid in a cytotoxicity assay led to inhibition of the target cell lysis only at higher concentrations (Fig. 4.14 A). In the conjugate decay assay, inhibitor treatment increased the half-life significantly, but only slightly (EtOH: 35.8 ± 2.1 min, okadaic acid: 38.3 ± 2.4 min) (Fig. 4.14 B). Calyculin A instead showed a stronger inhibitory effect on lysis and conjugate half-life. The half-life was reduced by about 52 % from 35.8 ± 2.1 min to 17.0 ± 1.8 min (Fig. 4.14 C, D). Since calyculin A is not inhibiting PP3 and the IC_{50} values for PP2A are comparable for both inhibitors, the effect seen with calyculin A is most likely due to the inhibition of PP1. This indicates a major role for this S/T phosphatase for the stability of conjugates and for the cytolytic function of NK cells.

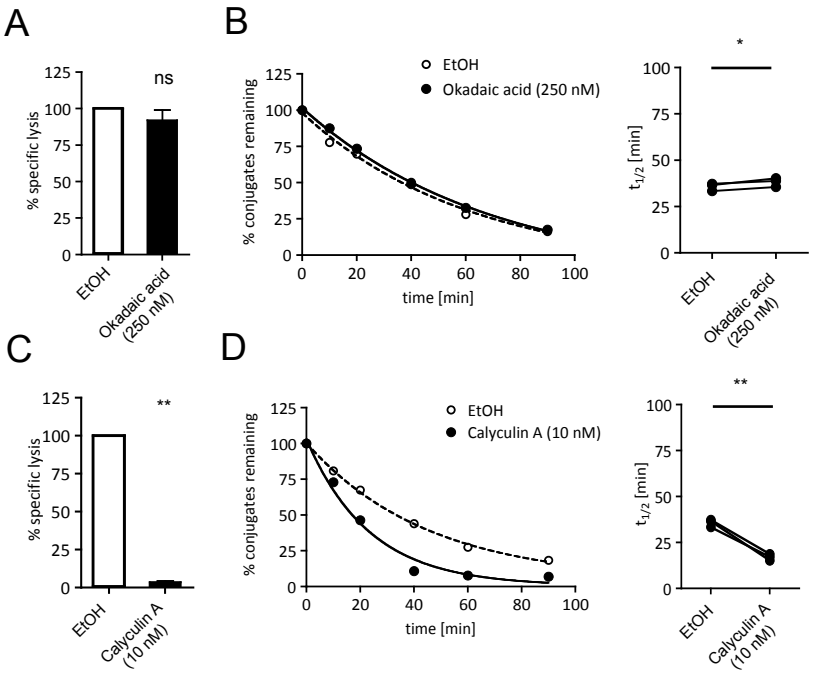

Fig. 4.14: Inhibition of serine-threonine phosphatases by calyculin A but not by okadaic acid decreases the cytolytic potential of NK cells and the stability of NK:target cell conjugates. (A, C) NK cells were pre-treated for 30 min with the respective inhibitor before addition of K562 target cells at an E:T of 5:1. The inhibitor concentration was kept constant during the 4 h standard ^{51}chromium release assay. Values are shown as mean ± SD. (n=3; paired two-tailed students t-test). (B, D) The inhibitors applied in the conjugate decay assay at the point of dilution. For each treatment a representative decay curve and the quantification of the experiments with 3 different donors are shown. (*< 0.05; ** < 0.01)

4.7 Energy level

In NK and T cells cytoskeleton dynamics, cell migration and also the granule exocytosis mediated by motor proteins as myosin II A are ATP-dependent processes (Samstag, 2003; Andzelm et al., 2007; Ilani et al., 2009; Sanborn et al., 2009 2011; Sanborn et al., 2011 2011; Kumari et al., 2012). However, Davis and colleagues showed that KIR-induced clustering of HLA-C in inhibitory NK cell synapses is not affected by depletion of intracellular ATP (Davis et al., 1999). The role of ATP for the aNKIS is not well understood yet. Therefore, the question arose if the intracellular energy level influences the detachment process. Azide is a potent inhibitor of ATP by interrupting mitochondrial respiration (Palmieri&Klingenberg, 1967; Fei et al., 2000).

We first analyzed the effect of sodium azide treatment on the intracellular ATP-level. After 2 h treatment with 50 mM sodium azide the ATP level in the cells was reduced by 63.8 ± 3.5 % (Fig. 4.15 A). The capability of ATP-depleted NK cells to form conjugates with K562 target cells was moderately decreased (Fig. 4.15 B). Interestingly, when azide was added directly before mixing with the target cells the effect was comparable to the inhibition observed when the NK cells were pre-treated for 2 h. A similar trend was seen for the lysis of K562 target cells. Under both conditions, 2 h pre-treated and not pre-treated NK cells, showed an equivalently reduced cytotoxicity (Fig. 4.15 C).

To determine the influence of the ATP level on the stability of conjugates sodium azide was applied in the conjugate decay assay. As for conjugate formation and cytotoxicity studies, the NK cells were either pre-treated before mixing with the target cells or the azide was added after 30 min pre-coincubation at the point of dilution. The pre-treated NK cells formed less conjugates, which is in consistence with the data for conjugate formation (Fig. 4.15 B). Interestingly, already after 10 min the decay curves for both conditions are nearly superimposable (Fig. 4.15 D). This trend was seen for all donors tested, indicating that the effect triggered by azide occurred very rapid. The stronger reduction of the half-life for conjugates with pre-treated NK cells results from the different percentages of NK cells in conjugates at time point 0. Compared to H_2O treated NK cells (41.5 ± 12.3 min), the conjugates with pre-treated NK cells showed a reduction of the half-life by 58 % to 17.0 ± 2.9 min. Addition of azide at the point of dilution diminished the half-life by 76.6 % to 9.6 ± 2.4 min (Fig. 4.15 E). These data indicate that effector functions like cytotoxicity as well as formation and maintenance of NK-target cell conjugates also depend on ATP.

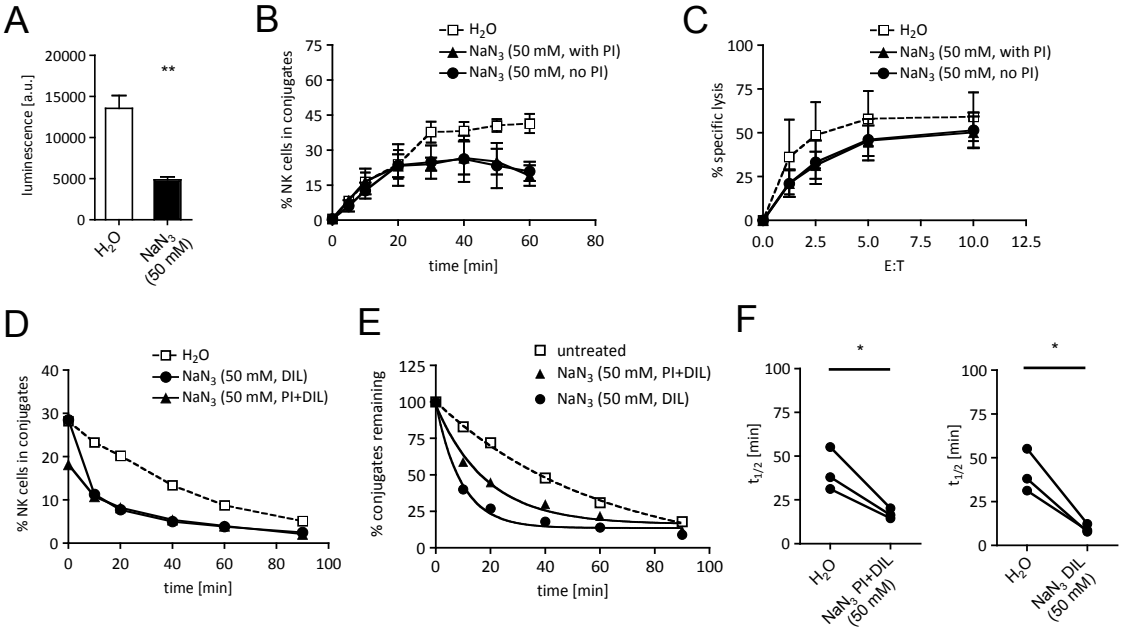

Fig. 4.15: Depletion of intracellular ATP by sodium azide impairs the potential of NK cells to form and maintain conjugates and reduces the lysis of K562 target cells. NK cells were either treated with 50 mM sodium azide or H_2O as solvent control. (A). The relative amount of ATP after 2 h treatment was determined using the ATPlite assay system. (B) Conjugate formation by treated NK cells with K562 target cells. NK cells were either pre-treated for 2 h or the inhibitor added at the time point of mixing with target cells. In both conditions the inhibitor concentration was present during the assay. (C) Pre-treated or not pre-treated NK cells were applied in a 4 h standard ^{51}chromium release assay against K562 target cells. Sodium azide was present in the assay. (A-C) Values are shown as mean ± SD. (n=3) (D-F) In the conjugate decay assay either pre-treated NK cells were applied with the inhibitor present during the assay or sodium azide was added at the point of dilution to untreated conjugates. One representative experiment is shown in (E) and (D), and the quantification of experiments with three different donors in (F). (*< 0.05).

4.8 Cytoskeleton dynamics

4.8.1 A dynamic actin cytoskeleton is indispensable for conjugate stability

The formation of the aNKIS is strongly depending on actin cytoskeleton rearrangement, which is considered to occur at the beginning of the effector stage (Orange, 2008; Mace et al., 2014). These rearrangements also play an important role for regulation and transit of lytic granules in the process of degranulation (Brown et al., 2011; Rak et al., 2011). It was shown that treatment with the actin cytoskeleton inhibitors cytochalasin D (cyto D) and jasplakinolide (jaspla) interfered with conjugate formation and reduced the cytotoxicity of NK cells (Cooper, 1987; Bubb et al., 1994; Orange et al., 2002; Wulfing et al., 2003; Rak et al., 2011). Therefore, we tested both substances in our system. Cyto D is a destabilizing reagent, leading to depolymerization of F-actin (Flanagan&Lin, 1980; Goddette&Frieden, 1986; Cooper, 1987). In contrast jasplakinolide stabilizes F-actin by preventing its degradation (Bubb et al., 1994; Bubb, 2000; Holzinger, 2009). NK cells were pre-treated for 30 min with the respective inhibitor before addition of the K562 target cells. Both treatments nearly abolished the cytolytic capacity (Fig. 4.16 A) and strongly affected the stability of the conjugates. Addition of cyto D to the conjugates at the point of dilution reduced the half-life by 89 % from 63.9 ± 25.1 min to 6.6 ± 1.5 min compared to the solvent control DMSO (Fig. 4.16 B). Similarly, use of jasplakinolide decreased the half-life to 7.7 ± 3.5 min (88 %; Fig. 4.16 C). This shows, in accordance with literature, that a dynamic cytoskeleton is indispensible for the function of NK cells and the maintenance of conjugates.

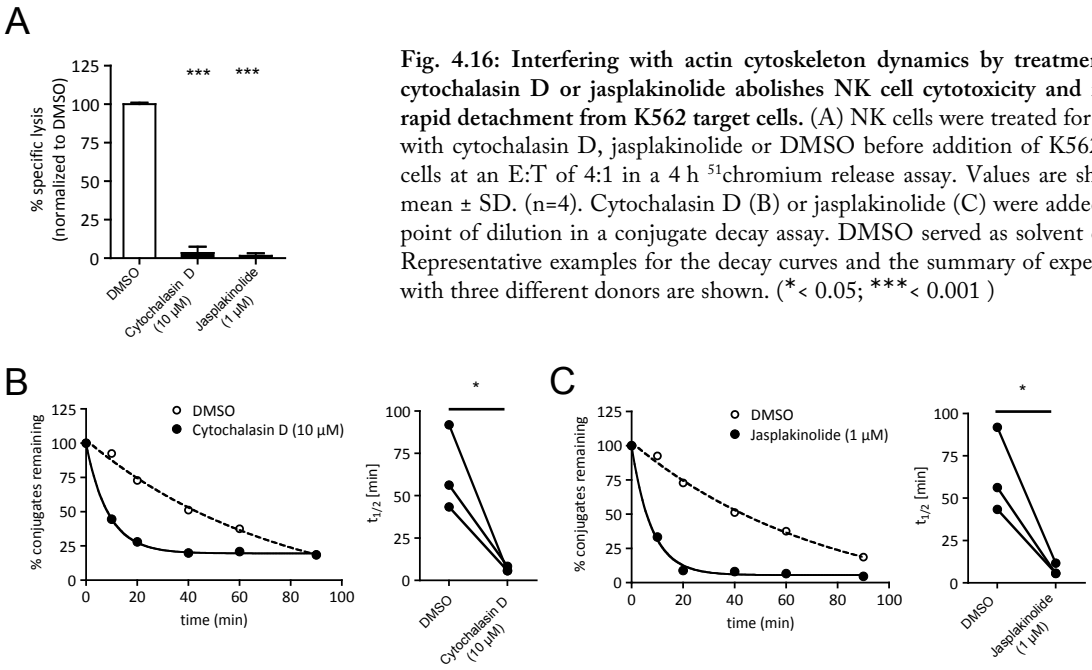

Fig. 4.16: Interfering with actin cytoskeleton dynamics by treatment with cytochalasin D or jasplakinolide abolishes NK cell cytotoxicity and induces rapid detachment from K562 target cells. (A) NK cells were treated for 30 min with cytochalasin D, jasplakinolide or DMSO before addition of K562 target cells at an E:T of 4:1 in a 4 h ^{51}chromium release assay. Values are shown as mean ± SD. (n=4). Cytochalasin D (B) or jasplakinolide (C) were added at the point of dilution in a conjugate decay assay. DMSO served as solvent control. Representative examples for the decay curves and the summary of experiments with three different donors are shown. (*< 0.05; ***< 0.001)

4.8.2 Tubulin

The degranulation process is not only strongly dependent on actin rearrangement but is considered to also depend on the microtubule cytoskeleton. The convergence of lytic granules to the microtubule organizing center (MTOC) and the recruitment to the synapse occur along microtubules (Katz et al., 1982; Stinchcombe et al., 2006; Banerjee et al., 2007). Here, we used two inhibitors to interfere with microtubules. Nocodazole destabilizes microtubules and induces their depolymerization (Vasquez et al., 1997). Paclitaxel on the contrary stabilizes microtubules (Amos&Lowe, 1999). Treatment of the NK cells with these inhibitors caused a minor, although for nocodazole (9.3 %) significant, reduction of the cytotoxicity towards K562 target cells (Fig. 4.1.5 A). If added to the standard decay assay with K562 cells at the point of dilution, only nocodazole decreased the half-life of the conjugates (DMSO: 29.3 ± 11.6 min, nocodazole: 18.1 ± 6.4 min; reduction: 41 %; Fig. 4.17 B), whereas paclitaxel seemed not to affect the conjugate stability (DMSO: 47.1 ± 10.1 min, paclitaxel 47.3 ± 17.3 min; Fig. 4.17 C). Thus, the interference with the microtubule cytoskeleton affects the cytotoxicity of NK cells only slightly. Considering that depolymerizing the microtubules by nocodazole reduced the half-life, whereas stabilizing by paclitaxel does not, indicates a necessity of formed microtubules for the maintenance of conjugates.

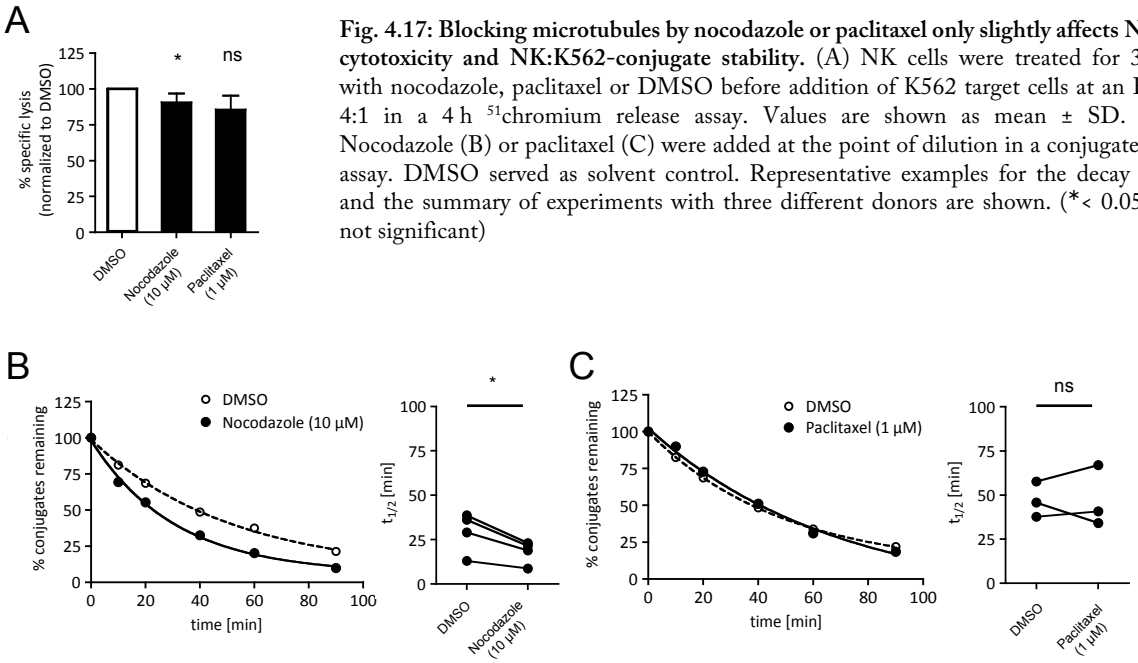

Fig. 4.17: Blocking microtubules by nocodazole or paclitaxel only slightly affects NK cell cytotoxicity and NK:K562-conjugate stability. (A) NK cells were treated for 30 min with nocodazole, paclitaxel or DMSO before addition of K562 target cells at an E:T of 4:1 in a 4 h ^{51}chromium release assay. Values are shown as mean ± SD. (n=4). Nocodazole (B) or paclitaxel (C) were added at the point of dilution in a conjugate decay assay. DMSO served as solvent control. Representative examples for the decay curves and the summary of experiments with three different donors are shown. (*< 0.05; ns = not significant)

4.9 MMP/ADAM inhibitors

Metalloproteinases as MMPs (matrix metalloproteinases) and ADAMs (a disintegrin and metalloproteinases) located at the cell surface play a pivotal role in immunology. For instance, they have been described to cleave CD16 and thereby regulate receptor down-modulation (Peruzzi et al., 2013; Romee et al., 2013; Zhou et al., 2013; Parsons et al., 2014). Additionally, these enzymes are found to play a role in cancer. As matrix-degrading enzymes they are implicated in invasion processes. Furthermore, they were also described to shed activating ligands, which then bind to NK cells rendering them hyporesponsive (Groth et al., 2011). As described for CD16, metalloproteinases might target other activating NK cell surface receptors and thereby regulate the interaction with the target cell. Therefore, we tested two inhibitors of MMPs and ADAMs to evaluate their impact on conjugate stability. Batimastat targets the MMPs-1, -2, -3, -7 and -9 as well as ADAM-17 and -8 with increasing IC_{50} value. GM6001 targets MMPs-8, -9, -1, -2 and -3. Neither of the inhibitors affected the cytotoxicity towards K562 cells, when the NK cells were pre-treated and the inhibitors were present in the assay (Fig. 4.18 A, C). If batimastat or GM6001 were applied in the conjugate decay assay with K562 cells at the point of dilution, no changes in the half-life were detectable (Fig. 4.18 B, C). Therefore, a role of these MMPs and ADAMs for NK cell cytotoxicity and the stability of NK:target cell conjugates most likely can be excluded.

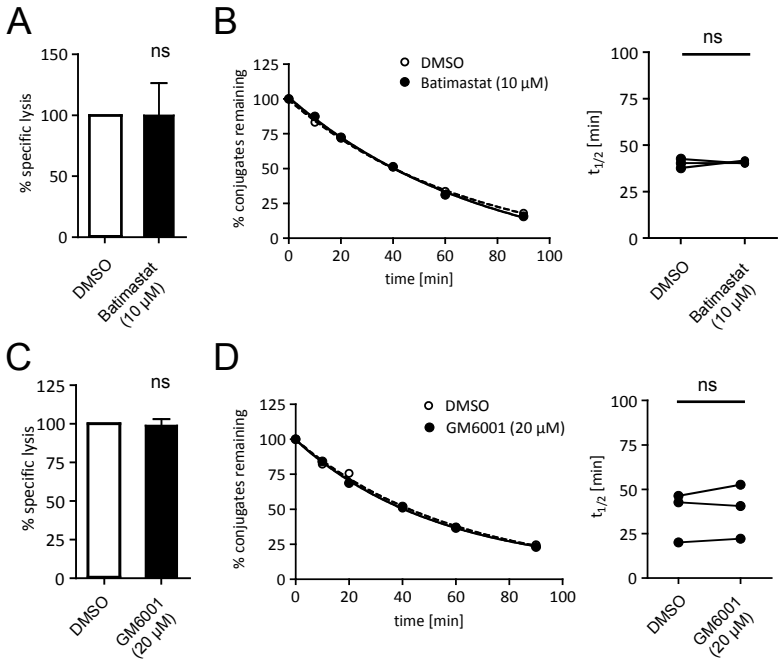

Fig. 4.18: Inhibition of metalloproteinases is not affecting NK cell-mediated cytotoxicity nor NK:K562-conjugate stability. NK cells were treated for 30 min with batimastat (A), GM6001 (B) or DMSO before addition of K562 target cells at an E:T of 4:1 in a 4 h ^{51}chromium release assay. Values are shown as mean ± SD. (n=3). In conjugate decay assays with K562 target cells batimastat (B), GM6001 (D) or DMSO were added at the point of dilution. Representative examples for the decay curves and the summary of experiments with three different donors are shown. (ns = not significant).

4.10 Target cell survival

The purpose of the formation of the activating NK cell synapse is the directed lysis of the target cell. An interesting emerging question was, which role the target cell death or survival plays for the kinetics of detachment of NK cells from target cells. It might be the death and the mechanisms that are induced during apoptosis, e.g. the phosphatidylserine flip or the loss of plasma-membrane integrity that induce detachment (Bouchier-Hayes et al., 2008; Wlodkowic et al., 2011). Thus, we tried different approaches to inhibit target cell lysis, or vice versa make the target cells more susceptible increasing the pace of lysis. To augment the sensitivity of K562 cells for NK cell-mediated lysis, the target cells were pre-incubated with the proteasome inhibitor Mg132. Unfortunately, the treatment did not induce the desired changes in the susceptibility towards NK cell cytotoxicity (data not shown).

4.10.1 Prevention of target cell death

In contrast to elevating the susceptibility of the target cells towards NK cell-mediated lysis, we aimed to prevent target cell death. If the detachment were influenced by target cell viability, a prolonged survival would suppress the detachment of the NK and thereby increase the conjugate half-life. A main mechanism of NK cells to induce target cell apoptosis is directed release of cytotoxic effector molecules, e.g. perforin and granzymes, into the synaptic cleft. Perforin forms pores in the target cell membrane inducing endocytosis as a rescue mechanism (Krzewski&Coligan, 2012). For the uptake of granzyme B different endocytosis mechanisms have been suggested. This includes fluid phase endocytosis, mannose 6-phosphate receptor-mediated endocytosis or heat shock protein 70 (HSP70)-mediated endocytosis (Gross et al., 2003). In the target cell, granzyme B initiates via different pathways caspase-cascades cumulating in apoptosis of the target cell. To counteract this effect we used the pan-caspase inhibitor Z-VAD-FMK (Sedelies et al., 2008). Unfortunately, we did not see increased survival of the treated target cells (data not shown) and therefore did not follow this idea further.

Instead of interfering with the induction of apoptosis in the target cell, we aimed to counteract the effector functions on the side of the NK cells. The first idea was to directly interfere with the release of the cytotoxic effector molecules, but prevention of NK cell-degranulation is a challenging task. One inhibitor known to reduce the amount of degranulation is blebbistatin. The compound inhibits myosin IIA, a motor protein that is required for the exocytosis of cytolytic granules in NK cells (Kovacs et al., 2004; Andzelm et al., 2007; Sanborn et al., 2009; Sanborn et al., 2011). To verify the inhibitory effect of blebbistatin on target cell-induced degranulation, the surface exposure of CD107a on treated NK cells after coincubation with K562 target cells was determined using flow cytometry.

The NK cells were pre-treated for 1 h with (-)-blebbistatin, the inactive enantiomer (+)-blebbistatin or the solvent control DMSO and the inhibitor present during the assays. A minor reduction of degranulation by 8 % was observed compared to the inactive analog (Fig. 4.19 A). The weak effect of the treatment could be due to the pre-activated status of the NK cells by culture with IL-2. Accordingly, the lysis of K562 target cells was reduced moderately by 28 % (Fig. 4.19 B). Since the NK cells were pre-treated, their ability to form conjugates was confirmed first. As shown in figure 4.19 C the treatment did not alter the capacity to form conjugates compared to the inactive (+)-blebbistatin or the solvent control. If NK cells pre-incubated with blebbistatin were applied in the conjugate decay assay the inhibition of myosin IIA increased the half-life of NK-target cell conjugates by 23 % from 40.8 ± 4.9 min for (+)-blebbistatin to 52.2 ± 4.10 min for (-)-blebbistatin (Fig 4.19 D). Myosin IIA is an ATPase, therefore we assessed if the treatment affects the cellular ATP level. The treatment did not change the level of ATP in the NK cells compared to the solvent control or the inactive analog (Fig. 4.19 E). Thus, reducing or inhibiting the degranulation of NK cells might increase the stability and thereby the half-life of NK:target cell conjugates. The reduced target cell death could be a possible cause for this observation. Even though, prevention of degranulation as such might also affect the detachment of NK cells from targets.

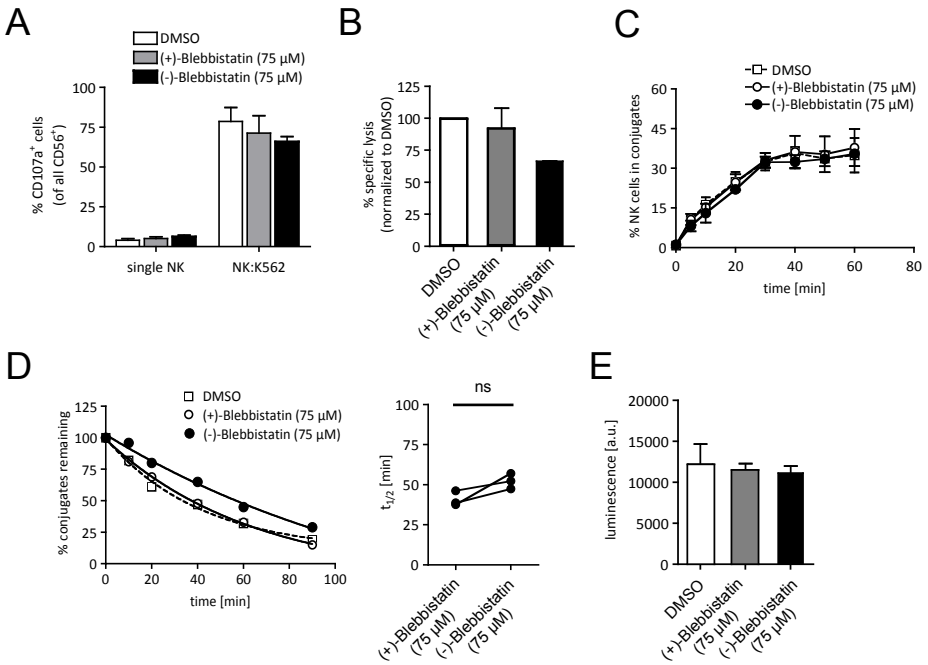

Fig. 4.19: Reduction of NK cell degranulation by blebbistatin reduces the lysis of K562 target cells and increases the half-life of NK:K562-conjugates. NK cells were pre-treated for 1 h with (-)-, (+)-blebbistatin or the solvent control DMSO. The inhibitor concentration was kept constant during the assays. K562 cells were used as targets. (A) CD107a (H4A3) surface expression after 4 h co-incubation with K562 cells (n=3). (B) Standard 4 h ^{51}chromium release assay. (E:T=4:1; n=3) (C) Conjugateformation assay. (n=3) (D) Conjugate decay assay. One representative decay curve and the quantification of experiments with three different donors are shown. (E) Relative intracellular ATP level of treated NK cells were determined in an ATPlite assay. (n=3) (A-C, E) Values are shown as mean ± SD. (ns = not significant)

As that degranulation was only partially inhibited by blebbistatin, we alternatively aimed to target perforin to effectively prevent target cell death induction. A known and established inhibitor for perforin is concanamycin A (CMA) (Kataoka, 1994; Kataoka et al., 1996). CMA belongs to the plecomacrolide-defined class of macrolide antibiotics that targets vacuolar-type, proton-translocating ATPases (V-ATPases) and ATPases with phosphorylated states (P-ATPases) (Drose&Altendorf, 1997). In eukaryotic cells V-H^+-ATPase is expressed on the plasma membrane as well as on the membrane of intracellular compartments. By the ATP-dependent transport of protons from the inside of the compartment into the cytosol it maintains an acidic pH in the compartments, e.g. lytic granules (Kataoka et al., 1996). This acidic pH in turn is required by cathepsin L which cleaves perforin from its immature to its mature active form by removing a glycosylated carboxy-terminal peptide (Uellner et al., 1997; Konjar et al., 2010). In preliminary studies we tested the inhibitor for its capacity to reduce mature perforin. NK cells were treated for 3 h with the inhibitor or the respective solvent control DMSO. The expression of perforin was assessed by western blot using the monoclonal anti-perforin1 antibody Pf344, which under denaturating, non-reducing conditions detects both isoforms. After treatment, although the inactive precursor was still detectable, the mature form was not, even after long exposure (Fig. 4.20 A, red rectangle). In the solvent control-treated samples the signal for the mature form is much stronger compared to the inactive form, indicating an exceeding amount of cleaved perforin. To test if the effect of CMA is reversible, we washed the cells after the treatment and incubated them for another 1 h and 4 h with or without the inhibitor present. In both conditions no mature perforin was detectable after 4 h. This shows that CMA treatment effectively and irreversibly induced to depletion of mature perforin in NK cells. To verify the results, we tested another monoclonal antibody against perforin in flow cytometry. We intracellularly stained treated cells with the anti-perforin antibody δG9, which does not distinguish between the both forms. After 3 h treatment with CMA the amount of perforin was significantly reduced by 73 % compared to untreated and solvent control-treated cells. The remaining perforin signal could be the immature form that is detected by the δG9 antibody. As control we stained for intracellular CD107a, another protein found in lytic granules. CD107a was still detectable after treatment and its expression rather increased slightly by 11 %. (Fig. 4.20 B). It was not clear whether the treatment with CMA leads to a passive reduction of mature perforin by preventing new formation and normal turnover, or if an active degradation process would be induced. Uellner and colleagues (1997) suggest, that the increased pH in the lytic granules by inhibition of V-H^+-ATPase induces an accelerated degradation of cleaved perforin (Uellner et al., 1997). Therefore, we treated NK cells with cycloheximide (CHX) that interferes with protein biosynthesis and thereby prevents the formation of new perforin precursor. The amount of perforin after treatment for up to 4 h with two different concentrations was monitored using western blot technology. As shown in Fig. 4.20 C in the long exposure of the film, the amount

of immature perforin decreased with advancing incubation time if the cells are treated with either concentration compared to the untreated cells. In contrast, the amount of mature active form does not change. Thus, the reduction of mature perforin induced by CMA could not be simply due to normal protein turnover but is rather due to increased degradation.

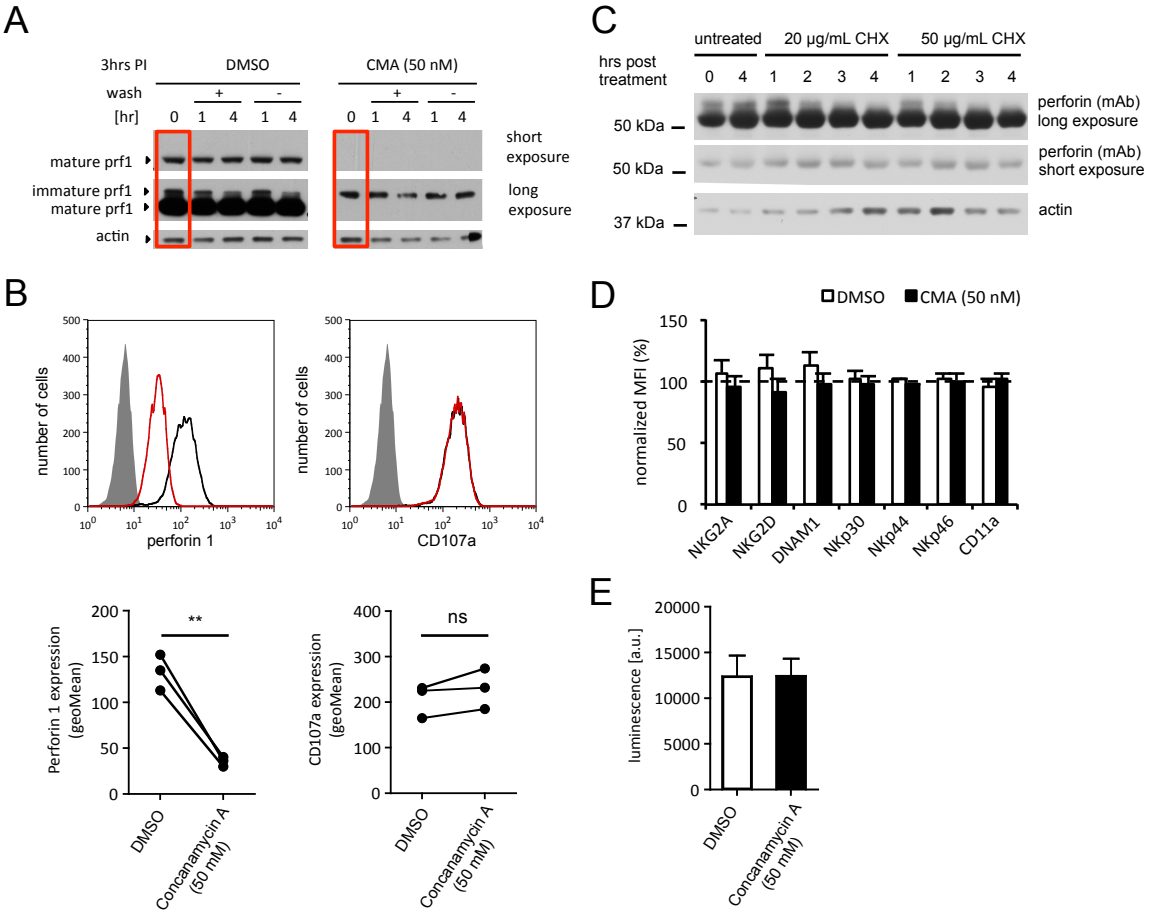

Fig. 4.20: Treatment of NK cells with concanamycin A (CMA) irreversibly depletes mature perforin. (A) NK cells were treated with CMA or solvent control for 3 h. Subsequently, the cells were washed and incubated for up to 4 h with (+) or without (-) the inhibitor present. Cell lysates were analyzed for perforin (prf1) expression (PF344). Actin levels were determined as loading control. Two different exposures for perforin detection are shown. (one representative example; n=3) (B) Intracellular staining for perforin (clone: δG9; *left*) and CD107a (clone: H4A3, *right*) after 3 h CMA treatment. Histograms of one representative experiment are shown (solid grey - isotype control of CMA-treated cells; specific staining of DMSO- (black line) and CMA-treated (red-line) NK cells). Lower panels show the quantification of three different donors. (C) NK cells were treated for 4 h with cycloheximide (CHX) in the indicated concentrations. Cell lysates were analyzed as in (A) (one representative example; n=3). (D) Surface expression of various NK cell receptors after 3 h treatment with CMA or DMSO was determined via flow cytometry. The mean fluorescent intensities (MFIs) were normalized to untreated cells. (n=3) (E) Relative intracellular ATP level of treated NK cells were determined in an ATPlite assay. (n=3) (D, E) Values are shown as mean ± SD.

Since the V-ATPases are implicated in various cell functions, e.g. vesicular transport, inhibition might have side effects besides depletion of mature perforin. To verify that the treated NK cells are still able to interact with target cells, we analyzed the surface expression of various receptors and the integrin alpha L chain (CD11a) that is part of the lymphocyte function-associated antigen-1 (LFA-1).

Compared to untreated or DMSO treated controls neither of the tested proteins showed significant changes in the surface expression detected by flow cytometry (Fig. 4.20 D).

The V-H$^+$-ATPase requires ATP for its proton transport function. To investigate if inhibition of the V-ATPase function affects the cellular ATP level, relative amount of intracellular ATP was determined. After 3 h CMA treatment the amount of ATP did not change compared to the controls indicating that the V-ATPase function has only limited impact on the intracellular energy level (Fig. 4.20 E).

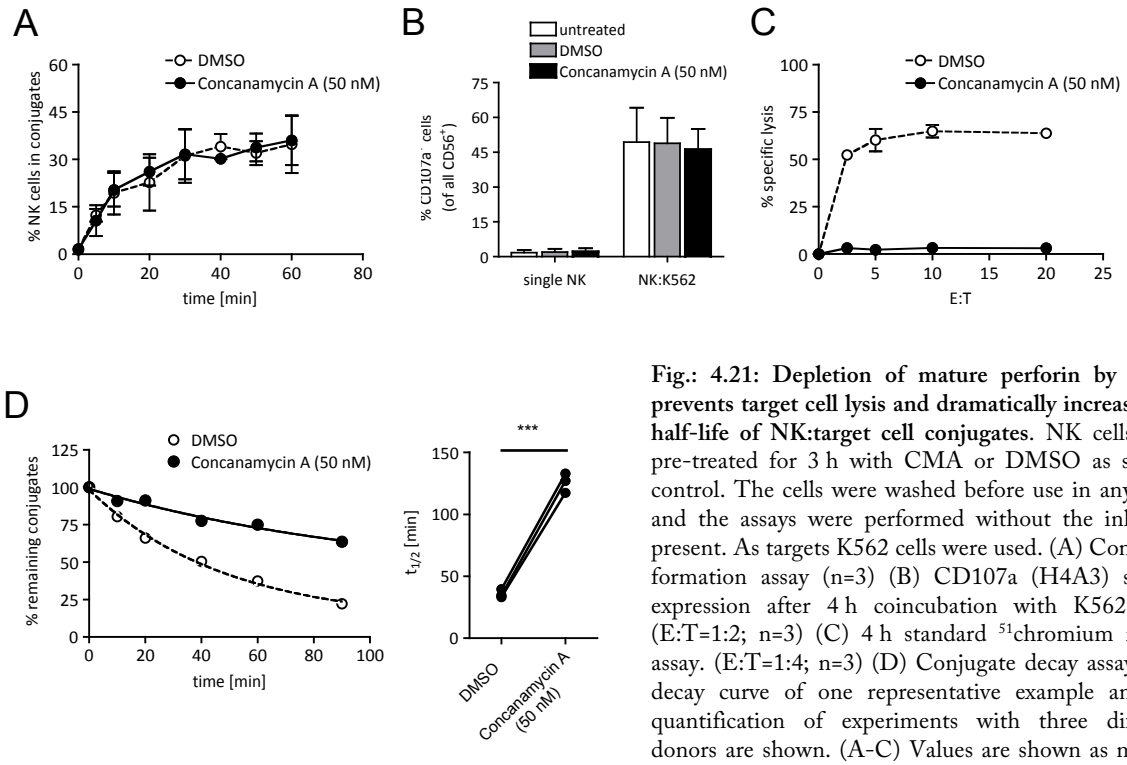

Fig.: 4.21: Depletion of mature perforin by CMA prevents target cell lysis and dramatically increases the half-life of NK:target cell conjugates. NK cells were pre-treated for 3 h with CMA or DMSO as solvent control. The cells were washed before use in any assay and the assays were performed without the inhibitor present. As targets K562 cells were used. (A) Conjugate formation assay (n=3) (B) CD107a (H4A3) surface expression after 4 h coincubation with K562 cells. (E:T=1:2; n=3) (C) 4 h standard ^{51}chromium release assay. (E:T=1:4; n=3) (D) Conjugate decay assay. The decay curve of one representative example and the quantification of experiments with three different donors are shown. (A-C) Values are shown as mean ± SD. (***< 0.001)

Since the effects induced by treatment with CMA are irreversible, functional assays were performed with pre-treated NK cells without inhibitor present in the assays. Thereby, the inhibitor does not influence the target cells. The potential of the mature perforin-depleted NK cells to form conjugates with K562 target cells was unchanged compared to solvent control treated cells (Fig. 4.21 A). Additionally, the target cell-induced degranulation detected by CD107a surface exposure was not influenced by the treatment (Fig. 4.21 B). As expected the lysis of the target cells was nearly abrogated by the depletion of mature perforin (Fig. 4.21 C). The detachment of perforin-depleted NK cells from target cells was drastically decelerated. The half-life (125.8 ± 7.8 min) determined in the conjugate decay assay was strongly increased by 352 % compared to solvent control DMSO (35.8 ± 3.3 min) (Fig. 4.21 D). These data suggest that either the function of the vacuolar H$^+$-ATPase is indispensable

for the detachment of NK cells from target cells or the survival of the target cells does prevent the dissociation of the conjugates.

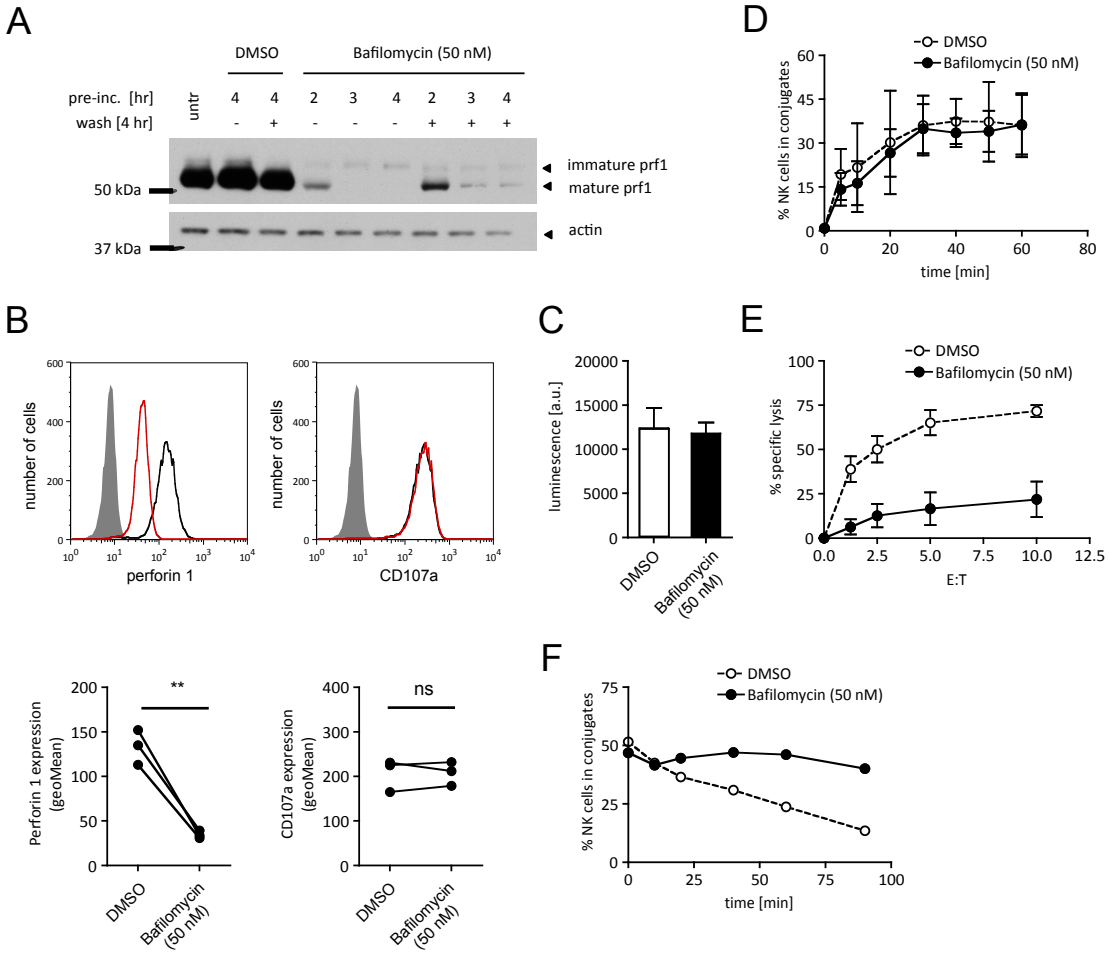

Fig. 4.22: **Treatment of NK cells with bafilomycin A1 reversibly depletes mature perforin and thereby reduces target cell lysis and increases NK:K562-conjugate stability.** (A) NK cells were treated with bafilomycin or solvent control for 3 h. Subsequently, the cells were washed and incubated for up to 4 h with (+) or without (-) the inhibitor present. Cell lysates probed for perforin (prf1) expression (PF344) and actin as loading control. One representative experiment is shown (n=2) (B-F) NK cells were pre-treated with bafilomycin or DMSO, washed and applied in the assays without the inhibitor present. (B) Intracellular staining for perforin (clone: δG9; *left*) and CD107a (clone: H4A3, *right*) after treatment. Histograms of one representative experiment are shown (solid grey - isotype control of bafilomycin-treated cells; specific staining of DMSO- (black line) and bafilomycin-treated (red-line) NK cells). Lower panels show the quantification of three different donors. (C) Relative intracellular ATP level in treated NK cells determined in an ATPlite assay (n=3) (D) Conjugate formation assay. (n=3) (E) 4 h standard ^{51}chromium release assay. (E:T=1:4; n=3) (F) Conjugate decay assay. The decay curve of one representative example of three experiments with different donors is shown. (C-E) Values are shown as mean ± SD.

To validate the effect seen with CMA we tested another V-H$^+$-ATPase inhibitor. Bafilomycin A1 is a member of the bafilomycin family that is structurally related to the class of concanamycins. As for CMA the effect of the treatment on the intracellular perforin level was determined first. NK cells were treated for up to 4 h and the perforin expression analyzed via western blot using the perforin-specific antibody Pf344. Compared to untreated and DMSO-treated cells the amount of mature perforin is

strongly reduced already after 2 h incubation and after 3 h it is not detectable anymore. If the inhibitor was removed and the cells incubated further without inhibitor the signal slightly increased again indicating that the observed effect is partially reversible (Fig. 4.22 A). Via intracellular flow cytometry a reduction of the perforin level by 74 % was detected. This was comparable to the effect seen by CMA-treatment (Fig. 4.20 B; Fig. 4.22 B). However, the level of intracellular CD107a was unchanged. As seen for the CMA-treatment inhibiting the V-H^+-ATPase has no influence on the intracellular ATP-level (Fig. 4.22 C). In the further experiments NK cells were pre-treated for 3 h and the assays were performed without the inhibitor present. The potential of the treated NK cells to form conjugates was not altered by the treatment compared to the DMSO-treated NK cells (Fig. 4.22 D). The cytotoxicity of bafilomycin A1-treated cells was reduced, but not fully abolished as seen for the CMA treatment (Fig. 4.21 C). This could be due to the restored mature perforin seen in western blot analysis after 4 h of incubation without the inhibitor. As seen for CMA the detachment of the NK cells from the target cells was dramatically decelerated (Fig. 4.22 F), for two of three experiments the half-life could not be determined since there was almost no decay of conjugates (data not shown). The observation that the detachment was decelerated this much although target cell lysis was not completely blocked, indicates that the effect seen is rather due to V-ATPase inhibition rather than to prevented target cell death.

To prove, if the effect seen is due to loss of mature perforin, we attempted to knock down the protein by RNA interference. We tested four different oligonucleotides targeting perforin 1-mRNA either separately or in various combinations and determined the amount of perforin after 48 h via western blot. Unfortunately, reduction of mature perforin was not achieved by any of the treatments (data not shown).

To interfere with the intracellular perforin level without affecting the vacuolar H^+-ATPase we used the ionophore monensin. Because of its effects on intracellular trafficking the compound is widely used for intracellular retention of proteins, e.g. cytokines (Tartakoff, 1983). As ionophore it allows H^+-exchange between intracellular compartments, e.g. acidic lytic granules and the cytosol and thereby leads to an increased pH in these compartments. The result, similar to the effect induced by CMA or bafilomycin A1, causes inhibition of important enzymes as the ones that are required for perforin cleavage. So far the effect of monensin on the perforin level has not been studied yet, therefore we first titrated the inhibitor and detected the level of intracellular perforin via western blot using the anti-perforin antibody Pf344. Already after 1 h treatment the amount was reduced in a dose-dependent manner. The concentration of 8.6 µM monensin effectively depleted mature perforin without affecting he amount of the immature precursor (Fig. 4.23 A). Additionally, the reversibility of perforin-

treduction was investigated. Pre-treated NK cells were incubated for another 24 h without the ionophore present and samples taken every 4 h. As seen before, after 1 h treatment the mature perforin is nearly undetectable. The signal reappeared after 4 h without monensin and further increased further over time. Although, it did not reach the levels detected in untreated or DMSO-treated cells. Additionally, as control the amount of granzyme B was detected using the monoclonal antibody Gb11. The treatment is not affecting the level of intracellular granzyme B in the NK cells (Fig. 4.23 B). Monensin-induced reduction of perforin was also verified via flow cytometry using the antibody δG9. In treated NK cells perforin was reduced by 69 % compared to control treated NK cells, whereas the amount of CD107a remained unaffected (Fig. 4.23 C). Interestingly, the different donors already showed large variation in their baseline expression of perforin and CD107a, but the trend was the same nevertheless.

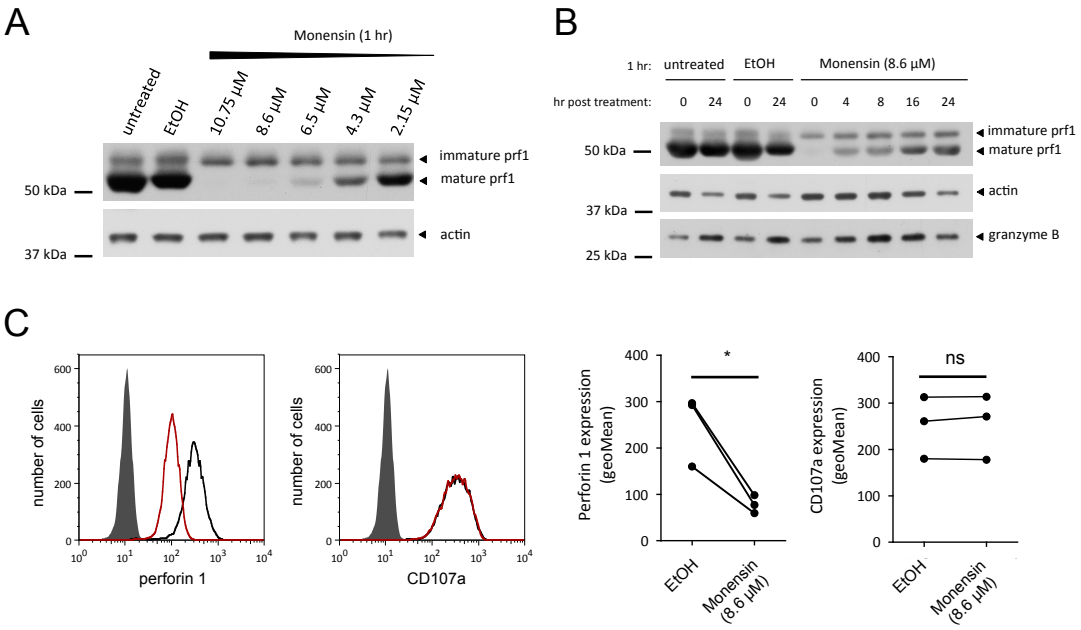

Fig. 4.23: Monensin leads to depletion of mature perforin in NK cells. (A) NK cells were treated for 1 h with different monensin concentrations or the solvent control EtOH. Subsequently, cell lysates probed for perforin (PF344) and actin as a loading control. (one representative example; n=3) (B) Pre-treated NK cells were washed and incubated for 24 h without the monensin present. Samples were taken every 4 h and analyzed for perforin and actin expression as in (A). (one representative experiment; n=3) (C) Intracellular staining for perforin (clone: δG9; *left*) and CD107a (clone: H4A3, *right*) after treatment. Histograms of one representative experiment are shown (solid grey - isotype control of monensin-treated cells; specific staining of EtOH- (black line) and monensin-treated (red-line) NK cells). Right panels show the quantification of three different donors.

For functional assays NK cells were pre-treated for 1 h with 8.6 µM monensin. Since the observed effect was reversible, the compound was present during the assays. Next the ability of pre-treated NK cells to form conjugates with K562 target cells was examined. The treatment slightly reduced conjugate formation compared solvent-treated cells (Fig. 4.24 A). On NK cells incubated with monensin, the surface expression of CD107a is slightly increased after 2 h co-incubation with the

targets. This was expected since monensin is widely used in degranulation assays to prevent the fast re-internalization and degradation of CD107a (Fig. 4.24 B). The titration of monensin in the cytotoxicity assay showed a dose-dependent reduction in lysis resembling the reduction of perforin seen in Fig. 4.24 A. The lowest concentration did not affect the lysis, whereas higher concentrations of 8.6 µM and 10.8 µM potently reduced the lysis to a similar extent (Fig. 4.24 C). Surprisingly, the half-life of conjugates formed by monensin-treated compared to EtOH-treated NK cells was not altered. Although the determined half-lives differed between individual donors the stability of the conjugates of monensin-treated NK cells was always comparable to control conditions (Fig. 4.24 D). Thus, although treatment with monensin prevents target cell death the detachment of NK cells from the target cells is unchanged.

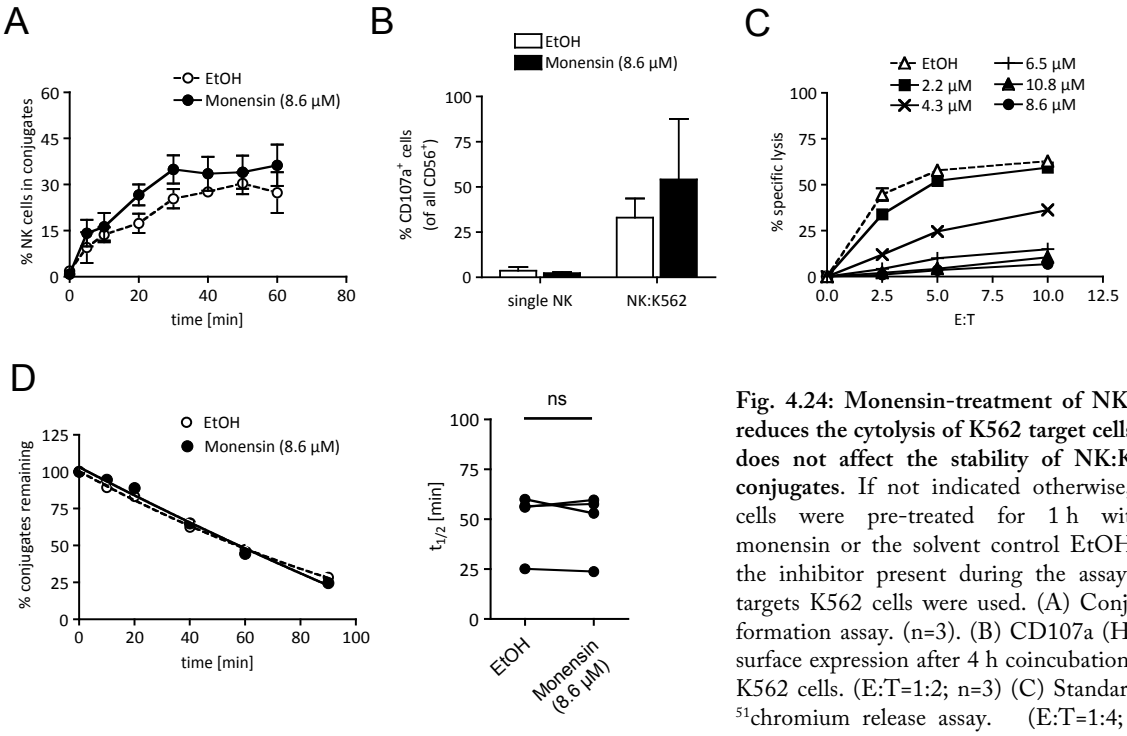

Fig. 4.24: Monensin-treatment of NK cells reduces the cytolysis of K562 target cells, but does not affect the stability of NK:K562-conjugates. If not indicated otherwise, NK cells were pre-treated for 1 h with 8 monensin or the solvent control EtOH and the inhibitor present during the assays. As targets K562 cells were used. (A) Conjugate formation assay. (n=3). (B) CD107a (H4A3) surface expression after 4 h coincubation with K562 cells. (E:T=1:2; n=3) (C) Standard 4 h ^{51}chromium release assay. (E:T=1:4; n=2) (D) Conjugate decay assay.
The decay curve of one representative example and the summary of 4 different donors are shown. (ns = not significant) (A-C) Values are shown as mean ± SD.

5. Discussion

5.1 Tools to investigate the detachment process

The understanding of NK cell mediated cytotoxicity and the requirement of the formation of the NK cell synapses are a main focus in NK cell research. The increasing understanding of its regulation and especially the deregulation in disease leads to new approaches in therapy. The steps of the synapse formation up to the release of lytic granules and the induction of apoptosis in target cells are fairly well, although not fully deciphered. Since it was found that NK cells can kill not only one target, but in some cases consecutively up to 16 (Bhat&Watzl, 2007; Choi&Mitchison, 2013; Vanherberghen et al., 2013), the question what leads to subsequent breakage of the synapse and the detachment from the target cell becomes more intriguing.

Here, we used a flow cytometry-based approach originally described in 2009 to determine factors influencing the detachment (Culley et al., 2009). The determined half-life for conjugates formed between human IL-2 activated NK cells and the target cell line K562 was about 47 min. It is important to take into consideration that this is an artificial *in vitro* system and therefore the half-life *in vivo* might be different. The duration of NK:target cell-contacts described in the literature is quite diverse most probably depending on multiple factors such as pre-activation of the NK cells, the type of effector or target cell or the assay system as such (Chauveau et al., 2010; Choi&Mitchison; Vanherberghen et al., 2013). Additionally, we observed differences in the half-lives between individual donors. This is in line with data from other groups, that also observed differences even between NK cells of single donors (Vanherberghen et al., 2013).

Minor changes in the assay set up as varying E:T ratios or pre-coincubation times have only slight influences on the determined half-life. This indicates that the half-life determined in the assay is consistent and changes most probably dependent only on cell-intrinsic factors.

Enabling conjugates to form normally and subsequently interfere with the detachment in our system e.g. by using inhibitors allows identification of factors that might be important for sustained conjugation or detachment. Once an important component is identified, more specific and more physiological approaches can be applied. Therefore, the established system provides a fast and comparably easy technique to determine events or molecules involved in the detachment process.

Furthermore, to visualize the detachment process of NK cells from target cells we established an assay based on life cell imaging and a flow chamber system. The low magnification did not allow definition of mature synapses, therefore we refrained from classifying the observed contacts as conjugates. Interestingly, the trend for the half-life of the NK:target cell contacts was similar compared to the results of flow cytometry-based assay. Varying the assay conditions of the microscopy-based assay, e.g.

application of inhibitors to the medium flow or changing target cell densities will allow gaining further information about the NK cell detachment.

5.2 Presence of a new susceptible target causes detachment

Serial killing increases the efficiency of NK cell cytotoxicity. Some NK cells are able to consecutively kill multiple times (Ullberg&Jondal, 1981; Bhat&Watzl, 2007; Tomescu et al., 2009; Choi&Mitchison, 2013; Lopez et al., 2013; Vanherberghen et al., 2013). Interestingly, Choi and Mitchison showed that the availability of a new target in close proximity induces detachment from a previous target. Moreover, it increases the speed of the killing events, a phenomenon they described as "kinetic priming" (Choi&Mitchison, 2013). In line with these observations, we found that addition of an exceeding amount of targets to pre-formed conjugates accelerated the NK cell detachment from the initial targets. This indicates that engagement of a new susceptible target induces processes leading to detachment. This could possibly include redistribution of adhesion molecules, activating receptors and the according signaling molecules. In contrast, fixed target cells did not decrease the conjugate half-life. This indicates, that only susceptible targets affect the NK cell detachment. It is known, that NK cells can interact with susceptible and unsusceptible targets at the same time (Eriksson et al., 1999). The spatial separation of activating and inhibitory signaling events is important to protect harmless bystander cells. Consequently, even though the remaining contact to a previous target keeps the NK cell in an activated status, the activating signaling that is locally induced by the new target still might have to overcome inhibition. This additional activating signaling at different location in the cell might induce mechanisms causing detachment. On the other side, bystander cells inducing local inhibitory signaling, e.g. by MHC class I molecule expression might not induce the detachment. Interestingly, in the study of Choi and Mitchison, the NK cells remained attached over long periods if no new target was in proximity, even after induction of apoptosis in the target cell. The remaining question is how much and for how long an apoptotic cell could provide activating stimuli.

5.3 Surface phenotype of detached NK cells

Cell-cell interactions influence the phenotype and induce gene-expression and many other functions. Ligation-induced up- or down-modulations of surface receptors have been described as mechanism for the regulation of NK cell function. Therefore, we investigated surface pattern changes of human NK cells induced by contact to HeLa cells. Some of the tested receptors were not regulated. For CD56 no ligand was found yet. The lack of a ligand could explain, why the expression of the receptor does not require regulation. Similarly, changes in the expression of LFA-1 were not expected. Although it is triggered by ICAMs during cell-cell interaction, ligation-induced modulation of its surface level was

not described so far. Its function is rather regulated via clustering and conformational changes. Although ligands for DNAM-1 and NKp44 are expressed on HeLa cells (El-Sherbiny et al., 2007; Jarahian et al. 2011; Baychelier et al., 2013), the surface expression of these receptors was not altered after detachment. This indicates, that the receptors are either not modulated or the down-regulation takes longer than the observation time of the assay. Alternatively, the expression of the ligands could be too low to induce effective changes in the receptor surface exposure. In contrast, levels of other receptors were either increased or decreased. In consistence with the literature, we found reduced expression of 2B4 and NKG2D after target cell contact (Sandusky et al., 2006; Roda-Navarro&Reyburn, 2009). The HeLa cells used here were transfected with CD48, the ligand for 2B4 and expression of stress-induced NKG2D-ligands on HeLa cells was described before (El Sherbiny et al., 2007). The reduction of surface levels of these receptors therefore most probably was due to ligand interaction. A similar trend was observed for NKp46, although it was not significant. That indicated that the same mechanism might also be true for this receptor. The hypothesis is supported by data that show binding of NKp46 to HeLa cells (El Sherbiny et al., 2007). The reduction in the surface levels of these receptors could also be due to exchange of membrane parts and the associated receptors with the target cell along the synapse. This process was suggested to be involved in the regulation of NK cell activity (Roda-Navarro et al., 2006; Jarahian et al., 2011; Baychelier et al., 2013). In contrast to reduced expression, some of the analyzed receptors showed increased surface levels on late-detaching NK cells. This was expected for CD69 and CD107a. CD69 was described as an early activation marker for lymphocytes, which is rapidly upregulated on the surface after activation. Similarly, increased CD107a expression as marker for degranulation indicates that the NK:target cell-contacts were functional leading to NK cell activation. Surprisingly, a similar trend of increased expression levels on late detaching NK cells was also seen for NKp30 and NKG2A. B7-H6 as ligand for NKp30 was found on HeLa cells (Zhang et al., 2012; Fiegler et al., 2013). Up-regulation of surface expression in this short time frame seems rather unlikely. A plausible cause for this observation could be due to an enrichment of certain subpopulations with increased expression of these receptors during the assay. This is particularly interesting for NKG2A, since this observation is in accordance with the "rheostat model" for NK cell education. It describes a possible mechanism, why NK cells that lack inhibitory receptors for self-MHC I become hyporesponsive instead of hyperresponsive. In other words, NK cells with a high expression of inhibitory receptors and thereby increased sensitivity to inhibition display a strong responsiveness to activating signals (Brodin et al., 2009; Joncker et al., 2009). Recently, a study showed that licensed NK cells form more stable conjugates than unlicensed NK cells (Thomas et al., 2013). Therefore, the high NKG2A expression on the detaching NK cells could mark a strong effector phenotype that shows increased ability to remain attached to the targets. Taken together these data indicate that licensing not only increases the initial adhesion, but also the ability to

maintain the conjugates. In this context it is important to note, that the receptor would not be triggered in this specific case, since there is no ligand expressed on HeLa cells (Palmisano et al., 2005). It would be interesting to also compare other inhibitory NK cell receptors, e.g. KIRs, for their expression after target cell contact. Unfortunately, the NK cells here expressed the KIRs analyzed only very little or not at all. In general, we conclude that the interaction of NK cells with target cells leads to alterations in the surface expression pattern of several receptors, possibly regulating their activity. But further studies are required to uncover the correlation between certain phenotypes and the ability to remain in conjugates. Additionally, considering the hypothesis that receptor down-modulation is a mechanism for reduction of activating signaling it would be interesting to prevent of internalization, e.g. by inhibition of endocytosis.

Surface levels of activating receptors are not only modulated by internalization. Cleavage of CD16 after activation by various cell surface metalloproteinases has been described recently (Peruzzi et al., 2013; Romee et al., 2013; Zhou et al., 2013; Parsons et al., 2014). Other surface receptors are possibly regulated in a similar way. Thus, we inhibited MMPs (matrix metalloproteinases) and ADAMs (a disintegrin and metalloproteinase) with broad-spectrum inhibitors. But the treatment neither affected the NK cell-mediated cytotoxicity nor the stability of NK:target cell conjugates. Thus, either the treatment was not efficient enough to inhibit all metalloproteinases at the cell surface, or they have no impact on the surface receptors and thereby on the strength of cell-cell interaction.

5.4 Signaling and detachment

NK cell activity is strictly regulated by integration of activating and inhibitory signaling. Triggering of integrins or activating receptors induces synergistic and redundant signaling pathways, which can be interrupted at early steps by ligation of inhibitory receptors (Long et al., 2013). Conjugate formation and induction of effector functions depend on certain key factors, e.g. Src- and Syk-family kinases, PI3K or PLCγ (Brumbaugh et al., 1997; Jiang et al., 2000; Watzl&Long, 2010). In accordance with the literature, we found that inhibition of these molecules, except for PI3K, reduced the cytotoxicity of the NK cells. Hence, we analyzed the influence of these signaling molecules on the stability of NK:target cell conjugates by applying the specific inhibitors in the decay assay.

To analyze their impact on the conjugate stability and detachment without disturbing initial steps of the synapse formation, the inhibitors were added after the conjugates were formed. All inhibitors tested reduced the half-life of the formed conjugates. The deceleration of the detachment was stronger when Src kinases, PI3K or PLCγ were targeted compared to the impact of Syk kinase inhibition. Src kinases or PLCγ inhibition had a very strong effect, leading to almost immediate collapse of most of

the conjugates. Considering the importance for Src family kinase-mediated phosphorylation in the signaling pathways of all activating receptors, this was not surprising (Watzl&Long, 2010; James et al., 2013). Similarly, PLCγ activity was described to be crucial for NK cell function (Regunathan et al., 2005; Tassi et al., 2005; Caraux et al., 2006). Inhibition of PI3K required for generation of PIP3 surprisingly only slightly affected the cytotoxicity, which is in contrast to literature (Eissmann&Watzl, 2006; James et al., 2013). A plausible cause could be the pre-activation of the NK cells by IL-2 that might render them less susceptible to PI3K inhibition. Nevertheless, interfering with PI3K activity affected the stability of conjugates, although less effective than Src kinase or PLCγ inhibition. The least effect on the conjugate half-life was induced by Syk kinase family inhibition. Specifically targeting Syk had the same effect as using an inhibitor with a broader spectrum also targeting other Syk family kinases. This shows, that inhibition of Syk is not compensated by other Syk family kinases and that it has less impact on conjugate stability. Thus, these data indicate that besides the initial activating trigger required for induction of synapse formation, the continuance of early signaling is mandatory to maintain contacts. The aNKIS is a dynamic structure. For instance receptor-ligand interactions are constantly broken and regenerated leading to new signals. Phosphorylation and dephosphorylation events as basis for regulation of signaling molecules are subject to a constant turn over. Consequently, to facilitate the NK cell to perform its task, constant reactivation of the signaling molecules is mandatory. A main process induced by these early signaling events is the formation of F-actin facilitating actin cytoskeleton rearrangements. Recruitment and clustering of receptors are dependent on F-actin. Hence, loss of the anchor provided by the actin cytoskeleton would induce the redistribution of receptors and integrins and thereby weaken the contact between NK and target cell.

Besides these early events, we were interested in the importance of events further down stream. The MAP kinase pathway induced by PI3K activation was described to be required for granule polarization and exocytosis (Vyas et al., 2002). We targeted MEK1/2 and p38 with chemical inhibitors. It was shown before, that MEK inhibition only partially influences NK cell-mediated cytotoxicity (Abraha&Whalen, 2009). In consistence with these data, interfering with MEK1/2 activity induced a moderate reduction of target cell lysis. Interestingly, MEK signaling was not required for conjugate stability. p38 was described to be activated by CD16 ligation or target cell contact (Chini et al., 2000; Trotta et al., 2000), although its inhibition was only partially reducing the lysis. In our experiments we did not observe an effect induced by p38 inhibition neither on cytotoxicity nor on the conjugate stability. Therefore, we concluded that later events such as MAP kinase signaling were required for full cytotoxicity, but not for the stability of conjugates.

Another signaling molecule described to be important for NK and T cell function is PKCθ. The serine-threonine kinase of the novel, Ca^{2+}-independent PKC subfamily, was described to have an essential role in the breakage of synapses of $CD4^+$ T cells in mice and humans (Sims et al., 2007; Beal et al., 2008). However, this is discussed controversially since PKCθ also was found to be required for IS stability by increasing LFA-1 avidity (Letschka et al., 2008; Kong&Altman, 2013). In the human NK cell line YTS PKCθ was shown to phosphorylate WASp-interacting protein (WIP). WIP phosphorylation is not required for its interaction with WASp, but was proposed to be required for the recruitment of actin and myosin IIA to the WIP-WASp-complex (Krzewski et al., 2006) and thereby may have a role in regulating actin cytoskeleton rearrangements. Inhibition of PKCθ reduced the NK cell-mediated cytotoxicity, but did not affect the detachment from target cells. To verify the results, we tested the θ-specific pseudosubstrate inhibitor or knocked down the PKCθ protein. Surprisingly, these treatments did not confirm the results induced by the broad-spectrum inhibitor. This indicates, that other PKC isoforms are required for NK cell cytotoxicity and that in contrast to the observation in T cells PKCθ does not affect the stability of the IS formed by NK cells.

Regulation of NK cell activity by inhibitory signaling is dependent on various phosphatases as e.g. SHP-1 or -2. The dephosphorylation of early signaling molecules such as Vav1 or the phosphorylation of Crk led to interruption of activating signaling pathways (Stebbins et al., 2003; Peterson&Long, 2008; Abeyweera et al., 2011). We hypothesized that activity of phosphatases at advanced stages of cytolytic interaction might be a regulatory mechanism. Pervanadate is a common inhibitor of protein-tyrosine phosphatases. It irreversibly oxidizes their catalytic cysteine (Huyer et al., 1997). Treatment of NK cells with pervanadate led to a reduction of their ability to form conjugates and consequently to a reduction of target cell lysis. Since already conjugate formation was impaired we were not able to analyze its effects on the detachment. Another family of phosphatases is serine-threonine (S/T) phosphatases. Several signaling molecules e.g. Akt and Erk are activated by phosphorylation of serine or threonine residues. Thus, we chemically inhibited the phosphatases PP1, PP2A and PP3A. Treatment with okadaic acid did not affect NK cell-mediated cytotoxicity or the detachment process. In contrast inhibition by calyculin A strongly decreases target cell lysis and interfered with conjugate stability. Bajpai and Brahmi found a similar effect of okadaic acid and calyculin A in the NK cell line YT-Indy and described two proteins that showed increased kinase activity in calyculin A-treated cells, but these proteins have not been identified yet (Bajpai&Brahmi, 1994; 1996). PP3A is only inhibited by okadaic acid. The specificity of both inhibitors for PP2A is comparable, whereas calyculin A has a higher inhibitory effect on PP1. Thus, since only calyculin A showed effects on the NK cell-function these effects are most likely due to inhibition of PP1. This finding reveals a possible role for this phosphatase for NK cell mediated cytotoxicity and for maintenance of NK:target cell contacts. In T

cells PP1 was described to dephosphorylate and thereby activate cofilin (Samstag, 2003). It is required in T cell migration and activation by depolymerizing and/or severing actin filaments (Samstag et al., 2013). So far, the role of cofilin in NK cells has not been studied. Therefore, the here observed effect could be due to a yet unknown role of cofilin A in NK cells or the activity of two yet unknown kinases.

5.5 Energy and detachment

Berke and Gabison stated already in 1975 that formation, but not maintenance of T:target cell conjugates is energy-dependent (Berke&Gabison, 1975). In 1999, Davis and colleagues found that formation of inhibitory synapses is not affected by depletion of ATP (Davis et al., 1999). The importance of ATP levels in NK cells for their function has not been evaluated yet. Reduction of intracellular ATP-levels by sodium azide treatment affected the ability of NK cells to form conjugates and moderately decreased their cytotoxic function. Additionally, depleting ATP led to a rapid loss of conjugate stability. For synapses between NK cell and macrophages it was described, that treatment with azide led to a reduction of formed conjugates. This and the data generated here indicate that NK cell functions are at least partly dependent on ATP. This is in line with observations made by Abarca-Rojano and colleagues (Abarca-Rojano et al., 2009). They found that NK cells upon target cell contact rapidly consume their metabolic energy and that mitochondria reorganize towards the synapse, possibly to compensate the local loss of energy. ATP is required as substrate for kinases (Hubbard&Till, 2000) as well as by ATPases as the vacuolar H^+-ATPase or myosin IIA (Sanborn et al., 2009; Stewart et al., 2013). Thus, ATP is a requirement for full NK cell function. We inhibited vacuolar H^+-ATPases and the ATPase myosin IIA. Neither of the molecules was influencing the intracellular ATP-level in NK cells that were not challenged with target cells. This might be different during NK:target cell interaction. Additionally, inhibiting a single molecule class might not strongly impact the ATP consumption, since many different steps require energy. Furthermore, the importance of ATP for conjugate stability is in line with the observations for the significance of early signaling events. The kinases recruited by activating receptors require ATP as substrate. Therefore, reduction of the substrate would decrease the activating signaling and thereby destabilize the NK:target cell conjugates.

5.6 The cytoskeleton and detachment

The dynamics of the cytoskeleton are indispensible for NK cell effector functions (Brown et al., 2011; Rak et al., 2011; Brown et al., 2012; Mace et al., 2014). Already very early steps in synapse formation, such as receptor clustering and polarization of the cell are dependent on a flexible actin cytoskeleton. It was shown, that either stabilizing or destabilizing the F-actin affects conjugate formation and cytolytic

activity (Orange et al., 2002; Wulfing et al., 2003; Rak et al., 2011). According to this finding, interfering with actin rearrangements abolished NK cell-mediated lysis of the target cell. When interfering with the actin dynamics in already formed conjugates, we saw a rapid detachment as early as 10 min after treatment in either condition. Therefore, we conclude that even in formed lytic synapses the actin cytoskeleton needs to reorganize in order to maintain the conjugates. Additionally, Gross and colleagues found, that also reorganization of the target cell cytoskeleton is required for conjugate formation (Gross et al., 2010). Since in our system NK as well as target cells are affected by the treatment, integrity of the target cell cytoskeleton might also be important to stabilize conjugates.

On the contrary, in our system microtubule dynamics were less important for these functions. When we either stabilized or destabilized microtubules the cytotoxicity of the NK cells was almost not affected. This was surprising since convergence of lytic granules to the MTOC, although it is independent of microtubule rearrangements, requires intact microtubules (Mentlik et al., 2010). However, polarization of the complex of MTOC and lytic granules to the contact site was described to be dependent on microtubule and actin reorganization (Mentlik et al., 2010; Lagrue et al., 2013). Katz and colleagues found, that conjugate formation is not affected by microtubule inhibition, whereas lysis was suppressed (Katz et al., 1982). In our approach to study detachment we only saw effects if microtubules were destabilized and these were minor compared to the effects seen by interference with the actin cytoskeleton. Therefore, the presence of microtubules but not their dynamics seems to be required for conjugate stability.

5.7 Target cell survival and detachment

Our data revealed a possible correlation between target cell death and NK cell detachment. Prevention of target cell death by inhibiting caspase-cascades induced by granzyme B failed. This could be partially explained by the observation that granzyme B also induces caspase-independent apoptosis mechanisms (Trapani et al., 1998; Beresford et al., 1999; Lieberman, 2003). Additionally, the impact on the target cell by NK cell effector functions could be too robust to be easily interfered with. Other cytotoxic molecules released besides granzymes during degranulation, e.g. perforin or granulysin are also affecting the survival of the target cell. Similarly, attempts to increase the susceptibility to lysis by inhibiting the target cell proteasome were not successful.

Consequently, we interfered with the effector mechanisms of the NK cells aiming to prevent target cell death. Targeting myosin IIA that is required for lytic granule exocytosis in NK cells (Kovacs et al.; Andzelm et al., 2007; Sanborn et al., 2009; Sanborn et al., 2011) only slightly reduced granule exocytosis and also affected the target cell lysis only partially. Myosin IIA-inhibited NK cells showed

normal conjugate formation, but interestingly the decay of their conjugates was decelerated. The observed effect was mild but consistent for all donors tested. On that account, either the degranulation as such or the reduced target cell death might have influence on the stability of conjugates.

Because we could not fully prevent degranulation and release of cytotoxic effector molecules, we depleted mature perforin in NK cells. By targeting the V-H^+-ATPase in the membrane of lytic granules we induced an increase in the pH of lytic granules. This led to inhibition of cathepsin L that cleaves immature perforin and thereby generates its active form. Additionally, the increased pH is assumed to induce degradation of mature perforin probably as mechanism to protect the NK cell (Kataoka, 1994; Kataoka et al., 1996). We used two different inhibitors of the V-H^+-ATPase. In both cases, NK cells were still able to normally form conjugates, but their cytotoxicity was abrogated or at least strongly decreased. And interestingly, in both cases the detachment of NK cells from target cells was dramatically decelerated. The arising question remains, if this is due to prevented target cell death or if this effect is caused by inhibition of the V-H^+-ATPase as such. Additionally, there could be unknown side effects of the compounds.

To interfere with perforin levels in a similar way, but without targeting the V-H^+-ATPase, we used monensin. The H^+-ionophore reversibly increases the pH in lytic granules and thereby induces depletion of mature perforin. As seen for V-ATPase inhibition this led to almost full reduction of NK cell-mediated cytotoxicity. But surprisingly monensin-treatment had no influence on the stability of the conjugates. The ionophor induces a broad spectrum of unspecific effects e.g. vacuolarization (Pedersen et al., 1982; Pohlmann et al., 1984). Thereby a prolonging effect on the half-life by perforin depletion could be masked by other changes in the cell induced by the treatment. Alternatively, the observation indicates that the effect seen by V-H^+-ATPase inhibition is not due to prevented target cell death, but reveals a new role of the ATPase.

The vacuolar H^+-ATPase has been reported to be involved in receptor-mediated endocytosis, intracellular membrane trafficking or also release of neurotransmitters. Additionally it was shown to be involved in virus-uptake e.g. via CD4 during HIV infections (Geyer et al., 2002; Jefferies et al., 2008). In osteoclasts the V-ATPase is required for acidification and interestingly was found to have an actin-binding site. Recently El Far and Seagar suggested a role of the V-ATPase in neurotransmitter release by interacting with SNARE proteins (El Far&Seagar, 2011). So far V-ATPases have not been specifically studied in NK cells. Therefore, no other function except for acidification in lytic granules was investigated yet. Our results indicate that there might be an additional functional role of V-ATPases in NK cells that has not been investigated yet.

In this study, we used three assay systems that characterize of the detachment process of NK cells from target cells. Using flow cytometry-based assays we show that recently detached NK cells display

changes in their surface expression pattern. This could be caused by regulatory mechanisms, which are important for controlling NK cell cytotoxicity. In line with this, we found that the stability of NK:target cell conjugates requires ongoing early activating signaling and a dynamic cytoskeleton. Supporting these findings, we observed that also ATP, e.g. as substrate for kinases or ATPases, must be available. In contrast signaling molecules further down-stream, or cell surface-located metalloproteinases are dispensable for the maintenance of conjugates. Inhibiting the vacuolar H^+-ATPase and thereby depleting mature perforin in the NK cells almost completely blocked the detachment of NK cells from target cells. The question remains if this is due to the prevention of the target cell death or induced by the interference with the V-ATPase function. The latter hypothesis would be supported by the observation that depletion of mature perforin by monensin did not affect the stability of NK:target cell conjugates. Further studies in this system and in addition, the visualization of the detachment process via life-cell imaging will increase the understanding of the events leading to detachment and resolving the sequence of this process. This might provide insights in NK cell function, which are important for augmentation of NK cell-mediated cytotoxicity by possibly increasing their ability for serial killing.

6. References

Abarca-Rojano, E., Muniz-Hernandez, S., Moreno-Altamirano, M. M., Mondragon-Flores, R., Enriquez-Rincon, F., & Sanchez-Garcia, F. J. 2009. **Re-organization of mitochondria at the NK cell immune synapse**. *Immunol Lett*, 122(1): 18-25.

Abeyweera, T. P., Merino, E., & Huse, M. 2011. **Inhibitory signaling blocks activating receptor clustering and induces cytoskeletal retraction in natural killer cells**. *J Cell Biol*, 192(4): 675-690.

Abraha, A. B., & Whalen, M. M. 2009. **The role of p44/42 activation in tributyltin-induced inhibition of human natural killer cells: effects of MEK inhibitors**. *J Appl Toxicol*, 29(2): 165-173.

Alter, G., Malenfant, J. M., & Altfeld, M. 2004. **CD107a as a functional marker for the identification of natural killer cell activity**. *J Immunol Methods*, 294(1-2): 15-22.

Amos, L. A., & Lowe, J. 1999. **How Taxol stabilises microtubule structure**. *Chem Biol*, 6(3): R65-69.

André, P., Spertini, O., Guia, S., Rihet, P., Dignat-George, F., Brailly, H., Sampol, J., Anderson, P. J., & Vivier, E. 2000. **Modification of P-selectin glycoprotein ligand-1 with a natural killer cell-restricted sulfated lactosamine creates an alternate ligand for L-selectin**. *Proceedings of the National Academy of Sciences of the United States of America*, 97(7): 3400-3405.

Andzelm, M. M., Chen, X., Krzewski, K., Orange, J. S., & Strominger, J. L. 2007. **Myosin IIA is required for cytolytic granule exocytosis in human NK cells**. *J Exp Med*, 204(10): 2285-2291.

Arulanandam, A. R. N., Moingeon, P., Concino, M. F., Recny, M. A., Kato, K., Yagita, H., Koyasu, S., & Reinherz, E. L. 1993. **A Soluble Multimeric Recombinant Cd2 Protein Identifies Cd48 as a Low Affinity Ligand for Human Cd2 - Divergence of Cd2 Ligands during the Evolution of Humans and Mice**. *Journal of Experimental Medicine*, 177(5): 1439-1450.

Bajpai, A., & Brahmi, Z. 1994. **Target cell-induced inactivation of cytolytic lymphocytes. Role and regulation of CD45 and calyculin A-inhibited phosphatase in response to interleukin-2**. *J Biol Chem*, 269(29): 18864-18869.

Bajpai, A., & Brahmi, Z. 1996. **Regulation of natural killer cell-mediated cytotoxicity by serine/threonine phosphatases: identification of a calyculin A-sensitive serine/threonine kinase**. *Biochem J*, 320 (Pt 1): 153-159.

Balagopalan, L., Sherman, E., Barr, V. A., & Samelson, L. E. 2011. **Imaging techniques for assaying lymphocyte activation in action**. *Nature Reviews Immunology*, 11(1): 21-33.

Balaji, K. N., Schaschke, N., Machleidt, W., Catalfamo, M., & Henkart, P. A. 2002. **Surface cathepsin B protects cytotoxic lymphocytes from self-destruction after degranulation**. *The Journal of experimental medicine*, 196(4): 493-503.

Banerjee, P. P., Pandey, R., Zheng, R., Suhoski, M. M., Monaco-Shawver, L., & Orange, J. S. 2007. **Cdc42-interacting protein-4 functionally links actin and microtubule networks at the cytolytic NK cell immunological synapse**. *J Exp Med*, 204(10): 2305-2320.

Baran, K., Dunstone, M., Chia, J., Ciccone, A., Browne, K. A., Clarke, C. J., Lukoyanova, N., Saibil, H., Whisstock, J. C., Voskoboinik, I., & Trapani, J. A. 2009. **The molecular basis for perforin oligomerization and transmembrane pore assembly**. *Immunity*, 30(5): 684-695.

Barber, D. F., Faure, M., & Long, E. O. 2004. **LFA-1 contributes an early signal for NK cell cytotoxicity**. *Journal of immunology*, 173(6): 3653-3659.

Barber, D. F., & Long, E. O. 2003. **Coexpression of CD58 or CD48 with intercellular adhesion molecule 1 on target cells enhances adhesion of resting NK cells**. *Journal of immunology*, 170(1): 294-299.

Baychelier, F., Sennepin, A., Ermonval, M., Dorgham, K., Debre, P., & Vieillard, V. 2013. **Identification of a cellular ligand for the natural cytotoxicity receptor NKp44**. *Blood*, 122(17): 2935-2942.

Beresford, P. J., Xia, Z., Greenberg, A. H., & Lieberman, J. 1999. **Granzyme A loading induces rapid cytolysis and a novel form of DNA damage independently of caspase activation**. *Immunity*, 10(5): 585-594.

Berke, G., & Gabison, D. 1975. **Energy requirements of the binding and lytic steps of T lymphocyte-mediated cytolysis of leukemic cells in vitro**. *Eur J Immunol*, 5(10): 671-675.

Bhat, R., & Watzl, C. 2007. **Serial killing of tumor cells by human natural killer cells--enhancement by therapeutic antibodies.** *PloS one*, 2(3): e326.

Blom, B., & Spits, H. 2006. **Development of human lymphoid cells**. *Annu Rev Immunol*, 24: 287-320.

Bouchier-Hayes, L., Munoz-Pinedo, C., Connell, S., & Green, D. R. 2008. **Measuring apoptosis at the single cell level**. *Methods*, 44(3): 222-228.

Brandt, C. S., Baratin, M., Yi, E. C., Kennedy, J., Gao, Z., Fox, B., Haldeman, B., Ostrander, C. D., Kaifu, T., Chabannon, C., Moretta, A., West, R., Xu, W., Vivier, E., & Levin, S. D. 2009. **The B7 family member B7-H6 is a tumor cell ligand for the activating natural killer cell receptor NKp30 in humans**. *The Journal of experimental medicine*, 206(7): 1495-1503.

Brodin, P., Karre, K., & Hoglund, P. 2009. **NK cell education: not an on-off switch but a tunable rheostat**. *Trends Immunol*, 30(4): 143-149.

Brown, A. C., Dobbie, I. M., Alakoskela, J. M., Davis, I., & Davis, D. M. 2012. **Super-resolution imaging of remodeled synaptic actin reveals different synergies between NK cell receptors and integrins**. *Blood*, 120(18): 3729-3740.

Brown, A. C., Oddos, S., Dobbie, I. M., Alakoskela, J. M., Parton, R. M., Eissmann, P., Neil, M. A., Dunsby, C., French, P. M., Davis, I., & Davis, D. M. 2011. **Remodelling of cortical actin where lytic granules dock at natural killer cell immune synapses revealed by super-resolution microscopy**. *PLoS Biol*, 9(9): e1001152.

Brumbaugh, K. M., Binstadt, B. A., Billadeau, D. D., Schoon, R. A., Dick, C. J., Ten, R. M., & Leibson, P. J. 1997. **Functional role for Syk tyrosine kinase in natural killer cell-mediated natural cytotoxicity**. *J Exp Med*, 186(12): 1965-1974.

Bryceson, Y. T., Ljunggren, H. G., & Long, E. O. 2009. **Minimal requirement for induction of natural cytotoxicity and intersection of activation signals by inhibitory receptors**. *Blood*, 114(13): 2657-2666.

Bryceson, Y. T., March, M. E., Barber, D. F., Ljunggren, H. G., & Long, E. O. 2005. **Cytolytic granule polarization and degranulation controlled by different receptors in resting NK cells**. *J Exp Med*, 202(7): 1001-1012.

Bryceson, Y. T., March, M. E., Ljunggren, H. G., & Long, E. O. 2006. **Activation, coactivation, and costimulation of resting human natural killer cells**. *Immunol Rev*, 214: 73-91.

Bubb, M. R. 2000. **Effects of Jasplakinolide on the Kinetics of Actin Polymerization. AN EXPLANATION FOR CERTAIN IN VIVO OBSERVATIONS**. *Journal of Biological Chemistry*, 275(7): 5163-5170.

Bubb, M. R., Senderowicz, A. M., Sausville, E. A., Duncan, K. L., & Korn, E. D. 1994. **Jasplakinolide, a cytotoxic natural product, induces actin polymerization and competitively inhibits the binding of phalloidin to F-actin**. *J Biol Chem*, 269(21): 14869-14871.

Burshtyn, D. N. 2010. **Natural Killer Cell Conjugate Assay Using Two-Color Flow Cytometry**. 612.

Butler, B., & Cooper, J. A. 2009. **Distinct roles for the actin nucleators Arp2/3 and hDia1 during NK-mediated cytotoxicity**. *Current biology : CB*, 19(22): 1886-1896.

Caligiuri, M. A. 2008. **Human natural killer cells**. *Blood*, 112(3): 461-469.

Campbell, K. S., & Hasegawa, J. 2013. **Natural killer cell biology: an update and future directions**. *J Allergy Clin Immunol*, 132(3): 536-544.

Capuano, C., Paolini, R., Molfetta, R., Frati, L., Santoni, A., & Galandrini, R. 2012. **PIP2-dependent regulation of Munc13-4 endocytic recycling: impact on the cytolytic secretory pathway**. *Blood*, 119(10): 2252-2262.

Caraux, A., Kim, N., Bell, S. E., Zompi, S., Ranson, T., Lesjean-Pottier, S., Garcia-Ojeda, M. E., Turner, M., & Colucci, F. 2006. **Phospholipase C-gamma2 is essential for NK cell cytotoxicity and innate immunity to malignant and virally infected cells**. *Blood*, 107(3): 994-1002.

Carlin, L. M., Evans, R., Milewicz, H., Fernandes, L., Matthews, D. R., Perani, M., Levitt, J., Keppler, M. D., Monypenny, J., Coolen, T., Barber, P. R., Vojnovic, B., Suhling, K., Fraternali, F., Ameer-Beg, S., Parker, P. J., Thomas, N. S., & Ng, T. 2011. **A targeted siRNA screen identifies regulators of Cdc42 activity at the natural killer cell immunological synapse**. *Sci Signal*, 4(201): ra81.

Casey, T. M., Meade, J. L., & Hewitt, E. W. 2007. **Organelle proteomics: identification of the exocytic machinery associated with the natural killer cell secretory lysosome**. *Mol Cell Proteomics*, 6(5): 767-780.

Chauveau, A., Aucher, A., Eissmann, P., Vivier, E., & Davis, D. M. 2010. **Membrane nanotubes facilitate long-distance interactions between natural killer cells and target cells**. *Proceedings of the National Academy of Sciences of the United States of America*, 107(12): 5545-5550.

Chávez-Galán, L., Arenas-Del Angel, M. C., Zenteno, E., Chávez, R., & Lascurain, R. 2009. **Cell death mechanisms induced by cytotoxic lymphocytes**. *Cellular & molecular immunology*, 6(1): 15-25.

Chen, L., Sung, S. S., Yip, M. L., Lawrence, H. R., Ren, Y., Guida, W. C., Sebti, S. M., Lawrence, N. J., & Wu, J. 2006. **Discovery of a novel shp2 protein tyrosine phosphatase inhibitor**. *Mol Pharmacol*, 70(2): 562-570.

Chini, C. C., Boos, M. D., Dick, C. J., Schoon, R. A., & Leibson, P. J. 2000. **Regulation of p38 mitogen-activated protein kinase during NK cell activation**. *European Journal of Immunology*, 30(10): 2791-2798.

Choi, P. J., & Mitchison, T. J. 2013. **Imaging burst kinetics and spatial coordination during serial killing by single natural killer cells**. *Proc Natl Acad Sci U S A*, 110(16): 6488-6493.

Claus, M., Meinke, S., Bhat, R., & Watzl, C. 2008. **Regulation of NK cell activity by 2B4, NTB-A and CRACC.** *Frontiers in bioscience : a journal and virtual library*, 13: 956-965.

Cohnen, A., Chiang, S. C., Stojanovic, A., Schmidt, H., Claus, M., Saftig, P., Janssen, O., Cerwenka, A., Bryceson, Y. T., & Watzl, C. 2013. **Surface CD107a/LAMP-1 protects natural killer cells from degranulation-associated damage**. *Blood*, 122(8): 1411-1418.

Comerci, C. J., Mace, E. M., Banerjee, P. P., & Orange, J. S. 2012. **CD2 promotes human natural killer cell membrane nanotube formation**. *PLoS One*, 7(10): e47664.

Cooper, J. A. 1987. **Effects of cytochalasin and phalloidin on actin**. *J Cell Biol*, 105(4): 1473-1478.

Cote, M., Menager, M. M., Burgess, A., Mahlaoui, N., Picard, C., Schaffner, C., Al-Manjomi, F., Al-Harbi, M., Alangari, A., Le Deist, F., Gennery, A. R., Prince, N., Cariou, A., Nitschke, P., Blank, U., El-Ghazali, G., Menasche, G., Latour, S., Fischer, A., & de Saint Basile, G. 2009. **Munc18-2 deficiency causes familial hemophagocytic lymphohistiocytosis type 5 and impairs cytotoxic granule exocytosis in patient NK cells**. *J Clin Invest*, 119(12): 3765-3773.

Crome, S. Q., Lang, P. A., Lang, K. S., & Ohashi, P. S. 2013. **Natural killer cells regulate diverse T cell responses**. *Trends Immunol*, 34(7): 342-349.

Culley, F. J., Johnson, M., Evans, J. H., Kumar, S., Crilly, R., Casasbuenas, J., Schnyder, T., Mehrabi, M., Deonarain, M. P., Ushakov, D. S., Braud, V., Roth, G., Brock, R., Kohler, K., & Davis, D. M. 2009. **Natural killer cell signal integration balances synapse symmetry and migration**. *PLoS Biol*, 7(7): e1000159.

Dabrazhynetskaya, A., Ma, J., Guerreiro-Cacais, A. O., Arany, Z., Rudd, E., Henter, J. I., Karre, K., Levitskaya, J., & Levitsky, V. 2012. **Syntaxin 11 marks a distinct intracellular compartment recruited to the immunological synapse of NK cells to colocalize with cytotoxic granules**. *J Cell Mol Med*, 16(1): 129-141.

Davis, D. M. 2009. **Mechanisms and functions for the duration of intercellular contacts made by lymphocytes**. *Nature Reviews Immunology*, 9(8): 543-555.

Davis, D. M., Chiu, I., Fassett, M., Cohen, G. B., Mandelboim, O., & Strominger, J. L. 1999. **The human natural killer cell immune synapse**. *Proc Natl Acad Sci U S A*, 96(26): 15062-15067.

de Andrade, L. F., Smyth, M. J., & Martinet, L. 2013. **DNAM-1 control of natural killer cells functions through nectin and nectin-like proteins**. *Immunol Cell Biol*.

Diefenbach, A., & Raulet, D. H. 2001. **Strategies for target cell recognition by natural killer cells**. *Immunological reviews*, 181: 170-184.

Drose, S., & Altendorf, K. 1997. **Bafilomycins and concanamycins as inhibitors of V-ATPases and P-ATPases**. *J Exp Biol*, 200(Pt 1): 1-8.

Dustin, M. L. 2009. **Modular design of immunological synapses and kinapses**. *Cold Spring Harb Perspect Biol*, 1(1): a002873.

Dustin, M. L., & Depoil, D. 2011. **New insights into the T cell synapse from single molecule techniques**. *Nat Rev Immunol*, 11(10): 672-684.

Dustin, M. L., Olszowy, M. W., Holdorf, A. D., Li, J., Bromley, S., Desai, N., Widder, P., Rosenberger, F., van der Merwe, P. A., Allen, P. M., & Shaw, A. S. 1998. **A novel adaptor protein orchestrates receptor patterning and cytoskeletal polarity in T-cell contacts**. *Cell*, 94(5): 667-677.

Eissmann, P., & Watzl, C. 2006. **Molecular analysis of NTB-A signaling: a role for EAT-2 in NTB-A-mediated activation of human NK cells.** *Journal of immunology*, 177(5): 3170-3177.

El Far, O., & Seagar, M. 2011. **A role for V-ATPase subunits in synaptic vesicle fusion?** *J Neurochem*, 117(4): 603-612.

El-Sherbiny, Y. M., Meade, J. L., Holmes, T. D., McGonagle, D., Mackie, S. L., Morgan, A. W., Cook, G., Feyler, S., Richards, S. J., Davies, F. E., Morgan, G. J., & Cook, G. P. 2007. **The requirement for DNAM-1, NKG2D, and NKp46 in the natural killer cell-mediated killing of myeloma cells**. *Cancer Research*, 67(18): 8444-8449.

Elstak, E. D., Neeft, M., Nehme, N. T., Voortman, J., Cheung, M., Goodarzifard, M., Gerritsen, H. C., van Bergen En Henegouwen, P. M., Callebaut, I., de Saint Basile, G., & van der Sluijs, P. 2011. **The munc13-4-rab27 complex is specifically required for tethering secretory lysosomes at the plasma membrane**. *Blood*, 118(6): 1570-1578.

Eriksson, M., Leitz, G., Fällman, E., Axner, O., Ryan, J. C., Nakamura, M. C., & Sentman, C. L. 1999. **Inhibitory receptors alter natural killer cell interactions with target cells yet allow simultaneous killing of susceptible targets**. *The Journal of experimental medicine*, 190(7): 1005-1012.

Evenou, J. P., Wagner, J., Zenke, G., Brinkmann, V., Wagner, K., Kovarik, J., Welzenbach, K. A., Weitz-Schmidt, G., Guntermann, C., Towbin, H., Cottens, S., Kaminski, S., Letschka, T., Lutz-Nicoladoni, C., Gruber, T., Hermann-Kleiter, N., Thuille, N., & Baier, G. 2009. **The potent protein kinase C-selective inhibitor AEB071 (sotrastaurin) represents a new class of immunosuppressive agents affecting early T-cell activation**. *J Pharmacol Exp Ther*, 330(3): 792-801.

Fassett, M. S., Davis, D. M., Valter, M. M., Cohen, G. B., & Strominger, J. L. 2001. **Signaling at the inhibitory natural killer cell immune synapse regulates lipid raft polarization but not class I MHC clustering**. *Proceedings of the National Academy of Sciences of the United States of America*, 98(25): 14547-14552.

Fei, M. J., Yamashita, E., Inoue, N., Yao, M., Yamaguchi, H., Tsukihara, T., Shinzawa-Itoh, K., Nakashima, R., & Yoshikawa, S. 2000. **X-ray structure of azide-bound fully oxidized cytochrome c oxidase from bovine heart at 2.9 A resolution**. *Acta Crystallogr D Biol Crystallogr*, 56(Pt 5): 529-535.

Fernandez, N. C., Treiner, E., Vance, R. E., Jamieson, A. M., Lemieux, S., & Raulet, D. H. 2005. **A subset of natural killer cells achieves self-tolerance without expressing inhibitory receptors specific for self-MHC molecules**. *Blood*, 105(11): 4416-4423.

Fiegler, N., Textor, S., Arnold, A., Rolle, A., Oehme, I., Breuhahn, K., Moldenhauer, G., Witzens-Harig, M., & Cerwenka, A. 2013. **Downregulation of the activating NKp30 ligand B7-H6 by HDAC inhibitors impairs tumor cell recognition by NK cells**. *Blood*, 122(5): 684-693.

Flanagan, M. D., & Lin, S. 1980. **Cytochalasins block actin filament elongation by binding to high affinity sites associated with F-actin**. *J Biol Chem*, 255(3): 835-838.

Galandrini, R., Capuano, C., & Santoni, A. 2013. **Activation of Lymphocyte Cytolytic Machinery: Where are We?** *Front Immunol*, 4: 390.

Geyer, M., Yu, H., Mandic, R., Linnemann, T., Zheng, Y. H., Fackler, O. T., & Peterlin, B. M. 2002. **Subunit H of the V-ATPase binds to the medium chain of adaptor protein complex 2 and connects Nef to the endocytic machinery**. *J Biol Chem*, 277(32): 28521-28529.

Gismondi, A., Bisogno, L., Mainiero, F., Palmieri, G., Piccoli, M., Frati, L., & Santoni, A. 1997. **Proline-rich tyrosine kinase-2 activation by beta 1 integrin fibronectin receptor cross-linking and association with paxillin in human natural killer cells**. *J Immunol*, 159(10): 4729-4736.

Goddette, D. W., & Frieden, C. 1986. **Actin polymerization. The mechanism of action of cytochalasin D**. *J Biol Chem*, 261(34): 15974-15980.

Gonzales, R. S., & Wick, T. M. 1996. **Hemodynamic modulation of monocytic cell adherence to vascular endothelium**. *Ann Biomed Eng*, 24(3): 382-393.

Graham, D. B., Cella, M., Giurisato, E., Fujikawa, K., Miletic, A. V., Kloeppel, T., Brim, K., Takai, T., Shaw, A. S., Colonna, M., & Swat, W. 2006. **Vav1 controls DAP10-mediated natural cytotoxicity by regulating actin and microtubule dynamics**. *Journal of immunology*, 177(4): 2349-2355.

Gross, C., Koelch, W., DeMaio, A., Arispe, N., & Multhoff, G. 2003. **Cell surface-bound heat shock protein 70 (Hsp70) mediates perforin-independent apoptosis by specific binding and uptake of granzyme B**. *The Journal of biological chemistry*, 278(42): 41173-41181.

Gross, C. C., Brzostowski, J. A., Liu, D., & Long, E. O. 2010. **Tethering of Intercellular Adhesion Molecule on Target Cells Is Required for LFA-1-Dependent NK Cell Adhesion and Granule Polarization**. *Journal of immunology (Baltimore, Md : 1950)*.

Groth, A., Kloss, S., von Strandmann, E. P., Koehl, U., & Koch, J. 2011. **Mechanisms of tumor and viral immune escape from natural killer cell-mediated surveillance**. *J Innate Immun*, 3(4): 344-354.

Gumbleton, M., & Kerr, W. G. 2013. **Role of inositol phospholipid signaling in natural killer cell biology**. *Front Immunol*, 4: 47.

Ham, H., Guerrier, S., Kim, J., Schoon, R. A., Anderson, E. L., Hamann, M. J., Lou, Z., & Billadeau, D. D. 2013. **Dedicator of cytokinesis 8 interacts with talin and Wiskott-Aldrich syndrome protein to regulate NK cell cytotoxicity**. *J Immunol*, 190(7): 3661-3669.

Hoffmann, P., Hofmeister, R., Brischwein, K., Brandl, C., Crommer, S., Bargou, R., Itin, C., Prang, N., & Baeuerle, P. A. 2005. **Serial killing of tumor cells by cytotoxic T cells redirected with a CD19-/CD3-bispecific single-chain antibody construct.** *Int J Cancer*, 115(1): 98-104.

Hoffmann, S. C., Cohnen, A., Ludwig, T., & Watzl, C. 2011. **2B4 Engagement Mediates Rapid LFA-1 and Actin-Dependent NK Cell Adhesion to Tumor Cells as Measured by Single Cell Force Spectroscopy.** *Journal of immunology (Baltimore, Md : 1950)*, 186(5): 2757-2764.

Hogg, N., Patzak, I., & Willenbrock, F. 2011. **The insider's guide to leukocyte integrin signalling and function**. *Nat Rev Immunol*, 11(6): 416-426.

Holzinger, A. 2009. **Jasplakinolide: an actin-specific reagent that promotes actin polymerization**. *Methods Mol Biol*, 586: 71-87.

Hubbard, S. R., & Till, J. H. 2000. **Protein tyrosine kinase structure and function.** *Annu Rev Biochem*, 69: 373-398.

Huyer, G., Liu, S., Kelly, J., Moffat, J., Payette, P., Kennedy, B., Tsaprailis, G., Gresser, M. J., & Ramachandran, C. 1997. **Mechanism of inhibition of protein-tyrosine phosphatases by vanadate and pervanadate**. *J Biol Chem*, 272(2): 843-851.

Ilani, T., Vasiliver-Shamis, G., Vardhana, S., Bretscher, A., & Dustin, M. L. 2009. **T cell antigen receptor signaling and immunological synapse stability require myosin IIA**. *Nat Immunol*, 10(5): 531-539.

Imai, K., Matsuyama, S., Miyake, S., Suga, K., & Nakachi, K. 2000. **Natural cytotoxic activity of peripheral-blood lymphocytes and cancer incidence: an 11-year follow-up study of a general population**. *Lancet*, 356(9244): 1795-1799.

James, A. M., Hsu, H. T., Dongre, P., Uzel, G., Mace, E. M., Banerjee, P. P., & Orange, J. S. 2013. **Rapid activation receptor- or IL-2-induced lytic granule convergence in human natural killer cells requires Src, but not downstream signaling**. *Blood*, 121(14): 2627-2637.

Jarahian, M., Fiedler, M., Cohnen, A., Djandji, D., Hammerling, G. J., Gati, C., Cerwenka, A., Turner, P. C., Moyer, R. W., Watzl, C., Hengel, H., & Momburg, F. 2011. **Modulation of NKp30- and NKp46-mediated natural killer cell responses by poxviral hemagglutinin**. *PLoS Pathog*, 7(8): e1002195.

Jefferies, K. C., Cipriano, D. J., & Forgac, M. 2008. **Function, structure and regulation of the vacuolar (H+)-ATPases**. *Arch Biochem Biophys*, 476(1): 33-42.

Jiang, K., Zhong, B., Gilvary, D. L., Corliss, B. C., Hong-Geller, E., Wei, S., & Djeu, J. Y. 2000. **Pivotal role of phosphoinositide-3 kinase in regulation of cytotoxicity in natural killer cells**. *Nat Immunol*, 1(5): 419-425.

Joncker, N. T., Fernandez, N. C., Treiner, E., Vivier, E., & Raulet, D. H. 2009. **NK cell responsiveness is tuned commensurate with the number of inhibitory receptors for self-MHC class I: the rheostat model**. *Journal of immunology*, 182(8): 4572-4580.

Joncker, N. T., Shifrin, N., Delebecque, F., & Raulet, D. H. 2010. **Mature natural killer cells reset their responsiveness when exposed to an altered MHC environment**. *The Journal of experimental medicine*.

Karre, K. 2002. **NK cells, MHC class I molecules and the missing self**. *Scand J Immunol*, 55(3): 221-228.

Kataoka, T. 1994. **Acidification is essential for maintaining the structure and function of lytic granules of CTL**.

Kataoka, T., Shinohara, N., Takayama, H., Takaku, K., Kondo, S., Yonehara, S., & Nagai, K. 1996. **Concanamycin A, a powerful tool for characterization and estimation of contribution of perforin- and Fas-based lytic pathways in cell-mediated cytotoxicity**. *J Immunol*, 156(10): 3678-3686.

Katz, P., Zaytoun, A. M., & Lee, J. H., Jr. 1982. **Mechanisms of human cell-mediated cytotoxicity. III. Dependence of natural killing on microtubule and microfilament integrity**. *J Immunol*, 129(6): 2816-2825.

Keefe, D., Shi, L., Feske, S., Massol, R., Navarro, F., Kirchhausen, T., & Lieberman, J. 2005. **Perforin triggers a plasma membrane-repair response that facilitates CTL induction of apoptosis**. *Immunity*, 23(3): 249-262.

Kellner, C., Maurer, T., Hallack, D., Repp, R., van de Winkel, J. G., Parren, P. W., Valerius, T., Humpe, A., Gramatzki, M., & Peipp, M. 2012. **Mimicking an induced self phenotype by coating lymphomas with the NKp30 ligand B7-H6 promotes NK cell cytotoxicity**. *J Immunol*, 189(10): 5037-5046.

Kim, S., Poursine-Laurent, J., Truscott, S. M., Lybarger, L., Song, Y. J., Yang, L., French, A. R., Sunwoo, J. B., Lemieux, S., Hansen, T. H., & Yokoyama, W. M. 2005. **Licensing of natural killer cells by host major histocompatibility complex class I molecules**. *Nature*, 436(7051): 709-713.

Koch, J., Steinle, A., Watzl, C., & Mandelboim, O. 2013. **Activating natural cytotoxicity receptors of natural killer cells in cancer and infection**. *Trends Immunol*, 34(4): 182-191.

Kong, K. F., & Altman, A. 2013. **In and out of the bull's eye: protein kinase Cs in the immunological synapse**. *Trends Immunol*, 34(5): 234-242.

Konjar, S., Sutton, V. R., Hoves, S., Repnik, U., Yagita, H., Reinheckel, T., Peters, C., Turk, V., Turk, B., Trapani, J. A., & Kopitar-Jerala, N. 2010. **Human and mouse perforin are processed in part through cleavage by the lysosomal cysteine proteinase cathepsin L**. *Immunology*, 131(2): 257-267.

Kovacs, M., Toth, J., Hetenyi, C., Malnasi-Csizmadia, A., & Sellers, J. R. 2004. **Mechanism of blebbistatin inhibition of myosin II**. *J Biol Chem*, 279(34): 35557-35563.

Krzewski, K., Chen, X., Orange, J. S., & Strominger, J. L. 2006. **Formation of a WIP-, WASp-, actin-, and myosin IIA-containing multiprotein complex in activated NK cells and its alteration by KIR inhibitory signaling**. *J Cell Biol*, 173(1): 121-132.

Krzewski, K., & Coligan, J. E. 2012. **Human NK cell lytic granules and regulation of their exocytosis**. *Front Immunol*, 3: 335.

Krzewski, K., Gil-Krzewska, A., Watts, J., Stern, J. N., & Strominger, J. L. 2011. **VAMP4- and VAMP7-expressing vesicles are both required for cytotoxic granule exocytosis in NK cells**. *Eur J Immunol*, 41(11): 3323-3329.

Krzewski, K., & Strominger, J. L. 2008. **The killer's kiss: the many functions of NK cell immunological synapses**. *Curr Opin Cell Biol*, 20(5): 597-605.

Kumari, S., Vardhana, S., Cammer, M., Curado, S., Santos, L., Sheetz, M. P., & Dustin, M. L. 2012. **T Lymphocyte Myosin IIA is Required for Maturation of the Immunological Synapse**. *Front Immunol*, 3: 230.

Lagrue, K., Carisey, A., Oszmiana, A., Kennedy, P. R., Williamson, D. J., Cartwright, A., Barthen, C., & Davis, D. M. 2013. **The central role of the cytoskeleton in mechanisms and functions of the NK cell immune synapse**. *Immunol Rev*, 256(1): 203-221.

Lanier, L. L., Ruitenberg, J. J., & Phillips, J. H. 1988. **Functional and biochemical analysis of CD16 antigen on natural killer cells and granulocytes**. *J Immunol*, 141(10): 3478-3485.

Letschka, T., Kollmann, V., Pfeifhofer-Obermair, C., Lutz-Nicoladoni, C., Obermair, G. J., Fresser, F., Leitges, M., Hermann-Kleiter, N., Kaminski, S., & Baier, G. 2008. **PKC-theta selectively controls the adhesion-stimulating molecule Rap1**. *Blood*, 112(12): 4617-4627.

Li, P., Katirai, F., Zheng, F., & Gong, F. 2011. **Recycling and reutilization of cytotoxic molecules, a new type of energy conservation of NK cells?** *Med Hypotheses*, 76(2): 293-295.

Lieberman, J. 2003. **The ABCs of granule-mediated cytotoxicity: new weapons in the arsenal**. *Nature Reviews Immunology*, 3(5): 361-370.

Liu, D., Bryceson, Y. T., Meckel, T., Vasiliver-Shamis, G., Dustin, M. L., & Long, E. O. 2009. **Integrin-dependent organization and bidirectional vesicular traffic at cytotoxic immune synapses**. *Immunity*, 31(1): 99-109.

Liu, D., Martina, J. A., Wu, X. S., Hammer, J. A., 3rd, & Long, E. O. 2011. **Two modes of lytic granule fusion during degranulation by natural killer cells**. *Immunol Cell Biol*, 89(6): 728-738.

Liu, D., Meckel, T., & Long, E. O. 2010. **Distinct Role of Rab27a in Granule Movement at the Plasma Membrane and in the Cytosol of NK Cells**. *PloS one*, 5(9).

Liu, D., Xu, L., Yang, F., Li, D., Gong, F., & Xu, T. 2005. **Rapid biogenesis and sensitization of secretory lysosomes in NK cells mediated by target-cell recognition**. *Proceedings of the National Academy of Sciences of the United States of America*, 102(1): 123-127.

Ljunggren, H. G., & Karre, K. 1990. **In search of the 'missing self': MHC molecules and NK cell recognition**. *Immunol Today*, 11(7): 237-244.

Long, E. O., Kim, H. S., Liu, D., Peterson, M. E., & Rajagopalan, S. 2013. **Controlling natural killer cell responses: integration of signals for activation and inhibition**. *Annu Rev Immunol*, 31: 227-258.

Lopez, J. A., Jenkins, M. R., Rudd-Schmidt, J. A., Brennan, A. J., Danne, J. C., Mannering, S. I., Trapani, J. A., & Voskoboinik, I. 2013. **Rapid and unidirectional perforin pore delivery at the cytotoxic immune synapse**. *J Immunol*, 191(5): 2328-2334.

López-Larrea, C., Suárez-Alvarez, B., López-Soto, A., López-Vázquez, A., & Gonzalez, S. 2008. **The NKG2D receptor: sensing stressed cells**. *Trends in Molecular Medicine*, 14(4): 179-189.

Mace, E. M., Dongre, P., Hsu, H. T., Sinha, P., James, A. M., Mann, S. S., Forbes, L. R., Watkin, L. B., & Orange, J. S. 2014. **Cell biological steps and checkpoints in accessing NK cell cytotoxicity**. *Immunol Cell Biol*.

Mace, E. M., Monkley, S. J., Critchley, D. R., & Takei, F. 2009. **A dual role for talin in NK cell cytotoxicity: activation of LFA-1-mediated cell adhesion and polarization of NK cells**. *Journal of immunology*, 182(2): 948-956.

Mace, E. M., Wu, W. W., Ho, T., Mann, S. S., Hsu, H. T., & Orange, J. S. 2012. **NK cell lytic granules are highly motile at the immunological synapse and require F-actin for post-degranulation persistence**. *J Immunol*, 189(10): 4870-4880.

Mace, E. M., Zhang, J., Siminovitch, K. A., & Takei, F. 2010. **Elucidation of the integrin LFA-1-mediated signaling pathway of actin polarization in natural killer cells**. *Blood*, 116(8): 1272-1279.

Mainiero, F., Soriani, A., Strippoli, R., Jacobelli, J., Gismondi, A., Piccoli, M., Frati, L., & Santoni, A. 2000. **RAC1/P38 MAPK signaling pathway controls beta1 integrin-induced interleukin-8 production in human natural killer cells**. *Immunity*, 12(1): 7-16.

March, M. E., & Long, E. O. 2011. **{beta}2 Integrin Induces TCR{zeta}-Syk-Phospholipase C-{gamma} Phosphorylation and Paxillin-Dependent Granule Polarization in Human NK Cells**. *Journal of immunology (Baltimore, Md : 1950)*, 186(5): 2998-3005.

Maul-Pavicic, A., Chiang, S. C. C., Rensing-Ehl, A., Jessen, B., Fauriat, C., Wood, S. M., Sjoqvist, S., Hufnagel, M., Schulze, I., Bass, T., Schamel, W. W., Fuchs, S., Pircher, H., McCarl, C. A., Mikoshiba, K., Schwarz, K., Feske, S., Bryceson, Y. T., & Ehl, S. 2011. **ORAI1-mediated calcium influx is required for human cytotoxic lymphocyte degranulation and target cell lysis**. *Proceedings of the National Academy of Sciences of the United States of America*, 108(8): 3324-3329.

Mellman, I., Fuchs, R., & Helenius, A. 1986. **Acidification of the endocytic and exocytic pathways**. *Annu Rev Biochem*, 55: 663-700.

Ménager, M. M., Ménasché, G., Romao, M., Knapnougel, P., Ho, C.-H., Garfa, M., Raposo, G., Feldmann, J., Fischer, A., & de Saint Basile, G. 2007. **Secretory cytotoxic granule maturation and exocytosis require the effector protein hMunc13-4**. *Nature Immunology*, 8(3): 257-267.

Mentlik, A. N., Sanborn, K. B., Holzbaur, E. L., & Orange, J. S. 2010. **Rapid lytic granule convergence to the MTOC in natural killer cells is dependent on dynein but not cytolytic commitment**. *Mol Biol Cell*, 21(13): 2241-2256.

Metkar, S. S., Wang, B., Aguilar-Santelises, M., Raja, S. M., Uhlin-Hansen, L., Podack, E., Trapani, J. A., & Froelich, C. J. 2002. **Cytotoxic cell granule-mediated apoptosis: perforin delivers granzyme B-serglycin complexes into target cells without plasma membrane pore formation**. *Immunity*, 16(3): 417-428.

Min-Oo, G., Kamimura, Y., Hendricks, D. W., Nabekura, T., & Lanier, L. L. 2013. **Natural killer cells: walking three paths down memory lane**. *Trends Immunol*, 34(6): 251-258.

Onfelt, B., Nedvetzki, S., Yanagi, K., & Davis, D. M. 2004. **Cutting edge: Membrane nanotubes connect immune cells**. *Journal of immunology*, 173(3): 1511-1513.

Orange, J. S. 2002. **Human natural killer cell deficiencies and susceptibility to infection.** *Microbes and Infection*: 1545–1558.

Orange, J. S. 2008. **Formation and function of the lytic NK-cell immunological synapse.** *Nat Rev Immunol*, 8(9): 713-725.

Orange, J. S., Harris, K. E., Andzelm, M. M., Valter, M. M., Geha, R. S., & Strominger, J. L. 2003. **The mature activating natural killer cell immunologic synapse is formed in distinct stages.** *Proc Natl Acad Sci U S A*, 100(24): 14151-14156.

Orange, J. S., Ramesh, N., Remold-O'Donnell, E., Sasahara, Y., Koopman, L., Byrne, M., Bonilla, F. A., Rosen, F. S., Geha, R. S., & Strominger, J. L. 2002. **Wiskott-Aldrich syndrome protein is required for NK cell cytotoxicity and colocalizes with actin to NK cell-activating immunologic synapses.** *Proceedings of the National Academy of Sciences of the United States of America*, 99(17): 11351-11356.

Palmieri, F., & Klingenberg, M. 1967. **Inhibition of respiration under the control of azide uptake by mitochondria.** *Eur J Biochem*, 1(4): 439-446.

Palmisano, G. L., Contardi, E., Morabito, A., Gargaglione, V., Ferrara, G. B., & Pistillo, M. P. 2005. **HLA-E surface expression is independent of the availability of HLA class I signal sequence-derived peptides in human tumor cell lines.** *Hum Immunol*, 66(1): 1-12.

Parsons, M. S., Tang, C. C., Jegaskanda, S., Center, R. J., Brooks, A. G., Stratov, I., & Kent, S. J. 2014. **Anti-HIV Antibody-Dependent Activation of NK Cells Impairs NKp46 Expression.** *J Immunol*, 192(1): 308-315.

Paul, W. E., & Seder, R. A. 1994. **Lymphocyte responses and cytokines.** *Cell*, 76(2): 241-251.

Pedersen, B., Norrild, B., & Krebs, H. J. 1982. **The effect of monensin on the antibody-dependent cell-mediated killing.** *Cell Immunol*, 72(1): 208-214.

Pende, D., Parolini, S., Pessino, A., Sivori, S., Augugliaro, R., Morelli, L., Marcenaro, E., Accame, L., Malaspina, A., Biassoni, R., Bottino, C., Moretta, L., & Moretta, A. 1999. **Identification and molecular characterization of NKp30, a novel triggering receptor involved in natural cytotoxicity mediated by human natural killer cells.** *J Exp Med*, 190(10): 1505-1516.

Peruzzi, G., Femnou, L., Gil-Krzewska, A., Borrego, F., Weck, J., Krzewski, K., & Coligan, J. E. 2013. **Membrane-Type 6 Matrix Metalloproteinase Regulates the Activation-Induced Downmodulation of CD16 in Human Primary NK Cells.** *J Immunol.*

Peterson, M. E., & Long, E. O. 2008. **Inhibitory receptor signaling via tyrosine phosphorylation of the adaptor Crk.** *Immunity*, 29(4): 578-588.

Pogge von Strandmann, E., Simhadri, V. R., von Tresckow, B., Sasse, S., Reiners, K. S., Hansen, H. P., Rothe, A., Boll, B., Simhadri, V. L., Borchmann, P., McKinnon, P. J., Hallek, M., & Engert, A. 2007. **Human leukocyte antigen-B-associated transcript 3 is released from tumor cells and engages the NKp30 receptor on natural killer cells.** *Immunity*, 27(6): 965-974.

Poggi, A., Massaro, A. M., Negrini, S., Contini, P., & Zocchi, M. R. 2005. **Tumor-induced apoptosis of human IL-2-activated NK cells: role of natural cytotoxicity receptors.** *Journal of immunology*, 174(5): 2653-2660.

Pohlmann, R., Kruger, S., Hasilik, A., & von Figura, K. 1984. **Effect of monensin on intracellular transport and receptor-mediated endocytosis of lysosomal enzymes**. *Biochem J*, 217(3): 649-658.

Pries, A. R., Secomb, T. W., & Gaehtgens, P. 1995. **Design principles of vascular beds**. *Circ Res*, 77(5): 1017-1023.

Rak, G. D., Mace, E. M., Banerjee, P. P., Svitkina, T., & Orange, J. S. 2011. **Natural killer cell lytic granule secretion occurs through a pervasive actin network at the immune synapse**. *PLoS Biol*, 9(9): e1001151.

Raulet, D. H. 2006. **Missing self recognition and self tolerance of natural killer (NK) cells**. *Semin Immunol*, 18(3): 145-150.

Raulet, D. H., & Vance, R. E. 2006. **Self-tolerance of natural killer cells**. *Nature Reviews Immunology*, 6(7): 520-531.

Raulet, D. H., Vance, R. E., & McMahon, C. W. 2001. **Regulation of the natural killer cell receptor repertoire**. *Annu Rev Immunol*, 19: 291-330.

Regunathan, J., Chen, Y., Wang, D., & Malarkannan, S. 2005. **NKG2D receptor-mediated NK cell function is regulated by inhibitory Ly49 receptors**. *Blood*, 105(1): 233-240.

Riteau, B., Barber, D. F., & Long, E. O. 2003. **Vav1 phosphorylation is induced by beta2 integrin engagement on natural killer cells upstream of actin cytoskeleton and lipid raft reorganization**. *The Journal of experimental medicine*, 198(3): 469-474.

Roda-Navarro, P., Mittelbrunn, M., Ortega, M., Howie, D., Terhorst, C., Sanchez-Madrid, F., & Fernandez-Ruiz, E. 2004. **Dynamic redistribution of the activating 2B4/SAP complex at the cytotoxic NK cell immune synapse**. *J Immunol*, 173(6): 3640-3646.

Roda-Navarro, P., & Reyburn, H. T. 2007. **Intercellular protein transfer at the NK cell immune synapse: mechanisms and physiological significance**. *FASEB J*, 21(8): 1636-1646.

Roda-Navarro, P., & Reyburn, H. T. 2009. **The traffic of the NKG2D/Dap10 receptor complex during natural killer (NK) cell activation**. *J Biol Chem*, 284(24): 16463-16472.

Roda-Navarro, P., Vales-Gomez, M., Chisholm, S. E., & Reyburn, H. T. 2006. **Transfer of NKG2D and MICB at the cytotoxic NK cell immune synapse correlates with a reduction in NK cell cytotoxic function**. *Proc Natl Acad Sci U S A*, 103(30): 11258-11263.

Romee, R., Foley, B., Lenvik, T., Wang, Y., Zhang, B., Ankarlo, D., Luo, X. H., Cooley, S., Verneris, M., Walcheck, B., & Miller, J. 2013. **NK cell CD16 surface expression and function is regulated by a disintegrin and metalloprotease-17 (ADAM17)**. *Blood*, 121(18): 3599-3608.

Rosental, B., Brusilovsky, M., Hadad, U., Oz, D., Appel, M. Y., Afergan, F., Yossef, R., Rosenberg, L. A., Aharoni, A., Cerwenka, A., Campbell, K. S., Braiman, A., & Porgador, A. 2011. **Proliferating Cell Nuclear Antigen Is a Novel Inhibitory Ligand for the Natural Cytotoxicity Receptor NKp44.** *Journal of immunology (Baltimore, Md : 1950)*, 187(11): 5693-5702.

Rothstein, T. L., Mage, M., Jones, G., & McHugh, L. L. 1978. **Cytotoxic T lymphocyte sequential killing of immobilized allogeneic tumor target cells measured by time-lapse microcinematography**. *J Immunol*, 121(5): 1652-1656.

Ruckrich, T., & Steinle, A. 2013. **Attenuated natural killer (NK) cell activation through C-type lectin-like receptor NKp80 is due to an anomalous hemi-immunoreceptor tyrosine-based activation motif (HemITAM) with impaired Syk kinase recruitment capacity**. *J Biol Chem*, 288(24): 17725-17733.

Samstag, Y. 2003. **Actin cytoskeletal dynamics in T lymphocyte activation and migration**. *Journal of Leukocyte Biology*, 73(1): 30-48.

Samstag, Y., John, I., & Wabnitz, G. H. 2013. **Cofilin: a redox sensitive mediator of actin dynamics during T-cell activation and migration**. *Immunol Rev*, 256(1): 30-47.

Sanborn, K. B., Mace, E. M., Rak, G. D., Difeo, A., Martignetti, J. A., Pecci, A., Bussel, J. B., Favier, R., & Orange, J. S. 2011. **Phosphorylation of the myosin IIA tailpiece regulates single myosin IIA molecule association with lytic granules to promote NK-cell cytotoxicity**. *Blood*, 118(22): 5862-5871.

Sanborn, K. B., Rak, G. D., Maru, S. Y., Demers, K., Difeo, A., Martignetti, J. A., Betts, M. R., Favier, R., Banerjee, P. P., & Orange, J. S. 2009. **Myosin IIA associates with NK cell lytic granules to enable their interaction with F-actin and function at the immunological synapse**. *J Immunol*, 182(11): 6969-6984.

Sancho, D., Nieto, M., Llano, M., Rodriguez-Fernandez, J. L., Tejedor, R., Avraham, S., Cabanas, C., Lopez-Botet, M., & Sanchez-Madrid, F. 2000. **The tyrosine kinase PYK-2/RAFTK regulates natural killer (NK) cell cytotoxic response, and is translocated and activated upon specific target cell recognition and killing**. *J Cell Biol*, 149(6): 1249-1262.

Sanderson, C. J. 1976. **The mechanism of T cell mediated cytotoxicity. II. Morphological studies of cell death by time-lapse microcinematography**. *Proc R Soc Lond B Biol Sci*, 192(1107): 241-255.

Sandusky, M. M., Messmer, B., & Watzl, C. 2006. **Regulation of 2B4 (CD244)-mediated NK cell activation by ligand-induced receptor modulation.** *European Journal of Immunology*, 36(12): 3268-3276.

Sedelies, K. A., Ciccone, A., Clarke, C. J., Oliaro, J., Sutton, V. R., Scott, F. L., Silke, J., Susanto, O., Green, D. R., Johnstone, R. W., Bird, P. I., Trapani, J. A., & Waterhouse, N. J. 2008. **Blocking granule-mediated death by primary human NK cells requires both protection of mitochondria and inhibition of caspase activity**. *Cell Death Differ*, 15(4): 708-717.

Selvaraj, P., Plunkett, M. L., Dustin, M., Sanders, M. E., Shaw, S., & Springer, T. A. 1987. **The T lymphocyte glycoprotein CD2 binds the cell surface ligand LFA-3**. *Nature*, 326(6111): 400-403.

Sims, T. N., Soos, T. J., Xenias, H. S., Dubin-Thaler, B., Hofman, J. M., Waite, J. C., Cameron, T. O., Thomas, V. K., Varma, R., Wiggins, C. H., Sheetz, M. P., Littman, D. R., & Dustin, M. L. 2007. **Opposing effects of PKCtheta and WASp on symmetry breaking and relocation of the immunological synapse**. *Cell*, 129(4): 773-785.

Sinai, P., Nguyen, C., Schatzle, J. D., & Wulfing, C. 2010. **Transience in polarization of cytolytic effectors is required for efficient killing and controlled by Cdc42**. *Proceedings of the National Academy of Sciences of the United States of America*, 107(26): 11912-11917.

Stebbins, C. C., Watzl, C., Billadeau, D. D., Leibson, P. J., Burshtyn, D. N., & Long, E. O. 2003. **Vav1 dephosphorylation by the tyrosine phosphatase SHP-1 as a mechanism for inhibition of cellular cytotoxicity**. *Molecular and Cellular Biology*, 23(17): 6291-6299.

Stewart, A. G., Sobti, M., Harvey, R. P., & Stock, D. 2013. **Rotary ATPases: models, machine elements and technical specifications**. *Bioarchitecture*, 3(1): 2-12.

Stinchcombe, J. C., Bossi, G., Booth, S., & Griffiths, G. M. 2001. **The immunological synapse of CTL contains a secretory domain and membrane bridges**. *Immunity*, 15(5): 751-761.

Stinchcombe, J. C., Majorovits, E., Bossi, G., Fuller, S., & Griffiths, G. M. 2006. **Centrosome polarization delivers secretory granules to the immunological synapse**. *Nature*, 443(7110): 462-465.

Stinchcombe, J. C., Salio, M., Cerundolo, V., Pende, D., Arico, M., & Griffiths, G. M. 2011. **Centriole polarisation to the immunological synapse directs secretion from cytolytic cells of both the innate and adaptive immune systems**. *BMC Biol*, 9: 45.

Taga, K., Yamauchi, A., & Bloom, E. T. 1999. **Target cell-induced apoptosis in IL-2-activated human natural killer cells**. *Leuk Lymphoma*, 32(5-6): 451-458.

Tager, A. M., Bromley, S. K., Medoff, B. D., Islam, S. A., Bercury, S. D., Friedrich, E. B., Carafone, A. D., Gerszten, R. E., & Luster, A. D. 2003. **Leukotriene B4 receptor BLT1 mediates early effector T cell recruitment**. *Nature Immunology*, 4(10): 982-990.

Tartakoff, A. M. 1983. **Perturbation of vesicular traffic with the carboxylic ionophore monensin**. *Cell*, 32(4): 1026-1028.

Tassi, I., Cella, M., Presti, R., Colucci, A., Gilfillan, S., Littman, D. R., & Colonna, M. 2008. **NK cell-activating receptors require PKC-theta for sustained signaling, transcriptional activation, and IFN-gamma secretion**. *Blood*, 112(10): 4109-4116.

Tassi, I., Presti, R., Kim, S., Yokoyama, W. M., Gilfillan, S., & Colonna, M. 2005. **Phospholipase C-gamma 2 is a critical signaling mediator for murine NK cell activating receptors**. *Journal of immunology*, 175(2): 749-754.

Thiery, J., Keefe, D., Boulant, S., Boucrot, E., Walch, M., Martinvalet, D., Goping, I. S., Bleackley, R. C., Kirchhausen, T., & Lieberman, J. 2011. **Perforin pores in the endosomal membrane trigger the release of endocytosed granzyme B into the cytosol of target cells.** *Nature Immunology*.

Thomas, L. M., Peterson, M. E., & Long, E. O. 2013. **Cutting edge: NK cell licensing modulates adhesion to target cells**. *J Immunol*, 191(8): 3981-3985.

Tian, Z., Gershwin, M. E., & Zhang, C. 2012. **Regulatory NK cells in autoimmune disease**. *J Autoimmun*, 39(3): 206-215.

Tomescu, C., Chehimi, J., Maino, V. C., & Montaner, L. J. 2009. **Retention of viability, cytotoxicity, and response to IL-2, IL-15, or IFN-alpha by human NK cells after CD107a degranulation**. *Journal of Leukocyte Biology*, 85(5): 871-876.

Trapani, J. A., Jans, D. A., Jans, P. J., Smyth, M. J., Browne, K. A., & Sutton, V. R. 1998. **Efficient nuclear targeting of granzyme B and the nuclear consequences of apoptosis induced by granzyme B and perforin are caspase-dependent, but cell death is caspase-independent**. *J Biol Chem*, 273(43): 27934-27938.

Trotta, R., Fettucciari, K., Azzoni, L., Abebe, B., Puorro, K. A., Eisenlohr, L. C., & Perussia, B. 2000. **Differential role of p38 and c-Jun N-terminal kinase 1 mitogen-activated protein kinases in NK cell cytotoxicity**. *J Immunol*, 165(4): 1782-1789.

Uellner, R., Zvelebil, M. J., Hopkins, J., Jones, J., MacDougall, L. K., Morgan, B. P., Podack, E., Waterfield, M. D., & Griffiths, G. M. 1997. **Perforin is activated by a proteolytic cleavage during biosynthesis which reveals a phospholipid-binding C2 domain**. *Embo Journal*, 16(24): 7287-7296.

Ullberg, M., & Jondal, M. 1981. **Recycling and target binding capacity of human natural killer cells**. *J Exp Med*, 153(3): 615-628.

Valiante, N. M., & Trinchieri, G. 1993. **Identification of a novel signal transduction surface molecule on human cytotoxic lymphocytes**. *J Exp Med*, 178(4): 1397-1406.

Vanherberghen, B., Olofsson, P. E., Forslund, E., Sternberg-Simon, M., Khorshidi, M. A., Pacouret, S., Guldevall, K., Enqvist, M., Malmberg, K. J., Mehr, R., & Onfelt, B. 2013. **Classification of human natural killer cells based on migration behavior and cytotoxic response**. *Blood*, 121(8): 1326-1334.

Vasquez, R. J., Howell, B., Yvon, A. M., Wadsworth, P., & Cassimeris, L. 1997. **Nanomolar concentrations of nocodazole alter microtubule dynamic instability in vivo and in vitro**. *Mol Biol Cell*, 8(6): 973-985.

Veillette, A. 2006. **NK cell regulation by SLAM family receptors and SAP-related adapters**. *Immunological reviews*, 214: 22-34.

Vitale, M., Bottino, C., Sivori, S., Sanseverino, L., Castriconi, R., Marcenaro, E., Augugliaro, R., Moretta, L., & Moretta, A. 1998. **NKp44, a novel triggering surface molecule specifically expressed by activated natural killer cells, is involved in non-major histocompatibility complex-restricted tumor cell lysis**. *The Journal of experimental medicine*, 187(12): 2065-2072.

Voskoboinik, I., Dunstone, M. A., Baran, K., Whisstock, J. C., & Trapani, J. A. 2010. **Perforin: structure, function, and role in human immunopathology**. *Immunol Rev*, 235(1): 35-54.

Voskoboinik, I., Thia, M. C., Fletcher, J., Ciccone, A., Browne, K., Smyth, M. J., & Trapani, J. A. 2005. **Calcium-dependent plasma membrane binding and cell lysis by perforin are mediated through its C2 domain: A critical role for aspartate residues 429, 435, 483, and 485 but not 491**. *J Biol Chem*, 280(9): 8426-8434.

Vyas, Y. M., Maniar, H., & Dupont, B. 2002. **Visualization of signaling pathways and cortical cytoskeleton in cytolytic and noncytolytic natural killer cell immune synapses**. *Immunological reviews*, 189: 161-178.

Vyas, Y. M., Mehta, K. M., Morgan, M., Maniar, H., Butros, L., Jung, S., Burkhardt, J. K., & Dupont, B. 2001. **Spatial organization of signal transduction molecules in the NK cell immune synapses during MHC class I-regulated noncytolytic and cytolytic interactions**. *Journal of immunology*, 167(8): 4358-4367.

Wahle, J. A., Paraiso, K. H., Kendig, R. D., Lawrence, H. R., Chen, L., Wu, J., & Kerr, W. G. 2007. **Inappropriate recruitment and activity by the Src homology region 2 domain-containing phosphatase 1 (SHP1) is responsible for receptor dominance in the SHIP-deficient NK cell.** *J Immunol*, 179(12): 8009-8015.

Warren, H. S. 2011. **Target-induced natural killer cell loss as a measure of NK cell responses.** *Journal of immunological methods*.

Watzl, C., & Long, E. O. 2010. **Signal transduction during activation and inhibition of natural killer cells.** *Current protocols in immunology / edited by John E Coligan [et al]*, Chapter 11: Unit 11.19B.

Watzl, C., & Urlaub, D. 2012. **Molecular mechanisms of natural killer cell regulation**. *Front Biosci (Landmark Ed)*, 17: 1418-1432.

Welte, S., Kuttruff, S., Waldhauer, I., & Steinle, A. 2006. **Mutual activation of natural killer cells and monocytes mediated by NKp80-AICL interaction**. *Nature Immunology*, 7(12): 1334-1342.

Westermann, J., & Pabst, R. 1992. **Distribution of lymphocyte subsets and natural killer cells in the human body**. *Clin Investig*, 70(7): 539-544.

Wiedemann, A., Depoil, D., Faroudi, M., & Valitutti, S. 2006. **Cytotoxic T lymphocytes kill multiple targets simultaneously via spatiotemporal uncoupling of lytic and stimulatory synapses**. *Proceedings of the National Academy of Sciences of the United States of America*, 103(29): 10985-10990.

Wlodkowic, D., Telford, W., Skommer, J., & Darzynkiewicz, Z. 2011. **Apoptosis and beyond: cytometry in studies of programmed cell death**. *Methods Cell Biol*, 103: 55-98.

Wood, S. M., Meeths, M., Chiang, S. C., Bechensteen, A. G., Boelens, J. J., Heilmann, C., Horiuchi, H., Rosthoj, S., Rutynowska, O., Winiarski, J., Stow, J. L., Nordenskjold, M., Henter, J. I., Ljunggren, H. G., & Bryceson, Y. T. 2009. **Different NK cell-activating receptors preferentially recruit Rab27a or Munc13-4 to perforin-containing granules for cytotoxicity**. *Blood*, 114(19): 4117-4127.

Wowk, M. E., & Trapani, J. A. 2004. **Cytotoxic activity of the lymphocyte toxin granzyme B**. *Microbes Infect*, 6(8): 752-758.

Wulfing, C., Purtic, B., Klem, J., & Schatzle, J. D. 2003. **Stepwise cytoskeletal polarization as a series of checkpoints in innate but not adaptive cytolytic killing**. *Proc Natl Acad Sci U S A*, 100(13): 7767-7772.

Yamauchi, A., Taga, K., Mostowski, H. S., & Bloom, E. T. 1996. **Target cell-induced apoptosis of interleukin-2-activated human natural killer cells: roles of cell surface molecules and intracellular events**. *Blood*, 87(12): 5127-5135.

Yokoyama, W. M., & Plougastel, B. F. 2003. **Immune functions encoded by the natural killer gene complex**. *Nat Rev Immunol*, 3(4): 304-316.

Zagury, D., Bernard, J., Thierness, N., Feldman, M., & Berke, G. 1975. **Isolation and characterizationof individual functionally reactive cytotoxic T lymphocytes: conjugation, killing and recycling at the single cell level**. *Eur J Immunol*, 5: 818-822.

Zamai, L., Ahmad, M., Bennett, I. M., Azzoni, L., Alnemri, E. S., & Perussia, B. 1998. **Natural killer (NK) cell-mediated cytotoxicity: differential use of TRAIL and Fas ligand by immature and mature primary human NK cells**. *J Exp Med*, 188(12): 2375-2380.

Zhang, T., Wu, M. R., & Sentman, C. L. 2012. **An NKp30-based chimeric antigen receptor promotes T cell effector functions and antitumor efficacy in vivo**. *J Immunol*, 189(5): 2290-2299.

Zheng, X., Wang, Y., Wei, H., Sun, R., & Tian, Z. 2009. **LFA-1 and CD2 synergize for the Erk1/2 activation in the Natural Killer (NK) cell immunological synapse**. *J Biol Chem*, 284(32): 21280-21287.

Zhou, Q., Gil-Krzewska, A., Peruzzi, G., & Borrego, F. 2013. **Matrix metalloproteinases inhibition promotes the polyfunctionality of human natural killer cells in therapeutic antibody-based anti-tumour immunotherapy**. *Clin Exp Immunol*, 173(1): 131-139.

7. Abbreviations

α	Alpha
ADCC	Antibody-dependent cellular cytotoxicity
AICL	Activation-induced C-type lectin
aNKIS	Activating NK cell immunological synapse
APC	Antigen presenting cell
ATP	Adenosine triphosphate
BID	BH3-interactin domain death agonist
BSA	Bovine serum albumin
CD	Cluster of differentiation
CMA	Concanamycin A
CMV	Cytomegalovirus
CTL	Cytotoxic T lymphocytes
DAPI	4',6-Diamidino-2-phenylindole-dihydrochloride
DC	Dendritic cell
DMEM	Dulbecco's Modified Eagle Medium
DMSO	Dimethyl sulfoxide
DNAM-1	DNAX accessory molecule-1
DOCK8	Dedicator of cytokinesis 8
EAT-2	Ewing's sarcoma-associated transcript-2
EBV	Eppstein-Barr virus
EDTA	Ethylenediaminetetraacetic acid
E:T ratio	Effector to target cell ratio
FACS	Fluorescence-activated cell sorting
Fc	Fragment crystallizable
FCS	Fetal calf serum
Fig.	Figure
FITC	Fluorescin isothiocyanate
γ	Gamma
GEF	Guanine nucleotide exchange factors
GMCSF	Granulocyte-macrophage colony stimulating factor
h	Hour
HLA	Human lymphocyte antigen
ICAM	Intercellular adhesion molecule
ID	Inner diameter
IFN	Interferon

Ig	Immunoglobulin
IgG	Immunoglobulin G
IL	Interleukin
ILT	Immunoglobulin -like transcript
IMDM	Iscove's Modified Dulbecco's Medium
iNKIS	Inhibitory NK cell immunological synapse
IS	Immunological synapse
ITAM	Immunoreceptor tyrosine-based activation motif
ITIM	Immunoreceptor tyrosine-based inhibition motif
ITSM	Immunoreceptor tyrosine-based switch motif
IU	International units
kDa	Kilo Dalton
KIR	Killer cell immunoglobuline-like receptor
LAT	Linker for the activation of T cells
LFA	Lymphocyte function-associated antigen
LSM	Lymphocyte separation medium
mAb	Monoclonal antibody
MAPK	Mitogen activated protein kinase
MCMV	Murine cytomeglovirus
MEK	Mitogen-activated protein kinase kinase
MFI	Mean fluorescence intensity
MHC	Major histocompatibility complex
min	Minutes
MMPs	Matrix metalloproteinases
MTOC	Microtubule organizing center
NCR	Natural cytotoxicity receptor
NEAA	Non-essential amino acids
NKC	Natural Killer gene complex
NK cell	Natural Killer cell
NKIS	NK cell immunological synapse
NRSB	Non-reducing sample buffer
NTAL	Non-T cell activation linker
PBL	Peripheral blood lymphocytes
PBMC	Peripheral blood mononuclear cells
PBS	Phosphate buffered saline
PCNA	Proliferating cell nuclear antigen
PE	Phycoerythrin
PFA	Paraformaldehyde

PI3K	Phosphatidyl-inositol-3-kinase
PIP_2	Phosphatidylinositol (4,5)-bisphosphate
PIP_3	Phosphatidylinositol 3,4,5-trisphosphate
PKC	Proteinkinase C
PLC	Phospholipase C
PLL	Poly-L-lysin
PMA	Phorbol 12-myristate 13-acetate
PMSF	Phenylmethysulfonyl fluoride
PVDF	Polyvinylidene fluoride
RNA	Ribonucleic acid
RNAi	RNA interference
RPMI	Roswell Park Memorial Institute
RSB	Reducing sample buffer
SAP	SLAM-associated protein
SDS	Sodium dodecyl sulfate
SDS-PAGE	SDS polyacrylamide gel electrophoresis
SHP	SH2 containing protein tyrosine phosphatases
siRNA	Small interfering RNA
SNARE	Soluble-N- ethylmaleimide-sensitive-factor accessory-protein receptor
SOCE	Store-operated Ca^{2+} entry
Syk	Spleen tyrosine kinase
θ	Theta
TCR	T cell receptor
TNF	Tumor necrosis factor
TRAIL	TNF-related apoptosis inducing ligand
Tyr	Tyrosine
WASp	Wiskott Aldrich-syndrome protein
WIP	WASp-interacting protein
WB	Western Blot
ζ	Zeta
ZAP70	Zeta chain-associated protein kinase 70